

Doctoral thesis

Analyses of symmetry enhancement in F-theory
from geometries and gauge theories

Naoto Kan

The Graduate University for Advanced Studies, SOKENDAI

Abstract

In this thesis, we consider F-theory compactifications. In the first half of the thesis, we study the roles of the loci of $f(z) = 0$ and $g(z) = 0$ that are the coefficient functions in the Weierstrass form, in F-theory. They are thought of as complex codimension-one objects and correspond to the two kinds of critical points of a dessin d'enfant of Grothendieck. The P^1 base space is divided into several cell regions bounded by some domain walls extending from these planes and D-branes, on which the imaginary part of the J -function vanishes. This amounts to drawing a dessin with a canonical triangulation. We show that the dessin provides a new way of keeping track of mutual non-localness among 7-branes without employing unphysical branch cuts or their base point. With the dessin we can see that weak- and strong-coupling regions coexist and are located across an S-wall from each other. We also present a simple method for computing a monodromy matrix for an arbitrary path by tracing the walls it goes through.

In the last half, we investigate higher-codimension singularities of Calabi-Yau manifolds. In F-theory, matters arise from codimension-two singularities of Calabi-Yau manifolds. For Calabi-Yau three-folds, the matters are the hypermultiplets that localize at the codimension-two singularities in six dimensions. The hypermultiplets are typically full-hypers, but in special cases become half-hypers. When the enhancements of the symmetries are $SU(6) \rightarrow E_6$, $SO(12) \rightarrow E_7$ and $E_7 \rightarrow E_8$, we obtain the half-hypers. We perform the resolutions of such singular Calabi-Yau three-folds. We obtain the intersection diagrams for such singularities. We also discuss the relation between the incomplete and complete resolutions.

Contents

1	Introduction	6
2	Basics of F-theory	11
2.1	Type IIB superstring theory and 7-branes	11
2.2	Elliptic fibrations and Weierstrass forms	16
2.3	Discriminant loci and $[p, q]$ -branes	19
2.4	Relations to M-theory	22
3	Enhancement of Gauge Symmetries and String Junctions	25
3.1	The Kodaira classification	25
3.2	String junctions and gauge enhancement	27
3.3	Self-intersection numbers of string junctions	30
3.4	Root systems and string junctions	33
3.4.1	An example: E_6	33
4	A dessin on the base	36
4.1	What is an elliptic point plane?	36
4.2	Relation to “dessin d’enfant” of Grothendieck	42
4.3	Basic properties of elliptic point planes	44
4.3.1	Basic properties of \mathbf{f} -planes	44
4.3.2	Basic properties of \mathbf{g} -planes	45
4.4	Simple method to compute the monodromy using the dessin	46

4.4.1	The method	46
4.4.2	Example: Monodromies of $N_f = 4$ $SU(2)$ Seiberg-Witten curves . . .	51
4.4.3	(p, q) -brane as an effective description	52
5	Higher-codimension singularities	57
5.1	Matters in F-theory	57
5.1.1	An example: $I_2 \rightarrow I_3$	59
5.1.2	Dual heterotic theory	61
5.2	Resolutions of Calabi-Yau four-folds from gauge theories	66
6	Half-hypermultiplets and incomplete/complete resolutions	71
6.1	Half-hypermultiplets in six-dimensional F-theory	71
6.1.1	$SU(6)$	72
6.1.2	$SO(12)$	74
6.1.3	E_7	75
6.2	Incomplete resolution: $D_6 \rightarrow E_7$	75
6.2.1	Blowing up p_1 first	75
6.2.2	Exceptional curves at $s = 0$: change from a root into a weight	80
6.2.3	Blowing up q_1 first	82
6.2.4	Exceptional curves at $s = 0$: Differences from the p_1 -first case	83
6.3	Complete resolution: $D_6 \rightarrow E_7$	84
6.3.1	Blowing up p_1 first	85
6.3.2	Blowing up q_1 first	86
7	Conclusions	89
A	The string junctions of E_6	93
B	Resolutions: $E_7 \rightarrow E_8$	96
B.1	Incomplete resolution: blowing up p_2 first	96
B.2	Exceptional curves at $s = 0$	102

B.3 Complete resolution: blow up p_2 first 103

Chapter 1

Introduction

In 1996, Vafa proposed F-theory [1]¹, which is a non-perturbative description of compactified type IIB superstring theory with 7-branes. Type IIB superstring theory has self S -duality [3]. This is a strong-weak duality since roughly speaking, S -duality maps a coupling constant g_s to $1/g_s$. S -duality in type IIB superstring theory plays a central role in the construction of F-theory.

S -duality appears in various places in physics. Historically, S -duality is first found in $\mathcal{N} = 4$ $SU(N)$ supersymmetric Yang-Mills (SYM) theory by Montonen and Olive [4]. $\mathcal{N}=2$ SYM theory also exhibits S -duality. The duality also plays an important role in Seiberg-Witten theory [5], which is characterized by Seiberg-Witten curve. The relation between Seiberg-Witten theory and F-theory is discussed in [6–8].

Type IIB superstring theory includes two scalars, the Ramond-Ramond (RR) 0-form C_0 and the dilaton ϕ [9]. Combining C_0 and ϕ , we can define the axio-dilaton field $\tau = C_0 + ie^{-\phi}$. The S -duality transformation converts τ to $(a\tau + b)/(c\tau + d)$, where $a, b, c, d \in \mathbb{Z}$ and $ad - bc = 1$, which is an $SL(2, \mathbb{Z})$ transformation. The transformation is identical to the modular transformation of the torus. In this sense, we can give a geometric interpretation to type IIB superstring theory, that is, we identify the axio-dilaton τ with the complex structure moduli of the torus. This is F-theory. The configuration space of the axio-dilaton field corresponds to the moduli space of the torus, which is similar to Seiberg-Witten theory.

¹We can also find good reviews [2].

In Seiberg-Witten theory, the τ that is identified to the moduli of the torus is a function of the Coulomb branch parameter.

It is sometimes said that F-theory is the twelve-dimensional theory. However, the extra two dimensions are *virtual* dimensions. This is in contrast to M-theory. In the case of M-theory, the extra one dimension is the eleventh *real* space. Indeed, the extra two dimensions in F-theory do not have the Kähler moduli. F-theory is a geometric interpretation that provides a definition of some compactifications of type IIB superstring theory.

The concrete description of F-theory is established as follows: We consider a torus with the complex moduli that depends on the coordinates of a compact subspace B of the ten-dimensional space-time. Combining B with the torus, the total manifold Y is described by an elliptic fibration. We call it the compactification of F-theory on Y . When B is n -dimensional complex manifold, we denote it as B_n , Y becomes $(n + 1)$ complex manifold, we denote as Y_{n+1} . In the language of type IIB superstring theory, it is a compactification on the manifold B_n with the non-trivial axio-dilaton background field that depends on the coordinates of B_n , namely,

$$\text{F}/Y_{n+1} \leftrightarrow \text{IIB}/B_n.$$

Supersymmetry requires that the first Chern class of Y_{n+1} needs to vanish, which means that Y_{n+1} is a Calabi-Yau manifold [10, 11]. For example, the base space B_n is P^1 when Y_{n+1} is a K3 manifold.

Existence of the axio-dilaton background field, which is a complex scalar field, implies the existence of 7-branes. Due to S -duality, 7-branes have not only RR charges but also Neveu-Schwarz-Neveu-Schwarz (NSNS) charges. The axio-dilaton field has non-trivial monodromies around singular points, which correspond to the positions of 7-branes. In the context of F-theory, the positions are points where the fibered torus shrinks. When we place all 7-branes in different points, the torus becomes singular, but the total space Y_{n+1} is not singular.

At a stack of 7-branes, not only the fibered torus but also total space becomes singular. The gauge symmetry enhances on the world-volume of the 7-brane stack. Information of the gauge symmetry is translated to the fiber type of the codimension-one singularities in F-theory. Such singularities are classified by Kodaira. In particular, the fiber types of IV^* ,

III^* and II^* are remarkable since the corresponding gauge symmetries are E_6 , E_7 and E_8 , respectively. If we have only D-branes (and orientifold planes), such exceptional groups do not appear. Indeed, we cannot construct the exceptional groups in type IIB compactifications. It is one of the advantages of F-theory that we can realize the exceptional groups.

In this thesis, we will review the relation between enhancement of the gauge symmetries and singularities of geometry. The fiber type of a codimension-one singularity can be labeled by the $SL(2, \mathbb{Z})$ monodromy around the fiber. It was shown that all types of Kodaira fibers can be represented by some product of monodromies of a basic set of 7-branes: $\mathbf{A} = [1, 0]$ -brane = D-brane, $\mathbf{B} = [1, 1]$ -brane and $\mathbf{C} = [1, -1]$ -brane, where a $[p, q]$ -brane is a 7-brane with p RR charges and q NSNS charges. The gauge symmetry on a coalescence of 7-branes has been clearly explained by using string junctions [12–28]. String junctions are also useful to describe chiral matter [29], non-simply laced Lie algebras [30], i.e., B_n , C_n , F_4 and G_2 types of simple Lie algebra, the Mordell-Weil lattice of a rational elliptic surface [31] and deformations of algebraic varieties [32, 33].

An elliptic fibration K3 manifold or a rational elliptic surface is defined by the Weierstrass equation, $y^2 = x^3 + fx + g$, where f and g depend on the coordinates of the base space P^1 . The positions of 7-branes are given by the discriminant locus, $\Delta = 0$, where $\Delta = 4f^3 + 27g^2$. One of the purposes of this thesis is that one investigates the role of the locus of $f = 0$ and $g = 0$ [34, 35]. We will identify the loci with the two kinds of critical points of a dessin d'enfant of Grothendieck. The base space P^1 is divided into several cell regions bounded by some domain walls extending from these planes and D-branes. This corresponds to drawing a dessin with a canonical triangulation. We also study how the locus of $f = 0$ and $g = 0$ and the cell regions depend on monodromies.

Perhaps the field of string phenomenology is the best place where F-theory fulfills its potential [36–52]. One readily realizes the $SU(5)$ grand unified theory (GUT), which can naturally explain the apparently complicated assignment of hypercharges to quarks and leptons, in F-theory. Moreover, F-theory also has good compatibility to the GUT with the exceptional gauge groups since the exceptional gauge groups, e.g. E_6 , naturally emerge in F-theory as we saw above.

In order to understand the relation between geometries and realized theories, we need to go beyond the Kodaira classification that associates with codimension-one singularities. Let us consider a F-theory compactification on an elliptic fibration singular Calabi-Yau four-fold. This compactification provide us a four-dimensional theory. The Calabi-Yau four-fold has not only codimension-one singularities but also codimension-two and three singularities. As we saw, information of a gauge symmetry is translated to the types of the codimension-one singularities. The data of the matter representations in four dimensions are encoded to the codimension-two singularities [53–60]. In addition, the codimension-three singularities correspond to the Yukawa coupling in the four-dimensional theory [37, 38, 61, 62].

Unfortunately, there is no a complete classification of the codimension-two and three singularities. This is a big problem in mathematics and physics. However, we can analyze some specific cases. In this thesis, we will review the case of a Calabi-Yau three-fold that is the elliptic fibration over the Hirzebruch surface. In this case, we can classify the singularities by Tate’s algorithm [55].

In addition, we can investigate resolutions of Calabi-Yau four-folds via the Coulomb branch of three-dimensional $\mathcal{N} = 2$ SYM theories [63, 64] [65–68]. This is motivated by the duality between F-theory and M-theory. The Coulomb branch is separated into some phases, and each phase corresponds to the different resolutions. As an example, we will analyze $SU(5)$ gauge group, and we will obtain a network of the resolutions of the Calabi-Yau four-fold.

For Calabi-Yau three-folds, the matters are the hypermultiplets in six-dimensions, which localize at the condimension-two singularities. The hypermultiplets are typically full-hypers, but in special cases half-hypers [53–55, 57, 60]. When the enhancements of the symmetries are $SU(6) \rightarrow E_6$, $SO(12) \rightarrow E_7$ and $E_7 \rightarrow E_8$, we obtain the half-hypers under some conditions. We will consider the resolutions of such singular Calabi-Yau three-folds. The first case was performed by Morrison and Taylor [57]. In the first case, we do not need small resolutions when we have the half-hypers. This is called the incomplete resolution. We focus on the second and third cases. We will find the same structure from the explicit resolutions of $SO(12) \rightarrow E_7$ and $E_7 \rightarrow E_8$ [69].

The organization of this thesis is as follows: In Chapter 2, we review basics of F-theory.

We start with type IIB superstring theory, and we introduce the idea of F-theory. We also provide some mathematical facts. We see that a discriminant locus of a Weierstrass form corresponds to a position of a 7-brane. In the last section of this chapter, we consider the duality between F-theory and M-theory. In Chapter 3, we consider codimension-one singularities. Singularity types are classified by Kodaira classification. We see that not only SU and SO gauge symmetry but also E type gauge symmetry appear. In addition, we introduce string junctions. The gauge enhancements can be interpreted as the possible string junctions under some conditions. In Chapter 4, we focus on the locus of $f = 0$ and $g = 0$ in the Weierstrass form. This is one of the main part of this thesis. We point out that they correspond to the two kinds of critical points of a dessin d'enfant of Grothendieck. We also provide simple method for computing a monodromy matrix for an arbitrary path by tracing the walls it goes through. In Chapter 5, we investigate higher-codimension singularities. We see that matter fields emerge when we have codimension-two singularities. We also analyze phases of resolutions of a Calabi-Yau four-fold by using three-dimensional supersymmetric gauge theories. In Chapter 6, we perform the resolutions for some special cases. When the gauge enhancements are $SU(6) \rightarrow E_6$, $SO(12) \rightarrow E_7$ and $E_7 \rightarrow E_8$, the half-hypers emerge under some conditions. We consider the case of $SO(12) \rightarrow E_7$ in this chapter. In Appendix A, we show the explicit solutions to E_6 string junctions. There are 72 solutions in the table. In Appendix B, we perform the resolution for the case of $E_7 \rightarrow E_8$. We consider the both the incomplete resolution and the complete resolution.

Chapter 2

Basics of F-theory

F-theory describes a non-perturbative expression of compactifications of type IIB superstring theory with 7-branes [1, 53, 54, 70–73]. Due to S -duality, there are not only D7-branes but also general $[p, q]$ -7-branes. We have twenty-four 7-branes if we require compactness of the internal space. F-theory is established by identifying the complex axio-dilaton field in type IIB superstring theory with the complex structure moduli of the torus. The compact space of F-theory needs to be Calabi-Yau elliptic fibrations, which is represented by the Weierstrass equation. We can obtain the complex structure moduli τ via the Jacobi J -function. The positions of the 7-branes correspond to the discriminant locus of the Weierstrass equation.

2.1 Type IIB superstring theory and 7-branes

We start with ten-dimensional $\mathcal{N} = (2, 0)$ supergravity theory which is the low energy effective theory of type IIB superstring theory. The action in the string frame are given by

$$\begin{aligned} S_{\text{string}} = & \frac{1}{2\kappa_{10}^2} \int d^{10}x e^{-2\phi} \sqrt{-g} (R + 4g^{MN} \partial_M \phi \partial_N \phi) - \frac{1}{4\kappa_{10}^2} \int e^{-2\phi} H_3 \wedge *H_3 \\ & - \frac{1}{8\kappa_{10}^2} \int F_1 \wedge *F_1 - \frac{1}{8\kappa_{10}^2} \int F_3 \wedge *F_3 - \frac{1}{8\kappa_{10}^2} \int F_5 \wedge *F_5 - \frac{1}{8\kappa_{10}^2} \int F_7 \wedge *F_7 \\ & - \frac{1}{8\kappa_{10}^2} \int F_9 \wedge *F_9 - \frac{1}{4\kappa_{10}^2} \int C_4 \wedge H_3 \wedge F_3 \\ & + (\text{fermionic terms}), \end{aligned} \tag{2.1.1}$$

where $\kappa_{10}^2 = 8\pi G_{10}$ is the ten-dimensional Newton constant, and $M, N = 0, 1, 2, \dots, 9$ are the indices of the ten-dimensional space-time. In string theory, the constant is given by

$$\frac{1}{2\kappa_{10}^2} = \frac{2\pi}{\ell_s^8}, \quad (2.1.2)$$

where $\ell_s = 2\pi\sqrt{\alpha'}$ is the string length. In this thesis, we choose $\ell_s^8 = 2\pi$. The field strengths in (2.1.1) are defined as

$$\begin{aligned} H_3 &= dB_2, & F_1 &= dC_0, & F_3 &= dC_2 - C_0 dB_2, \\ F_5 &= dC_4 - \frac{1}{2}C_2 \wedge dB_2 + \frac{1}{2}B_2 \wedge dC_2, & F_9 &= *F_1, & F_7 &= -*F_3, \end{aligned} \quad (2.1.3)$$

where C_p ($p = 0, 2, 4$) is the RR p -form and B_2 is the NSNS 2-form. ϕ is the dilaton field, which provides the string coupling constant:

$$g_s = e^\phi. \quad (2.1.4)$$

In addition, we must impose the duality relation at the level of the equation of motions:

$$F_5 = *F_5. \quad (2.1.5)$$

The action in the string frame is convenient when we consider the theory of the string world-sheet. On the other hand, we usually use the Einstein frame when we work on gravity theories. The action in the Einstein frame is given by the transformation for the metric,

$$g_{MN} \rightarrow e^{\phi/2} g_{MN}. \quad (2.1.6)$$

We introduce the combined field

$$\tau = C_0 + ie^{-\phi}, \quad (2.1.7)$$

which is called the complex axio-dilaton field. By using equations (2.1.6) and (2.1.7), we obtain the action in the Einstein frame

$$\begin{aligned} S_{\text{Einstein}} &= \int d^{10}x \sqrt{-g} \left(R - \frac{1}{2} g^{MN} \frac{\partial_M \tau \partial_N \bar{\tau}}{(\text{Im } \tau)^2} \right) - \frac{1}{2} \int (\text{Im } \tau)^2 H_3 \wedge *H_3 \\ &\quad - \frac{1}{4} \int F_3 \wedge *F_3 - \frac{1}{4} \int F_5 \wedge *F_5 - \frac{1}{4} \int F_7 \wedge *F_7 - \frac{1}{2} \int C_4 \wedge H_3 \wedge F_3 \\ &\quad + (\text{fermionic terms}). \end{aligned} \quad (2.1.8)$$

This action is invariant under $SL(2, \mathbb{Z})$ transformations

$$\begin{aligned} \tau &\rightarrow \frac{a\tau + b}{c\tau + d}, \quad \begin{pmatrix} C_2 \\ B_2 \end{pmatrix} \rightarrow M \begin{pmatrix} C_2 \\ B_2 \end{pmatrix}, \quad C_4 \rightarrow C_4 \\ g_{MN} &\rightarrow g_{MN} \quad M = \begin{pmatrix} a & b \\ c & d \end{pmatrix}, \end{aligned} \quad (2.1.9)$$

where $ad - bc = 1$ so that $M \in SL(2, \mathbb{Z})$ ¹. In particular, when we choose

$$M = \begin{pmatrix} 0 & -1 \\ 1 & 0 \end{pmatrix}, \quad (2.1.10)$$

then the τ transforms as

$$\tau \rightarrow -\frac{1}{\tau}. \quad (2.1.11)$$

From the definition of the τ (2.1.7), the imaginary part of the τ gives the inverse of the string coupling constant, $1/g_s$. Therefore, the $SL(2, \mathbb{Z})$ transformation (2.1.10) maps a strong coupling to a weak coupling, and vice versa. In this sense, S -duality is a strong-weak duality.

We construct a D7-brane solution. D7-branes couple to the RR 8-form. In other words, D7-branes are the magnetic source of the RR 0-form C_0 , which is the magnetic dual of C_8 . Since the D7-brane is the complex codimension-one object, we demand that all of the fields depend on the coordinates x^8 and x^9 , and we introduce the complex coordinate $z = x^8 + ix^9$. The Bianchi identity of F_9 in the existence of one D7-brane provide us

$$\oint_{S^1} *F_9 = \oint_{S^1} dC_0 = 1, \quad (2.1.12)$$

where we use that one D7-brane has one RR charge. The S^1 is a contour around the D7-brane in the (x^8, x^9) -plane.

In order to find the D7-brane solution, we set

$$B_2 = C_2 = C_4 = 0. \quad (2.1.13)$$

In addition, we also require that the vacuum expectation value (VEV) of all the fermions vanish. Under these constraints, the action becomes

$$S_{\text{Einstein}} = \int d^{10}x \sqrt{-g} \left(R - \frac{1}{2} g^{ij} \frac{\partial_i \tau \partial_j \bar{\tau}}{(\text{Im } \tau)^2} \right), \quad (2.1.14)$$

¹More precisely, the action is invariant under $SL(2, \mathbb{R})$ transformation. Due to the non-perturbative effects, the $SL(2, \mathbb{R})$ symmetry breaks to $SL(2, \mathbb{Z})$.

where $i, j = 8, 9$. We set the ansatz for the metric

$$ds^2 = \eta_{\mu\nu} dx^\mu dx^\nu + e^{\varphi(z, \bar{z})} dz d\bar{z}, \quad (2.1.15)$$

where $\mu, \nu = 0, 1, \dots, 7$ and $\eta_{\mu\nu} = \text{diag.}(-1, +1, \dots, +1)$. From the equation of motion of the $\bar{\tau}$, we obtain

$$\partial \bar{\partial} \tau = \frac{2}{\tau - \bar{\tau}} \partial \tau \bar{\partial} \tau, \quad (2.1.16)$$

where $\partial = \partial_z$ and $\bar{\partial} = \partial_{\bar{z}}$. Besides, the Einstein equation yields the two equations:

$$\partial \tau \partial \bar{\tau} - \bar{\partial} \tau \bar{\partial} \bar{\tau} = 0, \quad (2.1.17)$$

$$\partial \bar{\partial} \varphi = \frac{1}{(\tau - \bar{\tau})^2} (\partial \tau \bar{\partial} \bar{\tau} + \bar{\partial} \tau \partial \bar{\tau}). \quad (2.1.18)$$

The first equation (2.1.17) is given by the (89) component of the Einstein equation. The second equation (2.1.18) is presented by (aa) component of the Einstein equation, $a = 1, 2, \dots, 7$.

As a solution to (2.1.16) and (2.1.17), we take a holomorphic function², namely,

$$\bar{\partial} \tau = 0. \quad (2.1.19)$$

From the Bianchi identity (2.1.12), we can determine

$$\tau(z) = \frac{1}{2\pi i} \ln(z - z_0) + (\text{terms regular at } z_0), \quad (2.1.20)$$

where z_0 is the position of the D7-brane. Encircling z_0 , which means $(z - z_0) \rightarrow e^{2\pi i}(z - z_0)$, the $\tau(z)$ transform as

$$\tau \rightarrow \tau + 1 \quad (2.1.21)$$

since the $\tau(z)$ has the logarithmic term. The behavior under this transformation is called monodromy. The origin of monodromy is the $SL(2, \mathbb{Z})$ duality in type IIB superstring theory. Indeed, the monodromy around D7-brane (2.1.21) is generated by

$$M = \begin{pmatrix} 1 & 1 \\ 0 & 1 \end{pmatrix}, \quad (2.1.22)$$

²The D7-brane is a half BPS solution. We can derive this holomorphic condition from the requirement of supersymmetry [74].

where the matrix M is defined in (2.1.9).

Next, we would like to find the solution of the multiple 7-branes. We choose that the $\tau(z)$ is a holomorphic function again. Inserting the holomorphic function $\tau(z)$ into (2.1.18), we obtain

$$\partial\bar{\partial}\varphi = \frac{\partial\tau\bar{\partial}\bar{\tau}}{(\tau - \bar{\tau})^2} = \partial\bar{\partial}\ln\tau_2, \quad (2.1.23)$$

where $\tau_2 = \text{Im } \tau$. The general solution of this equation is given by

$$\varphi(z, \bar{z}) = \ln\tau_2(z, \bar{z}) + F(z) + \bar{F}(\bar{z}), \quad (2.1.24)$$

identically,

$$e^{\varphi(z, \bar{z})} = \tau_2(z, \bar{z})f(z)\bar{f}(\bar{z}), \quad (2.1.25)$$

where $F(z) = \ln f(z)$ is an arbitrary holomorphic function. We require modular invariance of $\varphi(z, \bar{z})$. With $\tau_2(z, \bar{z})$, we can construct a modular invariant combination

$$\tau_2(z, \bar{z})|\eta(\tau)|^4, \quad (2.1.26)$$

where $\eta(\tau)$ is Dedekind's η -function that is defined as

$$\eta(\tau) = q^{1/24} \prod_{n=1}^{\infty} (1 - q^n) \quad (2.1.27)$$

with $q = e^{2\pi i\tau}$. In addition, we also require that $e^{\varphi(z, \bar{z})}$ is non-vanish at everywhere. Using the one brane solution (2.1.20), we have $q \sim z - z_i$ near the positions of 7-branes z_i . The combination (2.1.26) becomes

$$\tau_2|\eta(\tau)|^4 \sim \tau_2 \left| (z - z_i)^{1/24} \right|^4, \quad (2.1.28)$$

near the $z \sim z_i$. Immediately, we see that the modular invariant combination (2.1.26) vanishes at the positions of 7-branes, $z = z_i$. In order to avoid this, we need to multiply the combination by

$$\left| \prod_{i=1}^N \left(\frac{1}{z - z_i} \right)^{1/24} \right|^4, \quad (2.1.29)$$

where N is the number of the 7-branes. Consequently, we find the multiple 7-branes solution of $\varphi(z, \bar{z})$:

$$e^{\varphi(z, \bar{z})} = \tau_2(z, \bar{z}) |\eta(\tau(z))|^4 \left| \prod_{i=1}^N \left(\frac{1}{z - z_i} \right)^{1/24} \right|^4. \quad (2.1.30)$$

We consider the behavior of the metric at infinity. At $|z| \rightarrow \infty$, we have

$$e^{\varphi(z, \bar{z})} \sim (z\bar{z})^{-N/12}, \quad (2.1.31)$$

since $\tau(z) \rightarrow \text{const.}$, thus the metric of the z -plane is given by

$$ds^2 \sim (z\bar{z})^{-N/12} dzd\bar{z} = dwd\bar{w} \quad (2.1.32)$$

where $w = z^{1-N/12}$. This expression imply that we have the deficit angle of $2\pi N/12$ around infinity. As a result, if we demand that the z -plane is compact, namely P^1 , N needs to be 24.

2.2 Elliptic fibrations and Weierstrass forms

The complex axio-dilaton field τ is transformed as

$$\tau \rightarrow \frac{a\tau + b}{c\tau + d}, \quad \begin{pmatrix} a & b \\ c & d \end{pmatrix} \in SL(2, \mathbb{Z}), \quad (2.2.1)$$

under the $SL(2, \mathbb{Z})$ duality. This transformation is identical to the transformation of the complex structure moduli of the torus. In order to establish F-theory, we identify the complex axio-dilaton field with the complex structure moduli of the torus. The axio-dilaton field depends on the coordinates of the compact space in type IIB superstring theory. In F-theory, compact spaces are described by elliptic fibrations.

We describe an elliptic curve³ as a hypersurface in the weighted projective space $WCP^2(2, 3, 1)$. The weighted projective space is a generalization of projective space. We denote the homogeneous coordinates of $WCP^2(2, 3, 1)$ as $(X : Y : Z)$. The identification of the coordinates is given by

$$(X, Y, Z) \sim (\lambda^2 X, \lambda^3 Y, \lambda Z), \quad (2.2.2)$$

³An elliptic curve is defined as a torus with the origin.

where $\lambda \in \mathbb{C}^* = \mathbb{C} - \{0\}$. We define the Weierstrass form as

$$P_W = Y^2 - X^3 - fXZ^4 - gZ^6, \quad (2.2.3)$$

where f and g are the parameters of torus. The elliptic curve is described as the zero-locus of the Weierstrass form P_W . In particular, when we choose the inhomogeneous coordinates as

$$x = \frac{X}{Z^2}, \quad y = \frac{Y}{Z^3}, \quad (2.2.4)$$

then the Weierstrass equation is expressed as

$$y^2 = x^3 + fx + g. \quad (2.2.5)$$

We can compute the complex structure moduli of the torus from the Weierstrass equation (or the Weierstrass form). The moduli τ is given by

$$\tau = \frac{\oint_{\beta} \omega}{\oint_{\alpha} \omega}, \quad \omega = \frac{dx}{y}, \quad (2.2.6)$$

where α and β represent the one-cycles of the elliptic curve. The ω is the holomorphic one-form on the elliptic curve⁴.

Next, we consider the elliptic fibrations:

$$\begin{array}{ccc} \pi : \mathbb{E}_\tau & \rightarrow & Y_{n+1} \\ & & \downarrow \\ & & B_n \end{array} \quad (2.2.7)$$

where \mathbb{E}_τ is an elliptic curve and B_n is a complex n -dimensional base space. When type IIB superstring theory is compactified on B_n , F-theory is compactified on Y_{n+1} . We can regard the elliptic fibration Y_{n+1} as the holomorphic line bundle \mathcal{L} over B_n (with a choice of sections). The first Chern class of Y_{n+1} is given by

$$c_1(Y_{n+1}) = c_1(B_n) - c_1(\mathcal{L}). \quad (2.2.8)$$

On the other hand, supersymmetry and the Einstein equation provide the relation [11]

$$c_1(B_n) = c_1(\mathcal{L}). \quad (2.2.9)$$

⁴In Seiberg-Witten theory, the ω is called Seiberg-Witten differential [5].

As a result, we have $c_1(Y_{n+1}) = 0$, which means Y_{n+1} is a Calabi-Yau manifold.

We focus on the $n = 1$ case. Y_2 is the two-dimensional Calabi-Yau manifold, namely, the K3 manifold. The base space B_1 becomes P^1 . We denote the coordinates of P^1 as z . The elliptic fibered K3 manifold is described by the Weierstrass equation,

$$y^2 = x^3 + f(z)x + g(z), \quad (2.2.10)$$

where $f(z)$ and $g(z)$ are the order eight and twelve polynomial of the z , respectively.

In order to obtain the τ from the Weierstrass equation (2.2.10), we introduce the Jacobi J -function:

$$J(\tau) = \frac{(\vartheta_2(\tau)^8 + \vartheta_3(\tau)^8 + \vartheta_4(\tau)^8)^3}{54\vartheta_2(\tau)^8\vartheta_3(\tau)^8\vartheta_4(\tau)^8}, \quad (2.2.11)$$

where the ϑ constants are defined as

$$\begin{aligned} \vartheta_2(\tau) &= \vartheta_2(0|\tau) = 2q^{1/8} \prod_{m=1}^{\infty} (1 - q^m) (1 + q^m)^2, \\ \vartheta_3(\tau) &= \vartheta_3(0|\tau) = \prod_{m=1}^{\infty} (1 - q^m) \left(1 + q^{m-1/2}\right)^2, \\ \vartheta_4(\tau) &= \vartheta_4(0|\tau) = \prod_{m=1}^{\infty} (1 - q^m) \left(1 - q^{m-1/2}\right)^2, \end{aligned} \quad (2.2.12)$$

with $q = e^{2\pi i\tau}$. The properties of the Jacobi J -function are as follows:

- The J -function is invariant under the modular transformations.
- The J -function is the one-to-one mapping of the fundamental domain into \mathbb{C} , and of the region $\text{Re } \tau < 0$ in the fundamental domain into the upper half-plane \mathbb{H} . The specific values $\tau = e^{2\pi i/3}, i, i\infty$ correspond to $J = 0, 1, \infty$, respectively.
- In the limit $q \rightarrow 0$, the asymptotic form of the J -function is

$$J(\tau) \rightarrow \left(\frac{1}{12}\right)^3 e^{2\pi\tau_2 - 2\pi i\tau_1}, \quad (2.2.13)$$

where $\tau_1 = \text{Re } \tau$ and $\tau_2 = \text{Im } \tau$.

We provide the procedure that read off a modular transformation of τ from a value of the J -function. For this purpose, we expand the second property. The J -function is one-to-one mapping of the fundamental domain into \mathbb{C} , while the function is one-to-many of the upper half-plane \mathbb{H} into \mathbb{C} . Since the J -function is the modular invariant, a value of the J -function of course goes back to the same value after the modular transformation. However, the trajectory of the values of the J -function depends on the modular transformation. As an example, let us consider T -transformation,

$$T : \tau \rightarrow \tau + 1. \quad (2.2.14)$$

For simplicity, we start from a point in the fundamental domain with $\text{Re } \tau < 0$. The point is mapped onto a point in the upper half-plane of the space of the J -function. Under the T -transformation (2.2.14), the value of τ crosses the line $(i, i\infty)$ and $(e^{2\pi i/3}, i\infty)$ in order. Correspondingly, the point in the space of the J -function crosses the line $(1, \infty)$ and $(\infty, 0)$ in order. Similarly, under the S -transformation,

$$S : \tau \rightarrow -\frac{1}{\tau}, \quad (2.2.15)$$

the point in the space of the J -function crosses the line $(1, \infty)$ and $(0, 1)$ in order. This method will be important in the later section.

2.3 Discriminant loci and $[p, q]$ -branes

In terms of $f(z)$ and $g(z)$ in the Weierstrass equation, the J -function (2.2.11) is given by

$$J(\tau(z)) = \frac{4f(z)^3}{4f(z)^3 + 27g(z)^2}. \quad (2.3.1)$$

Solving the equation for the τ , we obtain the $\tau(z)$ as the function of z . The $\tau(z)$ goes to $i\infty$ at the position of the 7-branes. This point corresponds to $J(\tau) = \infty$. Therefore, in terms of the Weierstrass equation, the positions of the 7-branes are given by

$$\Delta(z) = 0, \quad \Delta(z) = 4f(z)^3 + 27g(z)^2, \quad (2.3.2)$$

where the $\Delta(z)$ is called the discriminant. For the K3 manifold, $f(z)$ and $g(z)$ are the order eight and twelve polynomials of z , respectively. Hence, the discriminant locus $\Delta(z) = 0$ has

the twenty-four solutions in general, which means that there exist the twenty-four 7-branes. This is consistent with the previous section.

Note that the discriminant locus $\Delta(z) = 0$ is also the positions where the elliptic fiber becomes singular. The partial derivatives of Weierstrass form with respect to x and y vanish at the points where the elliptic fiber is singular:

$$3x^2 + f(z) = 0, \quad (2.3.3)$$

$$y = 0. \quad (2.3.4)$$

Inserting the two equations (2.3.3) and (2.3.4) to the Weierstrass equation (2.2.10), we have

$$2f(z)x + 3g(z) = 0. \quad (2.3.5)$$

We insert this equation to (2.3.3), so that we obtain

$$4f(z)^3 + 27g(z)^2 = 0, \quad (2.3.6)$$

where we assume $x \neq 0$ at the points of the singular torus. If $x = 0$ at the position of the singular torus, we have $f = 0$. Together with the Weierstrass equation, (2.3.6) is also satisfied when $x = 0$. As a result, we see the discriminant locus $\Delta(z) = 0$ is also the positions where the elliptic fiber becomes singular.

The 7-branes are classified by the monodromies around itself. As we saw in (2.1.21), the D7-brane has the monodromy $\tau \rightarrow \tau + 1$. If a 7-brane has the other monodromy, it is no longer the D7-brane. In order to label the 7-branes, we consider (p, q) -strings, which have the p NSNS charges and the q RR charges. We can obtain the (p, q) -string as the $SL(2, \mathbb{Z})$ transformation of the fundamental string (F1-string) or the D1-string. In other words, the (p, q) -string is the bound state of the p F1-strings and the q D1-strings. We define $[p, q]$ -branes. We can attach the (p, q) -string to $[p, q]$ -brane. In this notation, the D7-brane is denoted as the $[1, 0]$ -brane. The monodromy matrix of the $[1, 0]$ -brane is given by

$$M_{[1,0]} = \begin{pmatrix} 1 & 1 \\ 0 & 1 \end{pmatrix}. \quad (2.3.7)$$

Let us consider the relation between the general (p, q) -string and its monodromy matrix $M_{[p,q]}$. The gauge field on the theory of the world-volume of the 7-brane couples to the

NSNS two-form B_2 and the RR two-form C_2 at the point where the (p, q) -string is attached. Thereby we have a term

$$\int (q, p) \begin{pmatrix} C_2 \\ B_2 \end{pmatrix} \wedge *F, \quad (2.3.8)$$

where F is the two-form field strength and $*$ means the eight-dimensional Hodge dual. We require that the term is invariant under the monodromy transformation. Since the RR and NSNS two-forms transform as

$$\begin{pmatrix} C_2 \\ B_2 \end{pmatrix} \rightarrow M \begin{pmatrix} C_2 \\ B_2 \end{pmatrix} \quad (2.3.9)$$

under the $SL(2, \mathbb{Z})$ duality, we demand

$$(q, p)M = (q, p). \quad (2.3.10)$$

The solution to this equation is given by

$$M_{[p, q]} = \begin{pmatrix} 1 + pq & p^2 \\ -q^2 & 1 - pq \end{pmatrix}. \quad (2.3.11)$$

Equivalently, we see that

$$\tilde{M}_{[p, q]} = \begin{pmatrix} 0 & 1 \\ 1 & 0 \end{pmatrix} M_{[p, q]}^T \begin{pmatrix} 0 & 1 \\ 1 & 0 \end{pmatrix} = \begin{pmatrix} 1 - pq & p^2 \\ -q^2 & 1 + pq \end{pmatrix} \quad (2.3.12)$$

satisfies

$$\tilde{M}_{[p, q]} \begin{pmatrix} p \\ q \end{pmatrix} = \begin{pmatrix} p \\ q \end{pmatrix}. \quad (2.3.13)$$

Therefore, if the 7-brane has monodromy $M_{[p, q]}$, the (p, q) -string can be attached.

Note that any $[p, q]$ -branes can be transformed into the $[1, 0]$ -brane by the $SL(2, \mathbb{Z})$ transformation

$$M_{[1, 0]} = g_{[p, q]}^{-1} M_{[p, q]} g_{[p, q]}, \quad (2.3.14)$$

where $g_{[p, q]}$ is a $SL(2, \mathbb{Z})$ element. In this sense, any single 7-brane can be thought of as single D7-brane locally. However, two or more different types of 7-branes cannot be transformed

into the $[1, 0]$ -branes simultaneously. For instance, the $[p_1, q_1]$ -brane can be transformed to $[1, 0]$ -brane by $g_{[p_1, q_1]}$, but the $[p_2, q_2]$ -brane do not become the $[1, 0]$ -brane in general:

$$g_{[p_1, q_1]}^{-1} M_{[p_1, q_1]} g_{[p_1, q_1]} = M_{[1, 0]}, \quad (2.3.15)$$

$$g_{[p_1, q_1]}^{-1} M_{[p_2, q_2]} g_{[p_1, q_1]} \neq M_{[1, 0]}. \quad (2.3.16)$$

Such non-local 7-branes cannot be brought on top of each other in a supersymmetric way in general.

2.4 Relations to M-theory

M-theory is conjectured as a strong coupling limit of type IIA superstring theory [75]. This is an eleven-dimensional theory and a low energy effective theory of M-theory is $\mathcal{N} = 1$ eleven-dimensional supergravity. The action of the supergravity is given by

$$S = \frac{1}{2\kappa_{11}^2} \int d^{11}x \left(\sqrt{-g}R - \frac{1}{2}G_4 \wedge *G_4 - \frac{1}{6}A_3 \wedge G_4 \wedge G_4 \right) + (\text{fermionic terms}), \quad (2.4.1)$$

where A_3 is a three-form gauge field and $G_4 = dA_3$. The eleven-dimensional Planck length is defined as

$$\frac{1}{2\kappa_{11}^2} = \frac{2\pi}{\ell_p^9}. \quad (2.4.2)$$

The eleven-dimensional supergravity is related to type IIA supergravity via S^1 compactification of the eleventh direction. We provide the relation between the parameters in eleven dimensions and ten dimensions:

$$\frac{R_M}{\ell_p^9} = \frac{1}{\ell_s^8 g_s^2}, \quad (2.4.3)$$

where R_M is the radius of S^1 .

There are two kind of objects in M-theory, namely, M2-branes and M5-branes. M2-branes and M5-branes are coupled to the three-form gauge field A_3 electrically and magnetically, respectively. The solutions to M2-branes are given by

$$ds_{M2}^2 = f_{M2}(r)^{-2/3} \eta_{\mu\nu} dx^\mu dx^\nu + f_{M2}(r)^{1/3} dx^i dx^i, \quad (2.4.4)$$

$$G_4 = dx^0 dx^1 dx^2 df(r)^{-1}, \quad f_{M2}(r) = 1 + \frac{32\pi^2 \ell_p^6 N_{M2}}{r^6}, \quad r^2 = x^i x^i, \quad (2.4.5)$$

where $\mu, \nu = 0, 1, 2$ and $i = 3, \dots, 10$. N_{M2} is the number of M2-branes. The solution to M5-branes are as follows:

$$ds_{M5}^2 = f_{M5}^{-1/3}(r)\eta_{\mu\nu}dx^\mu dx^\nu + f_{M5}^{2/3}(r)dx^i dx^i, \quad (2.4.6)$$

$$G_4 = \frac{\epsilon_{ijklm}}{4!}\partial_i f(r)dx^j dx^k dx^l dx^m, \quad f(r) = 1 + \frac{\pi\ell_p^3 N_{M5}}{r^3}, \quad r^2 = x^i x^i, \quad (2.4.7)$$

where $\mu, \nu = 0, \dots, 5$ and $i, j, \dots = 6, \dots, 10$. N_{M5} is the number of M5-branes.

We can find relations between M- and F-theory through T -duality between type IIA and IIB superstring theory [76]. Let us consider a M-theory compactification on T^2 with

$$T^2 = S_M \times S_A. \quad (2.4.8)$$

We denote the radiuses of S_M and S_A as R_M and R_A , respectively. When $R_M \rightarrow 0$, the theory goes to type IIA theory on S_A . The components of the metric $g_{\mu,10}$ and $g_{10,10}$ become the RR 1-form C_1 and the dilation ϕ in type IIA theory, respectively. Taking T -dual along S_A , we find type IIB theory on S_B with the radius R_B given by

$$R_B = \frac{\ell_s^2}{R_A}, \quad (2.4.9)$$

where ℓ_s is the string length. The limit $R_A \rightarrow 0$, namely, $R_B \rightarrow \infty$, corresponds to the decompactified limit of type IIB theory. The component of the C_1 along S_A dualizes to the RR 0-form C_0 in type IIB side.

As a result, M-theory on T^2 with $V = \text{vol}(T^2)$ is dual to type IIB superstring theory. The duality is summarized in Table 2.1. The S -duality in type IIB is interpreted as the modular transformation of T^2 in M-theory side.

M-theory on T^2	Type IIB on S_B^1
complex structure moduli of T^2 , τ	axio-dilaton, $\tau = C_0 + ie^{-\phi}$
volume of T^2 , V	metric, $ds^2 = \eta_{\mu\nu}dx^\mu dx^\nu + \ell_s^4/V dy^2$ with $y \simeq y + 1$

Table 2.1: The duality between M-theory and type IIB theory

Next let us consider a fiberwise duality of M-theory. We compactify M-theory on Y_{n+1} , where Y_{n+1} is an elliptic fibration over B_n . Y_{n+1} is a Calabi-Yau manifold when we require

supersymmetry. Using the fiberwise duality, M-theory on Y_{n+1} is dual to type IIB theory on $B_n \times S^1_{\mathbb{B}}$. Now we can establish M/F-theory duality. Taking limit $V \rightarrow 0$, the dual IIB theory becomes the compactification on B_n , which is the F-theory compactification on Y_{n+1} . Furthermore, M2-branes wrapped on the torus (p, q) times correspond to (p, q) -strings, which will be introduced in the next chapter, wrapped on $S^1_{\mathbb{B}}$ in IIB theory. We summarize M/F-theory duality as follows:

M-theory on Y_{n+1} with $V \rightarrow 0$	F-theory on Y_{n+1}
complex structure moduli of fibered T^2 , τ	
M2-brane wrapped on T^2 (p, q) times	(p, q) -string

Table 2.2: The duality between M-theory and F-theory

Chapter 3

Enhancement of Gauge Symmetries and String Junctions

In the previous chapter, we considered the compactification of type IIB superstring theory with 7-branes. We identified the complex axio-dilaton field to the complex structure moduli of the torus so that we construct F-theory. The positions where the 7-branes are placed correspond to the discriminant locus.

In type II superstring theory, if we have N D-branes, $U(1)^N$ gauge symmetry emerges on the world-volume of the D-branes [77]. When the N D-branes make a stack, the gauge symmetry enhances to $U(N)$. Moreover, we have also $SO(2N)$ or $Sp(2N)$ when we introduce orientifold planes (O-planes). Now there are not only D7-branes but also general 7-branes. Due to this, we expect to emerge other gauge symmetries. Indeed, we will see appearance of E type symmetry.

3.1 The Kodaira classification

We expect that the types and configuration of the 7-branes have something to do with the gauge symmetry. In the previous section, we pointed out that the J -function has the data of the 7-branes. On the other hand, the J -function decides the K3 manifold in F-theory. Thus, we expect that one can obtain information of the gauge symmetry from the geometry of the K3 manifold.

We consider stacks of 7-branes. As we saw above, the discriminant locus $\Delta(z) = 0$ has a solution at each position of single 7-brane. When the 7-branes make a stack, the discriminant locus has a multiple root at a position of the stack. At such a point, not only the fibered torus but also the total K3 manifold becomes singular. The partial derivatives of Weierstrass form with respect to x , y and z become zero at the points where the elliptic fiber is singular:

$$3x^2 + f(z) = 0, \quad (3.1.1)$$

$$y = 0, \quad (3.1.2)$$

$$f'(z)x + g'(z) = 0. \quad (3.1.3)$$

The first two equations are the same as (2.3.3) and (2.3.4), respectively. In general, we can choose the singular point to be $z = 0$. The solution to the three equations and the Weierstrass equation (2.2.10) presents the singular point of the K3 manifold. We have the two cases: $x = y = 0$ or $x \neq 0$, $y = 0$.

Firstly, we consider the case of $x = y = 0$. Due to (3.1.1), we have $f(0) = 0$, that is, $\text{ord}(f) \geq 1$. In addition, (3.1.3) means $g'(0) = 0$, thus we obtain $\text{ord}(g) \geq 2$. Consequently, for the discriminant, we find $\text{ord}(\Delta) \geq 3$.

Secondly, we consider the case of $x \neq 0$, $y = 0$. Immediately, we see $f(0) \neq 0$ from (3.1.1), that is, $\text{ord}(f) = 0$. Inserting (3.1.1) and (3.1.2) to the Weierstrass equation, we have

$$2f(0)x + 3g(0) = 0, \quad (3.1.4)$$

so that we find $g(0) \neq 0$, i.e., $\text{ord}(g) = 0$. In addition, by using (3.1.1), (3.1.3) and (3.1.4), we obtain

$$\Delta'(0) = 12f^2(0)f'(0) + 54g(0)g'(0) = 0, \quad (3.1.5)$$

thus $\text{ord}(\Delta) \geq 2$. Therefore, when the discriminant has the multiple root, namely, the 7-branes make the stack, the elliptic K3 becomes singular.

Singularities of the elliptic K3 manifold are classified by Kodaira [19]. The singularities are labeled by not only the order of the discriminant but also the orders of the $f(z)$ and $g(z)$ in the Weierstrass equation. We show the table of the Kodaira classification in Table 3.1. We also show corresponding brane configurations. This classification is derived from resolutions of singular K3 surfaces.

Fiber type	ord(f)	ord(g)	ord(Δ)	Singularity type	7-brane configuration	Brane type
I_n	0	0	n	A_{n-1}	\mathbf{A}^n	A_{n-1}
II	≥ 1	1	2	A_0	\mathbf{CA}	H_0
III	1	≥ 2	3	A_1	$\mathbf{CA}^2(= \mathbf{A}^2\mathbf{B})$	H_1
IV	≥ 2	2	4	A_2	$\mathbf{CA}^3(= \mathbf{A}^2\mathbf{BA})$	H_2
I_n^*	≥ 2	3	$6+n$	D_{n+4}	$\mathbf{A}^{n+4}\mathbf{BC}$	D_{n+4}
I_n^*	2	≥ 3	$6+n$	D_{n+4}	$\mathbf{A}^{n+4}\mathbf{BC}$	D_{n+4}
II^*	≥ 4	5	10	E_8	$\mathbf{A}^7\mathbf{BC}^2$	E_8
III^*	3	≥ 5	9	E_7	$\mathbf{A}^6\mathbf{BC}^2$	E_7
IV^*	≥ 3	4	8	E_6	$\mathbf{A}^5\mathbf{BC}^2$	E_6

Table 3.1: The Kodaira classification

3.2 String junctions and gauge enhancement

In Section 2.3, we introduced the general 7-branes, i.e., the $[p, q]$ -branes. The $[p, q]$ -brane has the monodromy $M_{[p,q]}$. The (p, q) -string is invariant under the monodromy. However, the general (r, s) -string transform under the monodromy, where $(r, s) \neq (p, q)$. In this section, we will discuss the (r, s) -string, and in order to explain the effect of the monodromy, we introduce string junctions [13–20].

We consider the (r, s) -string which encircles around the $[p, q]$ -brane. The tension of the (r, s) -string is given by

$$T_{r,s} = \frac{1}{\sqrt{\tau_2}} |r + s\tau|. \quad (3.2.1)$$

Multiplying the metric of the 7-brane solution, we find the local mass of the (r, s) -string,

$$ds_{r,s} = \left| (r + s\tau)\eta^2(\tau) \prod_i (z - z_i)^{-1/12} dz \right|. \quad (3.2.2)$$

We require that the mass is invariant under the monodromy of the $[p, q]$ -brane, so that the

(r, s) -string transforms as

$$\begin{pmatrix} r \\ s \end{pmatrix} \rightarrow \begin{pmatrix} 0 & 1 \\ 1 & 0 \end{pmatrix} M_{[p,q]}^T \begin{pmatrix} 0 & 1 \\ 1 & 0 \end{pmatrix} \begin{pmatrix} r \\ s \end{pmatrix} = \begin{pmatrix} r \\ s \end{pmatrix} + (ps - qr) \begin{pmatrix} p \\ q \end{pmatrix} \quad (3.2.3)$$

under the monodromy transformation. We introduce the cut which are extended from the 7-brane. We interpret the monodromy that the τ and the (r, s) -string are affected as the effect of the cut.

According to (3.2.1), the difference of the charges are proportional to (p, q) , which can be attached to the $[p, q]$ -brane. Due to this, we can deform the contour of the string, and we find a string junction. In other words, we can interpret the string junction as the Hanany-Witten effect [78]. The charges of the strings are conserved at the junction.

Comparing the monodromy matrix around the singularity of the K3 manifold with $M_{[p,q]}$, we can identify the fiber type in the Kodaira classification with the 7-brane configuration. The 7-brane configurations for each fiber type is summarized in Table 3.1. Here we show notation and the monodromy matrices of the **A**, **B** and **C**-branes:

$$\mathbf{A} = [1, 0]; \quad M_{[1,0]} = \begin{pmatrix} 1 & 1 \\ 0 & 1 \end{pmatrix}, \quad (3.2.4)$$

$$\mathbf{B} = [1, 1]; \quad M_{[1,1]} = \begin{pmatrix} 2 & 1 \\ -1 & 0 \end{pmatrix}, \quad (3.2.5)$$

$$\mathbf{C} = [1, -1]; \quad M_{[1,-1]} = \begin{pmatrix} 0 & 1 \\ -1 & 2 \end{pmatrix}. \quad (3.2.6)$$

For example, let us see the fiber type *III*. The Weierstrass equation of this fiber type is represented by

$$y^2 = x^3 + zx. \quad (3.2.7)$$

The monodromy matrix around this singularity is given by

$$\begin{pmatrix} 0 & 1 \\ -1 & 0 \end{pmatrix}. \quad (3.2.8)$$

From the Table 3.1, we find that the 7-brane configuration is made from two **A**-branes and a **C**-brane. Indeed, the monodromy matrix around these 7-branes agrees with (3.2.8):

$$\mathbf{CA}^2 = M_{[1,-1]} M_{[1,0]}^2 = \begin{pmatrix} 0 & 1 \\ -1 & 0 \end{pmatrix}. \quad (3.2.9)$$

Note that the notation of **A**, **B** and **C**-branes is one of the choices of the bases¹.

Next, we see the correspondence between possible string junctions and gauge enhancement. Endpoints of a string are attached to two 7-branes, and the charges of the string at the endpoints need to consist with the types of the 7-branes. Due to monodromies, the charges of the string at each endpoint are different from each other in general. In other words, this is the origin of the string junctions. There exist strings that connect two 7-branes only when the two charges agree with the types of the 7-branes, respectively. The possible strings or string junctions correspond to the adjoint representation of the enhanced gauge symmetry.

Let us see a few examples. First, we consider the fiber type I_0^* . The brane configuration consist of **AAAABC**. We see that we have the strings that connect two **A**-branes directly since the $(1,0)$ -string is invariants under the monodromy of the **A**-brane:

$$\begin{pmatrix} 0 & 1 \\ 1 & 0 \end{pmatrix} M_{[1,0]}^T \begin{pmatrix} 0 & 1 \\ 1 & 0 \end{pmatrix} \begin{pmatrix} 1 \\ 0 \end{pmatrix} = \begin{pmatrix} 1 \\ 0 \end{pmatrix}. \quad (3.2.10)$$

Hence, we can obtain $SU(4)$ gauge group from the four **A**-branes. In order to find other possible strings, we decompose $SO(8)$ into $SU(4) \times U(1)$:

$$\mathbf{28} = \mathbf{15} + \mathbf{6} + \mathbf{6} + \mathbf{1}. \quad (3.2.11)$$

The **15** representation in the right hand side corresponds to the direct paths between the two **A**-branes and the Cartan subgroup of $SU(4)$. The singlet **1** represents the rest of the Cartan of $SO(8)$. The two **6**'s are strings that connect two different **A**-branes indirectly, which means that the strings start from an **A**-brane, stride across the cuts of the **B** and the **C**-branes and finally are connected with an **A**-brane. The reason for this is that the monodromy **BC** changes only the direction of the $(1,0)$ -string, namely,

$$\begin{pmatrix} 0 & 1 \\ 1 & 0 \end{pmatrix} (\mathbf{BC})^T \begin{pmatrix} 0 & 1 \\ 1 & 0 \end{pmatrix} \begin{pmatrix} 1 \\ 0 \end{pmatrix} = \begin{pmatrix} -1 \\ 0 \end{pmatrix}. \quad (3.2.12)$$

The indirect paths can be interpreted as string junctions.

Second example is the fiber type IV^* . The brane configuration consists of five **A**-branes,

¹More precisely, any monodromy can be described only two independent matrices. For instance, the monodromy matrix of the fiber type I_0^* is given by $\mathbf{A}^4\mathbf{BC}$, and this is equal to $(\mathbf{CA})^3$.

a **B**-brane and two **C**-branes. We decompose E_6 into $SU(5) \times SU(2) \times U(1)$:

$$\begin{aligned}
\mathbf{78} = & (\mathbf{24}, \mathbf{1}) + (\mathbf{1}, \mathbf{1}) \\
& + (\mathbf{10}, \mathbf{2}) + (\mathbf{10}, \mathbf{2}) \\
& + (\mathbf{5}, \mathbf{1}) + (\mathbf{5}, \mathbf{1}) \\
& + (\mathbf{1}, \mathbf{3}).
\end{aligned} \tag{3.2.13}$$

The first line in the right hand side corresponds to direct paths between the two different **A**-branes and Cartan's. The last one is also the direct paths of **C**-branes. The second and third lines represent the indirect paths between two **A**-branes and two **C**-branes, respectively.

3.3 Self-intersection numbers of string junctions

In the previous section, we introduced string junctions. The string junctions are another representation of monodromies. We roughly saw correspondence between string junctions and a gauge symmetry. However, not all possible string junctions are allowed as BPS states. In the previous section, we saw the string junctions of the fiber type I_0^* as a example. We considered only the indirect paths that connect two different **A**-branes, but we did not allow indirect paths that connect the same **A**-brane. Indeed, such a string junction does not satisfy the BPS condition. In this section, we show the BPS condition of the string junctions.

Originally, the string junctions are conjectured by the duality between M-theory on the torus and type IIB superstring theory on the circle [79]. As we saw in Section 2.4, M2-branes that are wrapped on the two cycles of the torus (p, q) times are identified with (p, q) -strings. Considering a M2-brane solution that is dual to three (p_i, q_i) -strings ($i = 1, 2, 3$) which are jointed at a point, we can show that the tensions vanish at the jointing point when the charges are conserved.

For our purpose, we introduce the *junction* **J**. A string junction consists of $Q_{\mathbf{A}}^i$ $(1, 0)$ -strings that are connected with a i -th **A**-brane, $Q_{\mathbf{B}}^j$ $(1, -1)$ -strings that are connected with j -th **B**-brane and $Q_{\mathbf{C}}^k$ $(1, 1)$ -strings that are connected with k -th **C**-brane. We represent **A**,

B and **C**-branes as \mathbf{a}_i , \mathbf{b}_i and \mathbf{c}_i , respectively. The junction \mathbf{J} is defined as

$$\mathbf{J} = \sum_i Q_{\mathbf{A}}^i \mathbf{a}_i + \sum_j Q_{\mathbf{B}}^j \mathbf{b}_j + \sum_k Q_{\mathbf{C}}^k \mathbf{c}_k. \quad (3.3.1)$$

The BPS condition is given by the condition for the self-intersection of the junction.

We consider the self-intersection of the junction. First we define the self-intersection number of the basis strings \mathbf{a} , \mathbf{b} and \mathbf{c} as -1 ,

$$(\mathbf{a}_i, \mathbf{a}_i) = (\mathbf{b}_i, \mathbf{b}_i) = (\mathbf{c}_i, \mathbf{c}_i) = -1. \quad (3.3.2)$$

In order to define a contribution to a self-intersection number from a junction point, we consider the (r, s) -string which encircles around the $[p, q]$ -brane. The self-intersection number of this setup is of course zero. We can regard this setup as the string junction, that is, the string junction is made from $(ps - qr)$ (p, q) -strings that are attached to $[p, q]$ -brane and the junction point. The contribution to the intersection number from the former is given by $[-(ps - qr)^2]$. Since the total self-intersection number needs to be zero, the contribution from the junction point, we denote as \mathbf{J}_3 , is given by

$$(\mathbf{J}_3, \mathbf{J}_3) = \begin{vmatrix} p_i & p_{i+1} \\ q_i & q_{i+1} \end{vmatrix}, \quad (3.3.3)$$

where $i = 1, 2, 3$ are the labels of the three (p_i, q_i) -strings in the string junction. We labeled in the clockwise direction. This contribution is independent of i with $p_4 = p_1$ and $q_4 = q_1$. Now we have $(p_1, q_1) = ((ps - qr)p, (ps - qr)q)$ and $(p_2, q_2) = (r, s)$, so $(\mathbf{J}_3, \mathbf{J}_3) = (ps - qr)^2$. Therefore, the total intersection number becomes zero.

We consider $\mathbf{J} = \mathbf{a}_i + \mathbf{a}_j$ with $i \neq j$. This junction has no junction points, namely, $(\mathbf{J}_3, \mathbf{J}_3) = 0$. A contribution from the $(1, 0)$ -strings that are attached to the **A**-branes is (-2) . Since

$$-2 = (\mathbf{a}_i + \mathbf{a}_j, \mathbf{a}_i + \mathbf{a}_j) = -1 + 2(\mathbf{a}_i, \mathbf{a}_j) - 1, \quad (3.3.4)$$

we have $(\mathbf{a}_i, \mathbf{a}_j) = 0$ for $i \neq j$. Similarly, we can also find $(\mathbf{b}_i, \mathbf{b}_j) = (\mathbf{c}_i, \mathbf{c}_j) = 0$. Next we consider $\mathbf{J} = \mathbf{a} + \mathbf{b}$. The self-intersection number (\mathbf{J}, \mathbf{J}) is given by

$$(\mathbf{J}, \mathbf{J}) = (\mathbf{a}, \mathbf{a}) + (\mathbf{b}, \mathbf{b}) + \begin{vmatrix} 1 & 1 \\ 0 & -1 \end{vmatrix} = -3. \quad (3.3.5)$$

By using (\mathbf{a}, \mathbf{b}) , this is expressed as

$$-3 = (\mathbf{a} + \mathbf{b}, \mathbf{a} + \mathbf{b}) = -2 + 2(\mathbf{a}, \mathbf{b}), \quad (3.3.6)$$

thus we find $(\mathbf{a}, \mathbf{b}) = -1/2$. In the same manner, we can determine the other intersections. We conclude that

$$(\mathbf{a}_i, \mathbf{a}_j) = (\mathbf{b}_i, \mathbf{b}_j) = (\mathbf{c}_i, \mathbf{c}_j) = -\delta_{ij}, \quad (3.3.7)$$

$$(\mathbf{a}, \mathbf{b}) = -\frac{1}{2}, \quad (3.3.8)$$

$$(\mathbf{a}, \mathbf{c}) = \frac{1}{2}, \quad (3.3.9)$$

$$(\mathbf{b}, \mathbf{c}) = 1. \quad (3.3.10)$$

Therefore, we can calculate the self-intersection number of the general string junction:

$$\begin{aligned} (\mathbf{J}, \mathbf{J}) = & - \sum_{i=1}^{n_{\mathbf{A}}} (Q_{\mathbf{A}}^i) - \sum_{i=1}^{n_{\mathbf{B}}} (Q_{\mathbf{B}}^i) - \sum_{i=1}^{n_{\mathbf{C}}} (Q_{\mathbf{C}}^i) \\ & - \sum_{i=1}^{n_{\mathbf{A}}} \sum_{j=1}^{n_{\mathbf{B}}} Q_{\mathbf{A}}^i Q_{\mathbf{B}}^j + \sum_{i=1}^{n_{\mathbf{A}}} \sum_{j=1}^{n_{\mathbf{C}}} Q_{\mathbf{A}}^i Q_{\mathbf{C}}^j + 2 \sum_{i=1}^{n_{\mathbf{B}}} \sum_{j=1}^{n_{\mathbf{C}}} Q_{\mathbf{B}}^i Q_{\mathbf{C}}^j. \end{aligned} \quad (3.3.11)$$

We provide the BPS condition. The BPS condition is encoded into the condition for the self-intersection numbers of the junctions. The condition is given by

$$(\mathbf{J}, \mathbf{J}) \geq -2. \quad (3.3.12)$$

This condition is derived from the duality between M-theory on the elliptic fibration K3 and IIB theory on the S^1 fibration over P^1 . Taking the decompactified limit of S^1 , the M-theory side corresponds to the limit where the fibered torus shrinks. In this limit, the string junctions that satisfy the BPS condition correspond to the holomorphic curves J' of the K3 surface [18, 80]. The self-intersection number of such curves is given by [81, 82]

$$(J', J') = 2g - 2 + b, \quad (3.3.13)$$

where g is the genus and b is the number of boundary. As a result, we find the condition (3.3.12).

3.4 Root systems and string junctions

In the previous section, we considered the BPS condition for the string junctions. As we saw in Section 3.1, the gauge enhancements are achieved by specific 7-brane configurations that are fixed by the Kodaira classification. The gauge fields that is in the adjoint representation are derived from some string junctions. In this section, we focus on such string junctions. We identify such string junctions with the root vectors of the gauge group [13, 17].

The adjoint representation consists of the string junctions that satisfy the following conditions:

$$p = q = 0, \tag{3.4.1}$$

$$(\mathbf{J}, \mathbf{J}) = -2, \tag{3.4.2}$$

where $p = \sum_i Q_{\mathbf{A}}^i + \sum_i Q_{\mathbf{B}}^i + \sum_i Q_{\mathbf{C}}^i$ and $q = -\sum_i Q_{\mathbf{B}}^i + \sum_i Q_{\mathbf{C}}^i$, namely, (p, q) are the total charges of the string junction. The first condition implies that the charges of the string junction become zero at infinity. The second condition is derived from the dual M-theory. In the M-theory side, enhanced gauge fields come from the M2-branes which are wrapped on the holomorphic curves with $g = 0$ (and $b = 0$).

3.4.1 An example: E_6

As an example, we consider the case of E_6 . The 7-brane configuration is given by $\mathbf{A}^5\mathbf{B}\mathbf{C}^2$. We obtain the general junction \mathbf{J} ,

$$\mathbf{J} = \sum_{i=1}^5 Q_{\mathbf{A}}^i \mathbf{a}_i + Q_{\mathbf{B}} \mathbf{b} + \sum_{i=1}^2 Q_{\mathbf{C}}^i \mathbf{c}_i. \tag{3.4.3}$$

The condition (3.4.1) yields

$$\sum_{i=1}^5 Q_{\mathbf{A}}^i + Q_{\mathbf{B}} + \sum_{j=1}^2 Q_{\mathbf{C}}^j = 0, \tag{3.4.4}$$

$$-Q_{\mathbf{B}} + \sum_{j=1}^2 Q_{\mathbf{C}}^j = 0. \tag{3.4.5}$$

In addition, we have

$$-\sum_{i=1}^5 (Q_{\mathbf{A}}^i) - (Q_{\mathbf{B}}) - \sum_{j=1}^2 (Q_{\mathbf{C}}^j) - \sum_{i=1}^5 Q_{\mathbf{A}}^i Q_{\mathbf{B}} + \sum_{i=1}^5 \sum_{j=1}^2 Q_{\mathbf{A}}^i Q_{\mathbf{C}}^j + 2 \sum_{j=1}^2 Q_{\mathbf{B}} Q_{\mathbf{C}}^j = -2 \quad (3.4.6)$$

from (3.4.2). We find the 72 solutions, which correspond to the roots of E_6 . We show all solutions in Appendix A.

E_6 group has the six simple roots. The string junctions that correspond to the simple roots are

$$\begin{aligned} \vec{Q}_1 &= (1, -1, 0, 0, 0, 0, 0, 0), \\ \vec{Q}_2 &= (0, 1, -1, 0, 0, 0, 0, 0), \\ \vec{Q}_3 &= (0, 0, 1, -1, 0, 0, 0, 0), \\ \vec{Q}_4 &= (0, 0, 0, 1, 1, -1, -1, 0), \\ \vec{Q}_5 &= (0, 0, 0, 0, 0, 0, 1, -1), \\ \vec{Q}_6 &= (0, 0, 0, 1, -1, 0, 0, 0), \end{aligned} \quad (3.4.7)$$

identically,

$$\begin{aligned} \alpha_1 &= \mathbf{a}_1 - \mathbf{a}_2, \\ \alpha_2 &= \mathbf{a}_2 - \mathbf{a}_3, \\ \alpha_3 &= \mathbf{a}_3 - \mathbf{a}_4, \\ \alpha_4 &= \mathbf{a}_4 + \mathbf{a}_5 - \mathbf{b} - \mathbf{c}_1, \\ \alpha_5 &= \mathbf{c}_1 - \mathbf{c}_2, \\ \alpha_6 &= \mathbf{a}_4 - \mathbf{a}_5, \end{aligned} \quad (3.4.8)$$

where $\vec{Q}_i = (Q_{\mathbf{A}}^1, Q_{\mathbf{A}}^2, Q_{\mathbf{A}}^3, Q_{\mathbf{A}}^4, Q_{\mathbf{A}}^5, Q_{\mathbf{B}}, Q_{\mathbf{C}}^1, Q_{\mathbf{C}}^2)$. We show the string junctions in Fig 3.1. We can see that the six string junctions provide the Cartan matrix $A_{ij}(E_6)$:

$$(\alpha_i, \alpha_j) = -A_{ij}(E_6). \quad (3.4.9)$$

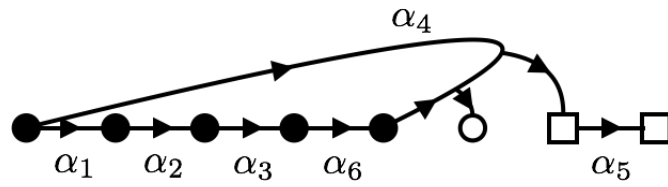


Fig. 3.1: We show the six string junctions in (3.4.7) or (3.4.8) which correspond to the simple roots of E_6 . The black circles denote the **A**-brane, the white circle is the **B**-brane and the squares are the **C**-branes.

Chapter 4

A dessin on the base

So far we considered F-theory compactifications on K3 manifolds, which are two-dimensional Calabi-Yau manifolds. This is required by the consequence of supersymmetry. The K3 surfaces are described by the Weierstrass equation (2.2.10). In this chapter, we consider a rational elliptic surface¹, which is one of the two rational elliptic surfaces arising in the stable degeneration limit of a K3 surface. The rational elliptic surface is not a Calabi-Yau manifold, but it is useful for investigating F-theory compactification. The rational elliptic surface is also described by the Weierstrass equation. In this chapter, we focus on not only the discriminant locus, $\Delta = 0$, but also the $f = 0$ and the $g = 0$ locus [34, 35].

4.1 What is an elliptic point plane?

We start with a Weierstrass equation

$$y^2 = x^3 + fx + g, \tag{4.1.1}$$

where y , x , f and g are sections of an $\mathcal{O}(3)$, an $\mathcal{O}(2)$, an $\mathcal{O}(4)$ and an $\mathcal{O}(6)$ bundle over the base P^1 . This equation defines a rational elliptic surface. We can also regard it as the total space of a Seiberg-Witten curve (with the “ u ”-plane being the base) of an $\mathcal{N} = 2$ $SU(2)$ gauge theory [5] or an E-string theory. [83–86] In an affine patch of P^1 with the coordinate z , the coefficient functions $f(z)$ and $g(z)$ are a 4th and a 6th order polynomial in z .

¹Sometimes this is called as a 1/2 K3 surface.

As is well known, the modulus τ of the elliptic fiber of (4.1.1) is given by the implicit function:

$$J(\tau) = \frac{4f^3}{4f^3 + 27g^2}, \quad (4.1.2)$$

where J is the elliptic modular function. The denominator of the right hand side

$$\Delta \equiv 4f^3 + 27g^2 \quad (4.1.3)$$

is called the discriminant. Near its zero locus $z = z_i$, $\text{Im}\tau$ goes to ∞ (if one has chosen the “standard” fundamental region) for generic (that is, nonzero) f and g . Examining the behavior of $J(\tau)$ around ∞ , we find

$$\tau(z) = \frac{1}{2\pi i} \log(z - z_i) (\text{const.} + O(z - z_i)), \quad (4.1.4)$$

which implies the existence of a D7-brane at each discriminant locus.²

On the other hand, since a locus of $f(z) = 0$ or $g(z) = 0$ alone does not mean $\Delta = 0$, it is not a D-brane. However, if the loci of $f(z) = 0$ and $g(z) = 0$ are present together with a D-brane, they play a significant role in generating a (p, q) -7-brane by acting $SL(2, \mathbb{Z})$ conjugate transformations on a D-brane or as components of an orientifold plane, as we show below. In this paper, we will collectively call the loci of $f(z) = 0$ and $g(z) = 0$ “*elliptic point planes*”.³

Elliptic point planes consist of two types, the loci of $f(z) = 0$ and $g(z) = 0$, which have different properties. In this paper, we call the locus of $f(z) = 0$ an $f=0$ *locus plane*, or an f -*plane* for short, and that of $g(z) = 0$ a $g=0$ *locus plane*, or a g -*plane* for short.⁴

At the location of an f -plane, the value of the J -function is

$$J(\tau) = \frac{4f^3}{4f^3 + 27g^2} = 0, \quad (4.1.5)$$

²Thus, henceforth in this paper, we refer to a locus of the discriminant as (a locus of) a “D-brane”. As we will see, however, the monodromy around it is not always T for a general choice of the reference point, due to the presence of the elliptic point planes.

³In the standard fundamental region of the modular group of a two-torus, there are two elliptic points $\tau = e^{\frac{2\pi i}{3}}$ and i . They are fixed points of actions of some elliptic elements of $SL(2, \mathbb{Z})$, hence the name.

⁴Despite the name “plane”, an elliptic point plane is no more a rigid object but a smooth submanifold when the elliptic fibration over \mathbb{P}^1 is further fibered over another manifold, just like a D-brane.

which corresponds to $\tau = e^{\frac{2\pi i}{3}}$. On the other hand, at the position of a g -plane ,

$$J(\tau) = \frac{4f^3}{4f^3 + 27g^2} = 1, \quad (4.1.6)$$

so this implies $\tau = i$. In their neighborhoods, $J(\tau)$ is expanded as

$$J(\tau) = \frac{1}{3!} J'''(e^{\frac{2\pi i}{3}}) (\tau - e^{\frac{2\pi i}{3}})^3 + O\left((\tau - e^{\frac{2\pi i}{3}})^4\right), \quad (4.1.7)$$

$$J(\tau) = 1 - \frac{12K\left(\frac{1}{\sqrt{2}}\right)^4}{\pi^2} (\tau - i)^2 + O((\tau - i)^3), \quad (4.1.8)$$

where $K(k)$ is the complete elliptic integral of the first kind

$$K(k) = \int_0^{\frac{\pi}{2}} \frac{d\theta}{\sqrt{1 - k^2 \sin^2 \theta}}. \quad (4.1.9)$$

Thus $\tau = e^{\frac{2\pi i}{3}}$ is a triple zero of $J(\tau)$ and $\tau = i$ is a double zero of $J(\tau) - 1$.

Suppose that $z = 0$ is a locus of $f = 0$. Since

$$J(\tau(z)) = \frac{4f(z)^3}{4f(z)^3 + 27g(z)^2}, \quad (4.1.10)$$

$J(\tau(z))$ is $O(z^3)$ at $z = 0$. So (4.1.7) shows that $\tau - e^{\frac{2\pi i}{3}}$ is $O(z)$ there, implying that the monodromy is trivial around the locus of f . Similarly, if $z = 0$ is a locus of $g = 0$, $J(\tau(z)) - 1$ is now $O(z^2)$. Comparing this with (4.1.8), we see that $\tau(z) - i$ is also $O(z)$, and hence there is no monodromy around the locus of $g = 0$, either.

However, this is not the end of the story. Fig. 4.2 shows the various choices of fundamental regions of the modulus τ and the corresponding complex plane as its image mapped by the J -function. From this we can see that if one goes around $\tau = e^{\frac{2\pi i}{3}}$ once on the upper half plane, one goes through *three* different fundamental regions to get back to the original position. Likewise if one goes around $\tau = i$, one undergoes *two* different fundamental regions. Thus an f -plane is a complex codimension-one submanifold at which three different regions on the z -plane corresponding to different fundamental regions meet, while a g -plane is similarly the place where two different regions meet. The regions on the z -plane corresponding to different fundamental regions are bounded by real codimension-one domain walls which consist of the zero loci of the imaginary part of the J -function.

Furthermore, each region on the z -plane corresponding to a definite fundamental region is divided by a domain wall

$$\{\tau \mid \text{Im}J(\tau) = 0, \text{Re}J(\tau) > 1\} \tag{4.1.11}$$

(a dashed green line) into two regions $\text{Im}J(\tau) > 0$ and $\text{Im}J(\tau) < 0$.

On the other hand, a D-brane resides at a discriminant locus $\Delta = 0$, from which two domain walls $\{\tau \mid \text{Im}J(\tau) = 0, \text{Re}J(\tau) < 0\}$ (a green line) and $\{\tau \mid \text{Im}J(\tau) = 0, \text{Re}J(\tau) > 1\}$ (a dashed green line) extend out into the bulk z space (\mathbb{P}^1) (Fig. 4.1).

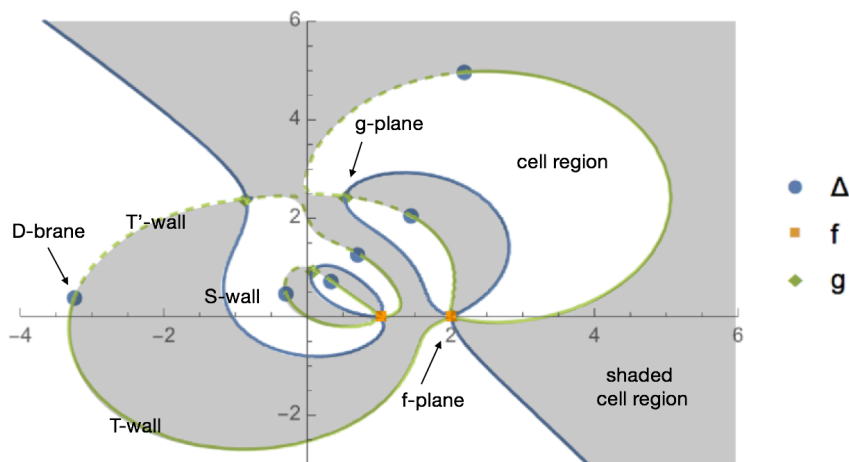


Fig. 4.1: An example configuration of D-branes, elliptic point planes and the cell regions bounded by the domain walls extended from them. D-branes are located at the loci of $\Delta = 0$, while elliptic point planes are at the loci of $f = 0$ and $g = 0$. In this example we can see two f -planes at $z = 1, 2$, three g -planes and six D-branes. (This figure is depicted for the Weierstrass equation (4.1.1) for f and g (4.4.19) with $\epsilon = 0.9$.)

Since the value of J is ∞ at a discriminant locus for generic (*i.e.* nonzero) values of f and g , D-branes can never, by definition, touch nor pass through (a non-end point of) the domain walls because $\text{Im}J(\tau)$ must vanish at the domain walls.

In this way, the z -space ($= \mathbb{P}^1$) is divided into several “*cell regions*”, which correspond to different fundamental regions in the preimage of the J -function, by the domain walls extended from the elliptic point planes ($= f$ -planes and g -planes) and D-branes (Fig. 4.1).

In particular, f -planes and g -planes extend the domain walls

$$\{\tau \mid \text{Im}J(\tau) = 0, 0 < \text{Re}J(\tau) < 1\} \quad (4.1.12)$$

(blue lines), and crossing through this wall implies that the type IIB coupling *locally gets S-dualized* (if starting from the standard choice of the fundamental region) (Fig. 4.2). Then there is a difference in monodromies between when one goes around a D-brane within a single cell region bounded by some domain walls and when one first crosses through a domain wall, moves around a D-brane and then crosses back through the wall again to the original position; they are different by an $SL(2, \mathbb{Z})$ conjugation. This is what's happening in what has been called a “**B**-brane” or a “**C**-brane” in the discussions of string junctions. That is, while the monodromy matrix is necessarily

$$T = \begin{pmatrix} 1 & 1 \\ 0 & 1 \end{pmatrix} \quad (4.1.13)$$

as long as the reference point is chosen to be in the standard fundamental region, a non-trivial (non-D-brane) (p, q) -brane arises if the monodromy is measured by going back and forth between regions corresponding to different fundamental regions in the preimage upper-half plane.

We would like to emphasize here that such a local S transformation never takes place without these “elliptic point planes” (= f -planes and g -planes). If it were not for elliptic point planes but there are only D-branes, the domain walls extended from them are only the ones

$$\{\tau \mid \text{Im}J(\tau) = 0, \text{Re}J(\tau) < 0\} \quad (4.1.14)$$

(green lines) and

$$\{\tau \mid \text{Im}J(\tau) = 0, \text{Re}J(\tau) > 1\} \quad (4.1.15)$$

(dashed green lines). So crossing through these walls only leads to a T transformation which commutes with the original monodromies of D-branes.

In the discussion below, we refer to the domain wall (4.1.14) (a green lines) as T -wall and the one (4.1.15) (a dashed green line) as T' -wall, whereas we call the type of domain wall (4.1.12) (a blue line) S -wall.

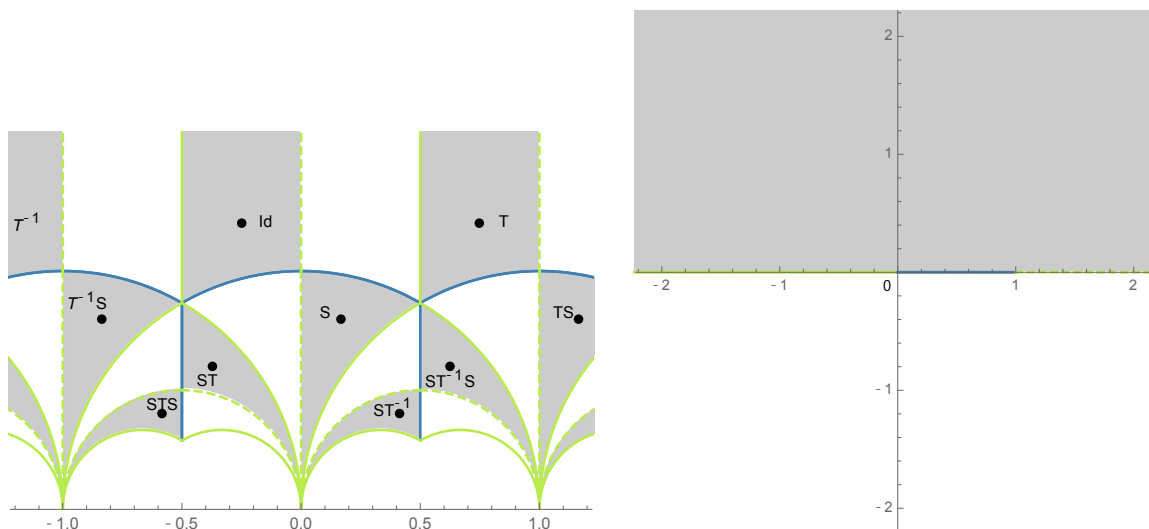


Fig. 4.2: Left: The upper half plane and various fundamental regions. The shaded regions are the regions in which the imaginary part of the image of the J -function $\text{Im}J(\tau)$ is positive. The symbol in each fundamental region (such as Id , T , S , ...) is the group element of $SL(2, \mathbb{Z})$ that maps the standard fundamental region to the fundamental region specified by the symbol. Right: The images of the J -function (= the whole complex plane). The green, blue and dashed green lines correspond to the respective boundary components of any one half of (the closure of) the fundamental regions.

To conclude this section we summarize the definitions of the new objects and notions introduced in this section as a mini-glossary.

Mini-glossary

f -plane A (complex) codimension-one object corresponding to a zero locus of $f(z)$ in the Weierstrass form on the z -plane. Represented by a small square in the figures.

g -plane A (complex) codimension-one object corresponding to a zero locus of $g(z)$ in the Weierstrass form on the z -plane. Represented by a small 45° -rotated square in the figures.

elliptic point plane The collective name for f -planes and g -planes.

T -wall A (real) codimension-one object (domain wall) corresponding to a zero locus of $\text{Im}J$ with $\text{Re}J < 0$, extending from a D-brane and a f -plane. Represented by a green line.

T' -wall A (real) codimension-one object (domain wall) corresponding to a zero locus of $\text{Im}J$ with $\text{Re}J > 1$, extending from a D-brane and a g -plane. Represented by a dashed green line.

S-wall A (real) codimension-one object (domain wall) corresponding to a zero locus of $\text{Im}J$ with $0 < \text{Re}J < 1$, extending from a f -plane and a g -plane. Represented by a blue line.

cell region A closed region on the z -plane (\mathbb{P}^1 base of the elliptic fibration) bounded by the T -, T' - and S -walls. Each cell region corresponds to either half of the (closure of the) ⁵ fundamental region with $\text{Im}J > 0$ or $\text{Im}J < 0$ of the fiber modulus.

shaded cell region The cell region corresponding to the (closure of the) half fundamental region with $\text{Im}J > 0$ (Fig. 4.1).

4.2 Relation to “dessin d’enfant” of Grothendieck

In fact, the construction in the previous section is nothing but drawing a “dessin d’enfant” of Grothendieck [87], known in mathematics, on the P^1 base with a canonical triangulation.⁶ A dessin d’enfant, meaning a drawing of a child, is a graph consisting of some black points, white points and lines connecting these points, drawn according to a special rule. To demonstrate the rule, let us consider, for example, a function [88]:

$$F(x) = -\frac{(x-1)^3(x-9)}{64x} = 1 - \frac{(x^2-6x-3)^2}{64x}, \quad (4.2.1)$$

where $x \in \mathbb{P}^1$. F is a map from \mathbb{P}^1 to \mathbb{P}^1 . At almost everywhere on \mathbb{P}^1 , F is a homeomorphism, sending a small disk to another in a one-to-one way. However, F maps a small disk centered at $x = 1$ to one centered at $F = 0$ in a three-to-one way. Similarly, F is a two-to-one map from a small disk centered at $x = 3 \pm 2\sqrt{3}$ to one centered at $F = 1$. The points $x = 1, 3 \pm 2\sqrt{3}$ are said *critical points*, and the corresponding values of F are said *critical values*. If the map from the neighborhood around a critical point to another around the corresponding critical value is k -to-one, we say that the *ramification index* of the critical point is k .

Now the rule to draw the dessin associated with (4.2.1) is as follows: Place a black point at every preimage of 0, and a white point at every preimage of 1. Next draw lines at preimages of the line segment $[0, 1]$. The result is shown in Fig. 4.3(a):

The equation (4.2.1) induces a branched covering over \mathbb{P}^1 . Treating this graph as a combinatorial object, one can reproduce the information of the branched covering as follows:

⁵Below we abuse terminology and refer to a “fundamental region” as one modulo points on its boundary.

⁶The contents of this section are triggered by a suggestion made by the anonymous referee of Phys. Rev. D.

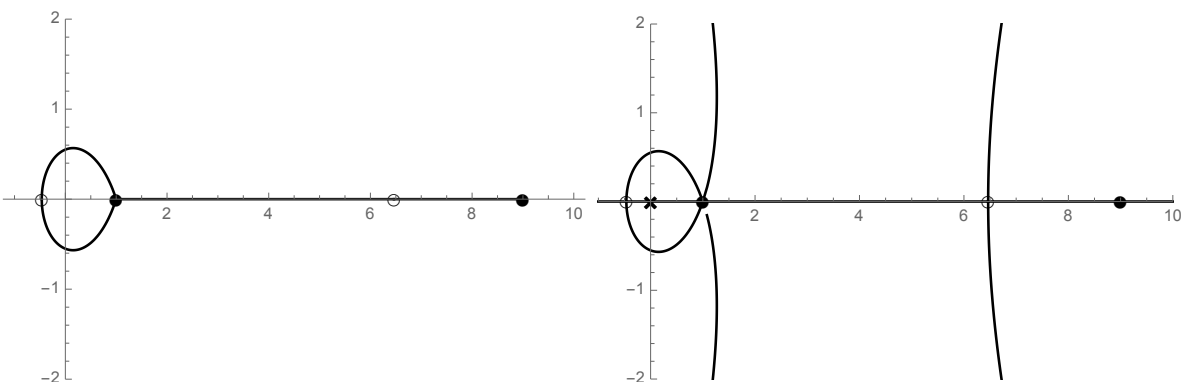


Fig. 4.3: (a)(left panel): The dessin for (4.2.1). (b)(right panel): The triangulated dessin. \times represents an ∞ point. The extra lines have been drawn at the preimages of the segment $[-\infty, 0]$ and $[1, \infty]$. The other ∞ point is not shown in this figure as it is infinitely far away.

One first adds a point ∞ to each region of the dessin. One then connects each ∞ with lines to the black or white points as many times as they appear on the boundary of the region. This yields a triangulation of the dessin. Assigning either the upper- or the lower-half plane to each triangle depending on the ordering of $0, 1, \infty$, and glueing these half planes together, one obtains a branched covering equivalent to the original one [88].

In the present case, the equation (4.1.10) defines a Belyi function, a holomorphic function whose critical values are only $0, 1$ and ∞ and nothing else. The black and white points in the dessin shown in Fig. 4.3(a) correspond to the f -planes and g -planes. The points ∞ added in the triangulation of the dessin are D-branes. The lines shown in Fig. 4.3(a) are the S -walls, while the lines connecting the ∞ points and the black or white points drawn in the triangulation are the T - and T' -walls.

What is special about (4.1.10) is that it induces a local homeomorphism between the \mathbb{P}^1 base and the upper-half plane. Indeed, as we saw in the previous section, the correspondence is one-to-one everywhere, even in the vicinity of the elliptic orbits $\tau = e^{\frac{2\pi i}{3}}$ and i . This is so because the $J = 0$ ($f = 0$) points are always critical points with ramification index three, and the $J = 1$ ($g = 0$) points are always with ramification index two. In this paper, we treat the dessin not as just a combinatorial graph, but draw the ∞ points and the triangulating lines (the T - and T' -walls) also as preimages of the J -function, as shown in Fig. 4.3(b). The

special feature of (4.1.10) then allows us to use the (triangulated) dessin as a convenient tool to compute monodromies, as we see below.

4.3 Basic properties of elliptic point planes

4.3.1 Basic properties of f -planes

As we defined in the previous sections, there are two kinds of elliptic point planes: f -planes and g -planes. In this section we describe the basic properties of f -planes.

As the name indicates, f -planes are the loci where the function f vanishes. As we saw in the previous section, these are the places where the J -function vanishes and τ becomes $e^{\frac{2\pi i}{3}}$ (or its $SL(2, \mathbb{Z})$ equivalents).

As we saw in the previous section, the expansion of $J(\tau)$ near $\tau = e^{\frac{2\pi i}{3}}$ is given by (4.1.7). If there is an f -plane at $z = 0$, $f = 0$ there, yielding

$$f(z) = f_{41}z + f_{42}z^2 + \cdots, \quad (4.3.1)$$

$$g(z) = g_{60} + g_{61}z + g_{62}z^2 + \cdots, \quad (4.3.2)$$

where f_{4i} , g_{6j} are constants with indices running over $i = 1, \dots, 8$ and $j = 1, \dots, 12$ for a K3 surface and $i = 1, \dots, 4$ and $j = 1, \dots, 6$ for a rational elliptic surface. Since

$$\frac{4f^3}{4f^3 + 27g^2} = \frac{4f_{41}^3}{27g_{60}^2} z^3 (1 + O(z)), \quad (4.3.3)$$

$\tau(z)$ asymptotically approaches

$$\tau(z) = e^{\frac{2\pi i}{3}} + \frac{2f_{41}}{(9g_{60}^2 J'''(e^{\frac{2\pi i}{3}}))^{\frac{1}{3}}} z \quad (4.3.4)$$

as $z \rightarrow 0$. Therefore, τ is regular near $z = 0$, and hence an f -plane does not carry D-brane charges.

Parameterize a small circle around $z = 0$ by $z = \epsilon e^{i\theta}$ ($\epsilon > 0$), then if one goes around along it once, so does τ once around $e^{\frac{2\pi i}{3}}$ along a small circle with a radius $\epsilon \left| \frac{2f_{41}}{(9g_{60}^2 J'''(e^{\frac{2\pi i}{3}}))^{\frac{1}{3}}} \right|$. Thus, although the monodromy around an f -plane is trivial, one passes through the boundary

of the half-fundamental region *six* times on the upper-half plane as one goes once around an f -plane. Since the neighborhoods of $z = 0$ and $\tau = e^{\frac{2\pi i}{3}}$ are homeomorphic, the neighborhood of $z = 0$ around an f -plane is also divided into six cell regions corresponding to different half-fundamental regions. The six domain walls separating these cell regions consist of three S -walls (blue) with $(0 < \operatorname{Re}J(\tau) < 1)$ and three T -walls (green) ($\operatorname{Re}J(\tau) < 0$), which are extended alternately from the f -plane, forming a locally \mathbb{Z}_3 -symmetric configuration.

On the upper-half plane, if one starts from the standard fundamental region and passes through preimages (of the J -function) of a T -wall (green) and an S -wall (blue) to go to the $SL(2, \mathbb{Z})$ equivalent point, then the $SL(2, \mathbb{Z})$ transformation mapping the original point to the final point is $T^{-1}S$. Further, if one crosses through preimages of a T -wall (green) and an S -wall (blue) again, the transformation to the final $SL(2, \mathbb{Z})$ equivalent point is $(T^{-1}S)^2 = -ST \sim ST$ (as $PSL(2, \mathbb{Z})$).

Since

$$(T^{-1}S)^3 = 1, \quad (4.3.5)$$

$T^{-1}S$ generates a \mathbb{Z}_3 group, which is the isotropy group of the elliptic point $\tau = e^{\frac{2\pi i}{3}}$. It is easy to show that this $T^{-1}S$ transformation acts on the neighborhood of this point as a $\frac{2\pi i}{3}$ rotation. Therefore, the configuration of τ near an f -plane is locally invariant under the simultaneous actions of the spacial \mathbb{Z}_3 rotation and the \mathbb{Z}_3 $SL(2, \mathbb{Z})$ transformation. The metric near an f -plane is locally \mathbb{Z}_3 invariant.

4.3.2 Basic properties of g -planes

Likewise, the expansion of $J(\tau)$ around $\tau = i$ is given by (4.1.8). Let a g -plane be at $z = 0$ this time. $f(z)$ and $g(z)$ are expanded as

$$f(z) = f_{40} + f_{41}z + f_{42}z^2 + \cdots, \quad (4.3.6)$$

$$g(z) = g_{61}z + g_{62}z^2 + \cdots. \quad (4.3.7)$$

Since

$$\frac{4f^3}{4f^3 + 27g^2} = 1 - \frac{27g_{61}^2}{4f_{40}^3}z^2(1 + O(z)), \quad (4.3.8)$$

$\tau(z)$ approaches

$$\tau(z) = i + \frac{3i\pi^{\frac{1}{2}}g_{61}}{4K(\frac{1}{\sqrt{2}})^2f_{40}^{\frac{3}{2}}}z \quad (4.3.9)$$

as $z \rightarrow 0$. Thus τ is again regular near a g -plane, therefore a g -plane does not have D-brane charges, either. The monodromy around a g -plane is also trivial, although if one goes around it, one will be passing through the S -walls (blue lines) and the T' -walls (dashed green lines) alternately, twice for each.

Suppose that on the upper-half plane one starts from an arbitrarily given point near $\tau = i$ in the standard fundamental region with $\text{Re}\tau < 0$ and goes through the preimages of an S -wall and a T' -wall to reach the $SL(2, \mathbb{Z})$ -equivalent point. This move can be achieved by the $SL(2, \mathbb{Z})$ S transformation. This S transformation acts on the neighborhood of $\tau = i$ as a \mathbb{Z}_2 rotation. The metric near a g -plane is also $SL(2, \mathbb{Z})$ invariant. Thus the vicinity of a g -plane is invariant under the \mathbb{Z}_2 rotation associated with the S transformation.

4.4 Simple method to compute the monodromy using the dessin

Drawing the contours of the walls and the positions of the D-branes and elliptic point planes, we can have a figure of the complex plane divided into several cell regions such as Fig. 4.1, which we call a *dessin*.⁷ For a given Weierstrass equation, the dessin provides us with a very simple method to compute the monodromy matrices along an arbitrary path around branes on the complex plane (= an affine patch of the \mathbb{P}^1 or the “ u -plane” of a Seiberg-Witten curve).

4.4.1 The method

To illustrate the method, let us consider the Seiberg-Witten curve of $\mathcal{N} = 2$ pure ($N_f = 0$) $SU(2)$ supersymmetric gauge theory [5]. The equation is

$$y^2 = x^3 - ux^2 + x. \quad (4.4.1)$$

⁷This corresponds to a *triangulated* dessin in the sense of Grothendieck.

Taking u as the coordinate z , we obtain a Weierstrass equation with

$$f(u) = -\frac{1}{3}u^2 + 1, \quad g(u) = -\frac{2}{27}u^3 + \frac{1}{3}u, \quad (4.4.2)$$

whose dessin is shown in the upper panel of Fig. 4.4. Let us compute the monodromy around each discriminant locus. Choosing a starting point near the left locus (shown as a cross), the left path crosses the walls as

$$\rightarrow \mathbf{G} \rightarrow \mathbf{B} \rightarrow \mathbf{G} \rightarrow \mathbf{dG} \rightarrow, \quad (4.4.3)$$

where \mathbf{G} denotes the T -wall, \mathbf{B} the S -wall and \mathbf{dG} the T' -wall.⁸

The monodromy matrices for various patterns of crossings are

$$\begin{aligned} \rightarrow \mathbf{dG} \rightarrow \mathbf{G} \rightarrow &= T, \\ \rightarrow \mathbf{G} \rightarrow \mathbf{dG} \rightarrow &= T^{-1}, \\ \rightarrow \mathbf{dG} \rightarrow \mathbf{B} \rightarrow = \rightarrow \mathbf{B} \rightarrow \mathbf{dG} \rightarrow &= S, \\ \rightarrow \mathbf{B} \rightarrow \mathbf{G} \rightarrow &= ST, \\ \rightarrow \mathbf{G} \rightarrow \mathbf{B} \rightarrow &= T^{-1}S, \end{aligned} \quad (4.4.4)$$

where the first wall of each row is the crossing from a shaded cell region ($\text{Im}J > 0$) to an unshaded one ($\text{Im}J < 0$), and the second is from an unshaded to a shaded one.⁹ The monodromy matrices are defined as

$$T = \begin{pmatrix} 1 & 1 \\ 0 & 1 \end{pmatrix}, \quad S = \begin{pmatrix} 0 & -1 \\ 1 & 0 \end{pmatrix} \quad (4.4.6)$$

⁸ \mathbf{G} , \mathbf{B} and \mathbf{dG} are respectively the first letters of Green, Blue and dashed Green. We have avoided using T , S or T' here as the monodromy matrices for the crossing do not coincide with the names of the walls.

⁹Therefore, these rules only apply when one computes a monodromy for a path that starts from and ends in a *shaded cell region* ($\text{Im}J > 0$). The rules for computing a monodromy for a path from an *unshaded cell region* ($\text{Im}J < 0$) to another are similar but different:

$$\begin{aligned} \rightarrow \mathbf{dG} \rightarrow \mathbf{G} \rightarrow &= T^{-1}, \\ \rightarrow \mathbf{G} \rightarrow \mathbf{dG} \rightarrow &= T, \\ \rightarrow \mathbf{dG} \rightarrow \mathbf{B} \rightarrow = \rightarrow \mathbf{B} \rightarrow \mathbf{dG} \rightarrow &= S, \\ \rightarrow \mathbf{B} \rightarrow \mathbf{G} \rightarrow &= ST^{-1}, \\ \rightarrow \mathbf{G} \rightarrow \mathbf{B} \rightarrow &= TS. \end{aligned} \quad (4.4.5)$$

as usual, where we say that the monodromy matrix is $\begin{pmatrix} a & b \\ c & d \end{pmatrix}$ if the modulus τ is changed to

$$\tau' = M \circ \tau \equiv \frac{a\tau + b}{c\tau + d}. \quad (4.4.7)$$

They are defined only in $PSL(2, \mathbb{Z})$, *i.e.* up to a multiplication of -1 .

By using the rule (4.4.4), we can immediately find the monodromy matrix for the path (4.4.3) as

$$\begin{aligned} T^{-1}S \cdot T^{-1} &= T^{-1}ST^{-1} \\ &\sim STS, \end{aligned} \quad (4.4.8)$$

where \sim denotes the equality in $PSL(2, \mathbb{Z})$.

Similarly, the crossed walls for the right path are

$$\rightarrow \mathbf{G} \rightarrow \mathbf{dG} \rightarrow \mathbf{G} \rightarrow \mathbf{dG} \rightarrow \mathbf{G} \rightarrow \mathbf{dG} \rightarrow \mathbf{B} \rightarrow \mathbf{G} \rightarrow . \quad (4.4.9)$$

Using rule (4.4.4) again, we find that the monodromy is

$$T^{-1} \cdot T^{-1} \cdot T^{-1} \cdot ST = T^{-3}ST. \quad (4.4.10)$$

A confusing but important point of the rule is that, in the first example, the monodromy matrix T^{-1} which corresponds to the crossings $\rightarrow \mathbf{G} \rightarrow \mathbf{dG} \rightarrow$ taking place *after* the crossings $\rightarrow \mathbf{G} \rightarrow \mathbf{B} \rightarrow$ is multiplied to $T^{-1}S$ from the *right*. This will be confusing because if $M = \begin{pmatrix} a & b \\ c & d \end{pmatrix}$, $M' = \begin{pmatrix} a' & b' \\ c' & d' \end{pmatrix}$ and $\tau' = M \circ \tau$, $\tau'' = M' \circ \tau'$, then the monodromy matrix $M'' = \begin{pmatrix} a'' & b'' \\ c'' & d'' \end{pmatrix}$ representing $\tau \mapsto \tau'' = M'' \circ \tau$ is given by

$$M'' = M'M, \quad (4.4.11)$$

in which M' is multiplied from the *left*.

More generally, the following statement holds: Let γ be a path specified by the series of the walls

$$\gamma := \rightarrow \mathbf{W}_1 \rightarrow \mathbf{W}_2 \rightarrow \cdots \rightarrow \mathbf{W}_k \rightarrow, \quad (4.4.12)$$

where \mathbf{W}_i ($i = 1, \dots, k$) are either of \mathbf{G} , \mathbf{B} or \mathbf{dG} , and let M_γ denote the associated monodromy matrix of γ . k is an even positive integer. (If it is odd, a shaded cell region is mapped to an unshaded cell region or vice versa, and the transformation cannot be an $SL(2, \mathbb{Z})$ transformation). Let γ_1, γ_2 be paths specified by the series of the walls crossed by them

$$\begin{aligned}\gamma_1 &: \rightarrow \mathbf{W}_1^{(1)} \rightarrow \mathbf{W}_2^{(1)} \rightarrow \dots \rightarrow \mathbf{W}_{k_1}^{(1)} \rightarrow, \\ \gamma_2 &: \rightarrow \mathbf{W}_1^{(2)} \rightarrow \mathbf{W}_2^{(2)} \rightarrow \dots \rightarrow \mathbf{W}_{k_2}^{(2)} \rightarrow,\end{aligned}\tag{4.4.13}$$

and let $\gamma_1 \bowtie \gamma_2$ be the jointed path

$$\gamma_1 \bowtie \gamma_2 : \rightarrow \mathbf{W}_1^{(1)} \rightarrow \dots \rightarrow \mathbf{W}_{k_1}^{(1)} \rightarrow \mathbf{W}_1^{(2)} \rightarrow \dots \rightarrow \mathbf{W}_{k_2}^{(2)} \rightarrow,\tag{4.4.14}$$

where we use the new symbol \bowtie to denote the operation of jointing two paths.¹⁰ Then

Proposition.

$$M_{\gamma_1 \bowtie \gamma_2} = M_{\gamma_1} M_{\gamma_2}.\tag{4.4.15}$$

Remark. As we noted above, the monodromy matrix corresponding to a later crossing comes to the *right*, unlike (4.4.11) in which the matrix for the later transformation is multiplied from the *left*.

Proof. By induction with respect to the total number of crossed walls, it is enough to show the statement for the cases when γ_2 is any of the crossing patterns (4.4.4). Suppose that γ_1 starts from a cell region C_0 and ends in another C_1 , and that γ_2 goes from the cell region C_1 to another C_2 , where γ_2 is taken to be any of the crossing patterns (4.4.4), say, $\gamma_2 = \Rightarrow \mathbf{dG} \rightarrow \mathbf{G} \rightarrow$ and $M_{\gamma_2} = T$. Let P_{γ_i} ($i = 1, 2$) be the associated maps which send points in the cell region C_{i-1} to those in the cell region C_i , respectively, such that the torus modulus over the point is $SL(2, \mathbb{Z})$ equivalent. We say two points on \mathbb{P}^1 are $SL(2, \mathbb{Z})$ equivalent if the torus fiber moduli over them are $SL(2, \mathbb{Z})$ equivalent. Using this terminology, we can say that P_{γ_i} ($i = 1, 2$) are the maps which send the points in C_{i-1} to their $SL(2, \mathbb{Z})$ equivalent points in C_i , respectively. Since $\tau(z)$ is holomorphic in z and $J(\tau)$ is holomorphic in τ , the

¹⁰We will not use the usual symbol for the addition “+” since this operation is noncommutative.

domain of the map P_{γ_1} is not necessarily restricted to only C_0 but can be extended to outside C_0 as far as it is in a small neighborhood of z_0 .

Let z_0 be a point in C_0 , and let $z_1 = P_{\gamma_1}(z_0) \in C_1$, $z_2 = P_{\gamma_2}(z_1) \in C_2$. If we denote τ_i ($i = 0, 1, 2$) be the modulus of the torus fiber over z_i ($i = 0, 1, 2$), they satisfy

$$J(\tau_i) = \frac{4f(z_i)^3}{4f(z_i)^3 + 27g(z_i)^2}, \quad (4.4.16)$$

where τ_1 and τ_2 are the values analytically continued from τ_0 along the paths γ_1 , and then γ_2 . Taking τ_0 in the *standard* fundamental region, the transformation from τ_0 to τ_1 is given by $\tau_1 = M_{\gamma_1} \circ \tau_0$, but consecutive transformation from τ_1 to τ_2 is *not* $M_{\gamma_2} \circ \tau_1$, as τ_1 does not belong to the standard fundamental region in general. Rather, since P_{γ_1} is locally an isomorphism between a neighborhood around z_0 and that around z_1 , the final point z_2 can be written as the P_{γ_1} image of z'_1 , where z'_1 is the $SL(2, \mathbb{Z})$ equivalent point in the cell region *reached along the path γ_2 first* from z_0 , if z_2 is close enough to z_1 (Fig. 4.5). If, on the other hand, z_2 is not close to z_1 , we can continuously deform the complex structure of the elliptic fibration so that z_2 may come close to z_1 . Since this is a continuous deformation, the monodromy transformation matrix does not change, as the entries of the matrix take discrete values. Thus we may assume that z_2 is close to z_1 .

Since τ_0 is taken in the standard fundamental region, τ'_1 , the modulus of the torus fiber over z'_1 , is given by

$$\tau'_1 = M_{\gamma_2} \circ \tau_0. \quad (4.4.17)$$

Therefore, since $\tau_2 = M_{\gamma_1} \circ \tau'_1$, we find

$$\begin{aligned} \tau_2 &= M_{\gamma_1} \circ M_{\gamma_2} \circ \tau_0 \\ &= (M_{\gamma_1} M_{\gamma_2}) \circ \tau_0, \end{aligned} \quad (4.4.18)$$

which is what the proposition claims.

In deriving (4.4.18), we did not use the fact that γ_2 was assumed to be a particular pattern among (4.4.4), but the relation (4.4.18) likewise holds for other patterns. This completes the proof of the proposition.¹¹

¹¹ In this proof, γ_2 is taken to be a path to the next adjacent cell region, whereas γ_1 is assumed to be some long path leading to a faraway cell region. If γ_1 is also a path to another next adjacent cell region, it can be explicitly checked that the proposition holds in this case as well.

4.4.2 Example: Monodromies of $N_f = 4$ $SU(2)$ Seiberg-Witten curves

The proposition (4.4.15) together with the rule (4.4.4) provides us with a very convenient method to compute the monodromy for an arbitrary Weierstrass model along an arbitrary path.

Fig. 4.6 is a dessin of $N_f = 4$ $SU(2)$ Seiberg-Witten curve with some mass parameters. The Weierstrass equation is (4.1.1) where

$$\begin{aligned} f &= (z-1)(z-2), \\ g &= \epsilon(z-i)(z-2i)(z-3i) \\ &\quad + (1-\epsilon) \left(-\frac{5}{16}i\sqrt{\frac{3}{2}}z^3 + \frac{17iz^2}{4\sqrt{6}} - i\sqrt{6}z + \frac{4}{3}i\sqrt{\frac{2}{3}} \right) \end{aligned} \quad (4.4.19)$$

with $\epsilon = 3 \times 10^{-7}$. This choice of g interpolates between the configuration in which all the g -locus planes are located on the imaginary axis at equal intervals ($\epsilon = 1$) and the one in which four of the six D-branes collide together at $z = 0$ to form a I_4 singular fiber ($\epsilon = 0$), with the f -planes fixed at $z = 1, 2$. The figure is the configuration very close to the latter limit.

As is well known, the one-parameter (“ u ”) family of tori describe the moduli space of the gauge theory and can be compactified into a rational elliptic surface by taking the variables and coefficient functions to be sections of appropriate line bundles, where the u parameter becomes the affine coordinate z of the base \mathbb{P}^1 . Note, however, that the dessin can be drawn on this affine patch independently of the choices of the bundles; it only affects how many D-branes are at the infinity of \mathbb{P}^1 .

This figure shows how the monodromies around the two D-branes on the right (located at $z \approx 1$ and ≈ 2) change depending on the choice of the reference point. If it is taken far enough (as marked as a white star), the monodromies along the black contours read $M_{2,1}$ and $M_{0,1}$. This means that, as we show later, a $(2, 1)$ and a $(0, 1)$ string become light near the respective D-branes, showing that the locations of the D-branes are the $(2, 1)$ dyon and the monopole point on the moduli space of the gauge theory, which is well known.

If the reference point is taken closer (as marked as a black star), then the monodromies

along the dashed black contours are $M_{1,1}(= \mathbf{B})$ and $M_{1,-1}(= \mathbf{C})$, which agrees with the **ABC** brane description of the I_0^* Kodaira singular fiber.

Finally, if the reference point is taken to be very close to the D-branes inside the cell regions surrounded by the S -walls, then the monodromies along the dotted contours are both T , showing that these branes look ordinary D-branes if they are observed from very close to them.

4.4.3 (p, q) -brane as an effective description

Of course, it is well known that the monodromy changes depending the choice of the reference point. A monodromy matrix measured from some reference point gets $SL(2, \mathbb{Z})$ conjugated if it is measured from another point. What is new here that, by drawing a dessin, we can precisely see how and from where the monodromy matrix changes and gets conjugated as we vary the position of the reference point.

For instance, we can see from Fig. 4.6 that the monodromies around the two D-branes on the right are either $M_{2,1}$, $M_{0,1}$ or $M_{1,1}(= \mathbf{B})$, $M_{1,-1}(= \mathbf{C})$ for most choices of the reference point on the $z(\equiv u)$ -plane, and they are recognized as ordinary ($M_{1,0} = \mathbf{A}$) D-branes only when they are viewed from the points in the tiny regions surrounded by the S -walls. Thus we see that the effective description of the two branes as $(1, 1)(= \mathbf{B})$ - and $(1, -1)(= \mathbf{C})$ -branes are good at the energy scale lower than the scale of the size of the small cell regions surrounded by the S -walls.

However, one can also set the mass parameters of the same gauge theory so that the dessin of the Seiberg-Witten curve looks as shown in Fig. 4.1. In this case, the S -walls spread into wide areas of the \mathbb{P}^1 . There is not much difference among the six D-branes, and there is no obvious reason to distinguish particular two as **B** or **C** from the other four D-branes.

Remark. We have seen that a cluster of a D-brane and two elliptic point planes, in which the former is surrounded by the S -walls extended from the latter, may be effectively identified as a **B**- or a **C**-brane, if viewed from a distance of the size of the cluster. Thus one might think that an “exact” (p, q) -brane (whose monodromy is $M_{p,q}$ along arbitrary small loop) can

be obtained by taking the f - and g -planes on top of each other so that the size of the cell region the S -walls surround becomes zero. This is not the case, however, since if the f - and g -planes collide, the order of the discriminant becomes two, implying that another D-brane also automatically comes on top of the D-brane, f -plane and g -plane. Since it contains two D-branes, it cannot be identified as a *single* (p, q) -brane in the **ABC**-brane description.

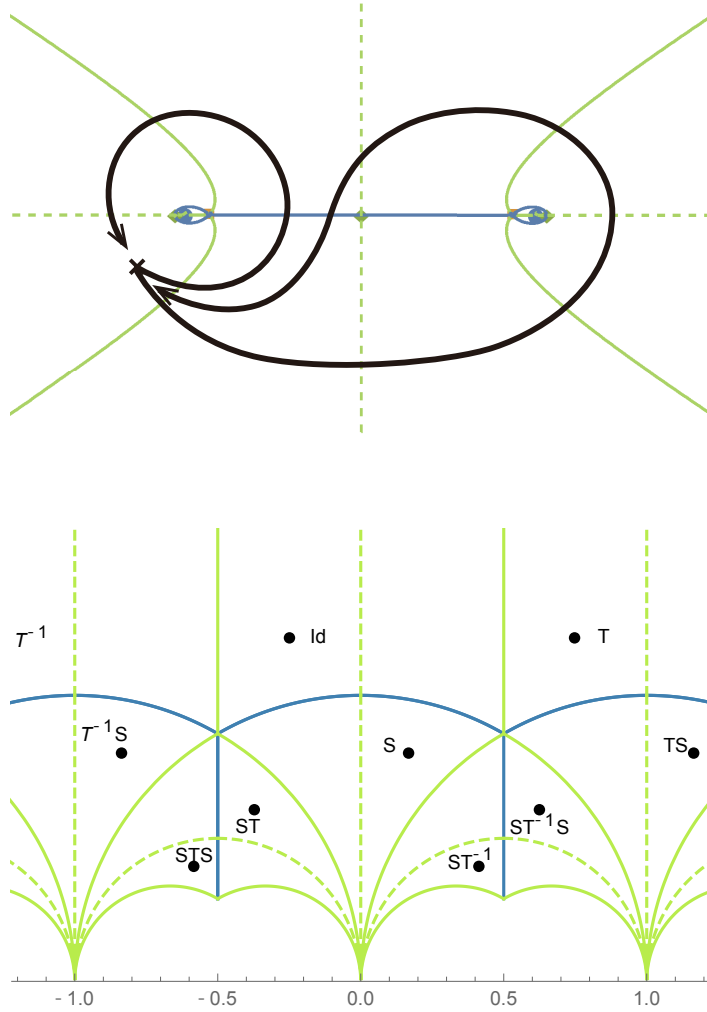


Fig. 4.4: The upper panel: The dessin of $N_f = 0$ SW curve ($f(u) = -\frac{1}{3}u^2 + 1$, $g(u) = -\frac{2}{27}u^3 + \frac{1}{3}u$). The lower panel: The crossed walls and the corresponding monodromies.

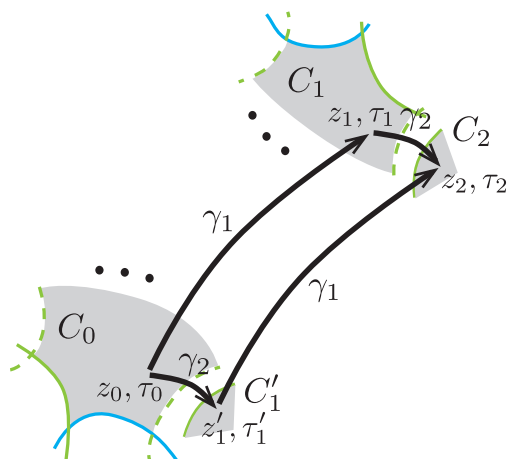


Fig. 4.5: Taking τ_0 in the *standard* fundamental region, the transformation from τ_0 to τ_1 is given by $\tau_1 = M_{\gamma_1} \circ \tau_0$, but consecutive transformation from τ_1 to τ_2 is *not* $M_{\gamma_2} \circ \tau_1$, as τ_1 does not belong to the standard fundamental region in general. Rather, we have $\tau_2 = M_{\gamma_1} \circ \tau'_1$ with $\tau'_1 = M_{\gamma_2} \circ \tau_0$ as P_{γ_1} induces an isomorphism.

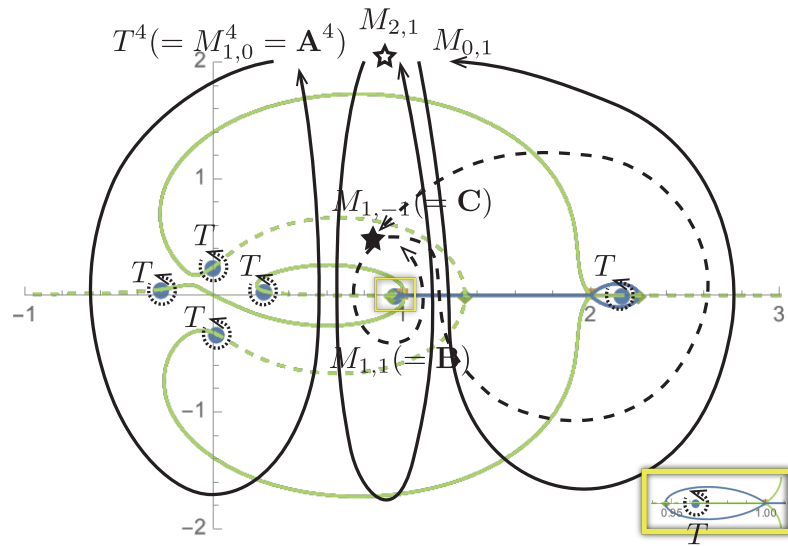


Fig. 4.6: Monodromies of $N_f = 4$ $SU(2)$ Seiberg-Witten curve. It shows how the monodromies around the two D-branes on the right (located at $z \approx 1$ and $z \approx 2$) change depending on the choice of the reference point. If it is taken far enough (as marked as a white star), the monodromies along the black contours read $M_{2,1}$ and $M_{0,1}$. If the reference point is taken closer (as marked as a black star), then the monodromies along the dashed black contours are $M_{1,1}(= \mathbf{B})$ and $M_{1,-1}(= \mathbf{C})$. If, on the other hand, the reference point is taken to be very close to the D-branes inside the cell regions surrounded by the S -walls, then the monodromies along the dotted contours are both T .

Chapter 5

Higher-codimension singularities

So far we considered eight-dimensional compactifications of F-theory. Enhancement of gauge symmetries arise from the singularities of the K3 surface. They are the codimension-one singularities, namely, the points in the base space of the elliptic K3 surface.

In this chapter we consider higher-codimension singularities. Supersymmetry requires that the compact space need to be a Calabi-Yau manifold. The Calabi-Yau three-fold can have not only the codimension-one singularities but also the codimension-two singularities. As we will see, such codimension-two singularities provide massless matters in F-theory [53–56].

In addition, we also consider the Calabi-Yau four-fold. We will see that phases of resolutions of the Calabi-Yau four-fold can be investigated by the Coulomb branch of three-dimensional $\mathcal{N} = 2$ supersymmetric gauge theories [65–68].

5.1 Matters in F-theory

Let us consider F-theory compactifications on the Calabi-Yau three fold. In particular, we concentrate on the elliptic fibered Calabi-Yau three-fold over the Hirzebruch surface F_n . The Hirzebruch surface is a P^1 fibration over P^1 , which is characterized single integer n . The Calabi-Yau three-fold is defined as follows: We start with the four homogeneous coordinates

(u', v', u, v) . We introduce the two charges of the coordinates as follows:

$$\begin{array}{cccc} & u' & v' & u & v \\ Q^{(\lambda)} : & 1 & 1 & n & 0 \\ Q^{(\mu)} : & 0 & 0 & 1 & 1 \end{array} \quad (5.1.1)$$

In other words, we introduce the two identifications between the four coordinates as

$$(u', v', u, v) \sim (\lambda u', \lambda v', \lambda^n u, v) \quad (5.1.2)$$

$$(u', v', u, v) \sim (u', v', \mu u, \mu v), \quad (5.1.3)$$

where $\lambda, \mu \in \mathbb{C}$ and $n \in \mathbb{Z}$. The Hirzebruch surface is defined as

$$F_n = \{\mathbb{C}^4 - (0, 0, 0, 0)\} / \sim, \quad (5.1.4)$$

which is labeled by an integer n . If $n = 0$, the surface becomes the direct product $P^1 \times P^1$.

The elliptic fibered Calabi-Yau three-fold over the Hirzebruch surface is described by the Weierstrass form. We introduce the affine coordinates as

$$z' = \frac{u'}{v'}, \quad z = \frac{u}{v}. \quad (5.1.5)$$

The Weierstrass equation is given by

$$y^2 = x^3 + f(z, z')x + g(z, z'), \quad (5.1.6)$$

where

$$f(z, z') = \sum_{i=0}^8 z^i f_{(4-i)n+8}(z'), \quad (5.1.7)$$

$$g(z, z') = \sum_{j=0}^{12} z^j g_{(6-j)n+12}(z'). \quad (5.1.8)$$

The subscripts of $f_{(4-i)n+8}(z')$ and $g_{(6-j)n+12}(z')$ represent the degree of the polynomial. The each terms of f and g is determined by the charges in (5.1.1), i.e. the each polynomials have the same charges. The charges of x and y are assigned as follows:

$$\begin{array}{cc} & x & y \\ Q^{(\lambda)} : & 2n + 4 & 3n + 6 \\ Q^{(\mu)} : & 4 & 6 \end{array} \quad (5.1.9)$$

The discriminant is given by

$$\begin{aligned}
\Delta(z, z') &= 4f^3(z, z') + 27g^2(z, z') \\
&= (4f_{4n+8}^3(z') + 27g_{6n+12}^2(z')) \\
&\quad + (12f_{4n+8}^2(z')f_{3n+8}(z') + 54g_{6n+12}(z')g_{5n+12}(z'))z \\
&\quad + (12f_{4n+8}^2(z')f_{2n+8}(z') + 12f_{4n+8}(z')f_{3n+8}^2(z') + 54g_{6n+12}(z')g_{4n+12}(z') + 27g_{5n+12}^2(z'))z^2 \\
&\quad + \cdots \\
&\quad + (4f_{-4n+8}^3(z') + 27g_{-6n+12}^2(z'))z^{24}.
\end{aligned} \tag{5.1.10}$$

5.1.1 An example: $I_2 \rightarrow I_3$

As an example, let us consider the codimension-two singularity where the fiber type I_2 enhances to I_3 . The stack of two 7-branes intersects with another 7-brane at this point. Matters appear at the singular point. The corresponding gauge groups are $SU(2) \rightarrow SU(3)$. We assume that the codimension-one singularity where we have the fiber type I_2 is localized at $z = 0$. The orders of f , g and Δ are given by

$$\text{ord}(f) = 0, \quad \text{ord}(g) = 0, \quad \text{ord}(\Delta) = 2. \tag{5.1.11}$$

The first two equations imply $f_{4n+8}(z') \neq 0$ and $g_{6n+12}(z') \neq 0$ at $z = 0$. The last equation means

$$\begin{cases} 4f_{4n+8}^3(z') + 27g_{6n+12}^2(z') = 0, & (5.1.12) \end{cases}$$

$$\begin{cases} 12f_{4n+8}^2(z')f_{3n+8}(z') + 54g_{6n+12}(z')g_{5n+12}(z') = 0 & (5.1.13) \end{cases}$$

at $z = 0$. As a solution to (5.1.12), we choose

$$\begin{cases} f_{4n+8}(z') = -3h_{2n+4}^2(z'), \\ g_{6n+12}(z') = 2h_{2n+4}^3(z'), \end{cases} \tag{5.1.14}$$

where $h_{2n+4}(z')$ is a polynomial that has the degree of $(2n + 4)$ and where we assume $h_{2n+4}(z') \neq 0$. Then, the second equation (5.1.13) provides

$$g_{5n+12}(z') = -f_{3n+8}(z')h_{2n+4}(z'), \tag{5.1.15}$$

thus when the identity is satisfied, we have $SU(2)$ symmetry at $z = 0$.

Inserting (5.1.14) and (5.1.15), we obtain

$$\begin{aligned} \Delta(z, z') &= (108f_{2n+8}(z')h_{2n+4}^2(z') + 108h_{2n+4}(z')g_{4n+12}(z') - 9f_{3n+8}^2(z'))h_{2n+4}^2(z')z^2 + O(z'^3), \end{aligned} \quad (5.1.16)$$

where $O(z'^3)$ represents the terms whose the degrees are 3 or higher. When

$$108f_{2n+8}(z')h_{2n+4}^2(z') + 108h_{2n+4}(z')g_{4n+12}(z') - 9f_{3n+8}^2(z') = 0, \quad (5.1.17)$$

the order of the discriminant is enhanced to 3, namely, $\text{ord}(\Delta) = 2 \rightarrow 3$, which means that the fiber type I_2 is enhanced to I_3^1 .

The matters are localized at the codimension-two singularity where the equation (5.1.17) is satisfied. Let us count the number of the matters. In the sense of $\mathcal{N} = (1, 0)$ supersymmetry in six dimensions, the matters are the hypermultiplets. There are the two types of the hypermultiplets; the neutral and the charged hypermultiplets. The number of the neutral hypermultiplets corresponds to the dimensions of complex moduli for $i = 0, 1, 2, 3$ and $j = 0, 1, 2, 3, 4, 5$ in (5.1.7) and (5.1.8)². The Weierstrass equation that satisfy (5.1.14) and (5.1.15) is given by

$$\begin{aligned} y^2 = & x^3 - 3xh_{2n+4}^2(z') + 2h_{2n+4}^3(z') - zf_{3n+8}(z')h_{2n+4}(z') \\ & + x \sum_{i=1}^8 z^i f_{(4-i)n+8}(z') + \sum_{j=2}^{12} z^j g_{(6-j)n+12}. \end{aligned} \quad (5.1.18)$$

The dimensions of complex moduli are given by the number of the coefficients of the polynomials. We obtain

$$\begin{aligned} n_{\text{H}}^{(\text{neutral})} &= (2n + 5) + (3n + 9) + (2n + 9) + (n + 9) \\ &+ (4n + 13) + (3n + 13) + (2n + 13) + (n + 13) - 1 \\ &= 18n + 83, \end{aligned} \quad (5.1.19)$$

¹When $h_{2n+4}(z') = 0$, the order of the discriminant also becomes $\text{ord}(\Delta) = 3$. In this case, we have $f_{4n+8}(z') = g_{6n+12}(z') = g_{5n+12}(z') = 0$, that is, $\text{ord}(f) = 1$ and $\text{ord}(g) = 2$. This corresponds to the fiber type *III*.

²When we consider elliptic fibered K3 surfaces, singular fibers are placed at $z = 0$. In the case of the elliptic fibered Calabi-Yau three-fold over the Hirzebruch surface, however, fibers become singular at $z = 0$ and ∞ . The fact that we consider $z = 0$ is reflected on $i = 0, 1, 2, 3$ and $j = 0, 1, 2, 3, 4, 5$. As we will see in the next subsection, the two lines $z = 0, \infty$ correspond to each E_8 in $E_8 \times E_8$ heterotic superstring theory.

where the last -1 implies an overall factor.

The charged matters arise from the extra zero-locus (5.1.17). The degree of the left hand side in (5.1.17) is $6n + 16$. In general, when a gauge group H is enhanced to G , the matters of $G/(H \times U(1))$ emerge. In this case, $SU(2)$ is enhanced to $SU(3)$. We decompose the adjoint representation of $SU(3)$ into $SU(2) \times U(1)$:

$$\mathbf{8} = \mathbf{3} + \mathbf{2} + \mathbf{2} + \mathbf{1}, \quad (5.1.20)$$

that is, the hypermultiplets are in $\mathbf{2}$. Therefore, number of charged matters is given by

$$n_{\text{H}}^{(\text{charged})} = 2 \cdot (6n + 16). \quad (5.1.21)$$

We get the total number of the matters

$$\begin{aligned} n_{\text{H}} &= n_{\text{H}}^{(\text{charged})} + n_{\text{H}}^{(\text{neutral})} \\ &= 30n + 115. \end{aligned} \quad (5.1.22)$$

As we will see in the next subsection, the number n_{H} is consistent with the six-dimensional anomaly cancellation in the heterotic side.

5.1.2 Dual heterotic theory

The F-theory compactification on a Calabi-Yau three-fold whose base space is a Hirzebruch surface is dual to $E_8 \times E_8$ heterotic superstring theory compactified on an elliptic fibered K3 surface. This is interpreted as the fiberwise duality between F-theory on K3 and $E_8 \times E_8$ heterotic theory on T^2 .

First of all, the three-form that is introduced in order to cancel an anomaly is given by

$$H = dB + \omega_{3L} - \omega_{3Y}, \quad (5.1.23)$$

where ω_{3L} and ω_{3Y} are the Lorentz and the Yan-Mills Chern-Simons three-form, respectively. Since the three-form H needs to be globally well defined, the integration of the exterior derivative of H over $K3$ must be zero³:

$$\frac{1}{2} \frac{1}{8\pi^2} \int_{K3} \left(\text{tr} R^2 - \frac{1}{30} \text{Tr} F^2 \right) = 0, \quad (5.1.24)$$

³We denote traces in the fundamental representation as “tr”, and the adjoint representation as “Tr”.

where we multiply the factor $1/(16\pi^2)$. The first term in the left hand side is half of the Pontryagin number, and it gives 24 for K3. On the other hand, the second term in the left hand side represents the instanton number. As a result, the configuration of the gauge field has the 24 instantons in the K3 surface.

We denote the instanton numbers as $(12 + n, 12 - n)$ for each E_8 . The parameter n corresponds to the label of the Hirzebruch surface F_n in dual F-theory. When the $12 + n$ instantons break the first E_8 to some gauge group G , we obtain the charged hypermultiplets and the neutral hypermultiplets.

Next we consider the numbers of the charged hypermultiplets and the neutral hypermultiplets. Spin-half particles in six dimensions come from gravitinos and gauginos in ten dimensions. We concentrate on the latter. When a gauge group G is broken to G' by the gauge field getting a value on H , the adjoint representation of G is decomposed into a sum of the representation of (G', H) :

$$\mathbf{G} = \sum_i (\mathbf{L}_i, \mathbf{C}_i), \quad (5.1.25)$$

where \mathbf{G} is the adjoint representation of G , \mathbf{L}_i and \mathbf{C}_i are the representations of G' and H , respectively. Thus the number of the spin-half particles in \mathbf{L}_i is given by the index of the spin-half particles in \mathbf{C}_i of K3:

$$n_i = \frac{1}{8\pi^2} \int_{\text{K3}} \left(\frac{1}{2} \text{tr}_{\mathbf{C}_i} F^2 - \frac{1}{48} \dim(\mathbf{C}_i) \text{tr} R^2 \right) \quad (5.1.26)$$

$$= \frac{r_i}{8\pi^2} \int_{\text{K3}} \frac{1}{2} \text{Tr} F^2 - \dim(\mathbf{C}_i), \quad (5.1.27)$$

where

$$r_i = \frac{\text{tr}_{\mathbf{C}_i} F^2}{\text{Tr} F^2} \quad (5.1.28)$$

is depend only on the representation \mathbf{C}_i . The r_i is given by Table 5.1.

$G' \times H \subset G = E_8$	$\mathbf{G} = 248$	$\text{tr}_{\mathbf{C}_i} F^2$
$E_7 \times SU(2)$	$(\mathbf{133}, \mathbf{1}) + (\mathbf{56}, \mathbf{2}) + (\mathbf{1}, \mathbf{3})$	$\text{tr}_3 F^2 = 4\text{tr}_2 F^2$
$E_6 \times SU(3)$	$(\mathbf{78}, \mathbf{1}) + 2(\mathbf{27}, \mathbf{3}) + (\mathbf{1}, \mathbf{8})$	$\text{tr}_8 F^2 = 6\text{tr}_3 F^2$
$SO(12) \times (SU(2) \times SU(2))$	$(\mathbf{66}, (\mathbf{1}, \mathbf{1})) + (\mathbf{32}, (\mathbf{2}, \mathbf{1})) + (\mathbf{32}, (\mathbf{1}, \mathbf{2}))$ $+ (\mathbf{12}, (\mathbf{2}, \mathbf{2})) + (\mathbf{1}, (\mathbf{3}, \mathbf{1})) + (\mathbf{1}, (\mathbf{1}, \mathbf{3}))$	$\text{tr}_{(\mathbf{2}, \mathbf{2})} F^2 = 2(\text{tr}_{(\mathbf{2}, \mathbf{1})} F^2 + \text{tr}_{(\mathbf{1}, \mathbf{2})} F^2)$ $\text{tr}_{(\mathbf{3}, \mathbf{1})} F^2 = 4\text{tr}_{(\mathbf{2}, \mathbf{1})} F^2$
$SO(10) \times SU(4)$	$(\mathbf{45}, \mathbf{1}) + (\mathbf{16}, \mathbf{4}) + (\mathbf{10}, \mathbf{6}) + (\mathbf{1}, \mathbf{15})$	$\text{tr}_6 F^2 = 2\text{tr}_4 F^2$ $\text{tr}_{15} F^2 = 8\text{tr}_4 F^2$
$SO(8) \times SO(8)$	$(\mathbf{28}, \mathbf{1}) + 3(\mathbf{8}, \mathbf{8}) + (\mathbf{1}, \mathbf{28})$	$\text{tr}_{28} F^2 = 6\text{tr}_8 F^2$
$SU(6) \times (SU(2) \times SU(3))$	$(\mathbf{35}, (\mathbf{1}, \mathbf{1})) + (\mathbf{20}, (\mathbf{2}, \mathbf{1})) + 2(\mathbf{15}, (\mathbf{1}, \mathbf{3}))$ $+ 2(\mathbf{6}, (\mathbf{2}, \mathbf{3})) + (\mathbf{1}, (\mathbf{3}, \mathbf{1})) + (\mathbf{1}, (\mathbf{1}, \mathbf{8}))$	$\text{tr}_{(\mathbf{3}, \mathbf{1})} F^2 = 4\text{tr}_{(\mathbf{2}, \mathbf{1})} F^2$ $\text{tr}_{(\mathbf{1}, \mathbf{8})} F^2 = 6\text{tr}_{(\mathbf{1}, \mathbf{3})} F^2$ $\text{tr}_{(\mathbf{2}, \mathbf{3})} F^2 = 3\text{tr}_{(\mathbf{2}, \mathbf{1})} F^2 + 2\text{tr}_{(\mathbf{1}, \mathbf{3})} F^2$
$SU(5) \times SU(5)$	$(\mathbf{24}, \mathbf{1}) + 2(\mathbf{5}, \mathbf{10}) + 2(\mathbf{10}, \mathbf{5}) + (\mathbf{1}, \mathbf{24})$	$\text{tr}_{10} F^2 = 3\text{tr}_5 F^2$ $\text{tr}_{24} F^2 = 10\text{tr}_5 F^2$
$SU(4) \times SO(10)$	$(\mathbf{15}, \mathbf{1}) + (\mathbf{6}, \mathbf{10}) + (\mathbf{4}, \mathbf{16}) + (\mathbf{1}, \mathbf{45})$	$\text{tr}_{16} F^2 = 2\text{tr}_{10} F^2$ $\text{tr}_{45} F^2 = 8\text{tr}_{10} F^2$
$SU(3) \times E_6$	$(\mathbf{8}, \mathbf{1}) + 2(\mathbf{3}, \mathbf{27}) + (\mathbf{1}, \mathbf{78})$	$\text{tr}_{78} F^2 = 4\text{tr}_{27} F^2$
$SU(2) \times E_7$	$(\mathbf{3}, \mathbf{1}) + (\mathbf{2}, \mathbf{56}) + (\mathbf{1}, \mathbf{133})$	$\text{tr}_{133} F^2 = 4\text{tr}_{56} F^2$

Table 5.1: The decompositions of the adjoint representation of E_8 .

When the gauge field F has $12 + n$ instantons in E_8 , the number of the hypermultiplet is given by

$$n_i = 30r_i(12 + n) - \dim(\mathbf{C}_i). \quad (5.1.29)$$

We summarize the numbers of the charged hypermultiplets and the neutral (singlet) hypermultiplets in Table 5.2. Note that H consists of the direct product of the two groups for the cases of $G' = SO(12)$ and $SU(6)$. This is the reason why there is the parameter r in the case of rank 6 in Table 5.2, that is, we denote the instanton numbers of $SU(2)$ and $SU(3)$ as $4 + r$ and $8 + n - r$, respectively.

Let us see the case of $SU(2)$, which we considered in the previous subsection from the

point of view of F-theory. We see that the numbers of the charged and the neutral hypermultiplets in Table 5.2 coincide with $n_{\text{H}}^{(\text{charged})}$ and $n_{\text{H}}^{(\text{neutral})}$ that are derived from the F-theory compactification on the Calabi-Yau three-fold.

Finally, we consider anomaly cancellation in six dimensions. The condition of anomaly cancellation is given by

$$H - V = 273 - 29T, \quad (5.1.30)$$

where H , V and T are the numbers of hypermultiplets, vector multiplets and tensor multiplets, respectively. The tensor multiplet comes from the gravity multiplet in ten dimensions, so that $T = 1$. H includes 20 hypers which come from the gravity multiplet. For each E_8 which has $12 + n$ or $12 - n$ instantons, the conditions of anomaly cancellation are

$$n_{\text{H}} - n_{\text{V}} = 112 + 30n \text{ or } 112 - 30n. \quad (5.1.31)$$

For the $SU(2)$ case, according to (5.1.22), $n_{\text{H}} = 30n + 115$, and $n_{\text{V}} = 3$. We can see that the condition of anomaly cancellation is satisfied.

Gauge group	Charged hypers	Neutral hypers
E_7	$\left(\frac{n+8}{2}\right) \mathbf{56}$	$2n + 21$
$E_6 \times U(1)$	$\left(\frac{n+8}{2}\right) (\mathbf{27} + \mathbf{27} + \mathbf{1} + \mathbf{1})$	$2n + 21$
$SO(12) \times SU(2)$	$\left(\frac{n+8}{2}\right) [(\mathbf{32}, \mathbf{1}) + (\mathbf{12}, \mathbf{2})]$	$2n + 21$
E_6	$(n + 6) \mathbf{27}$	$3n + 28$
$SO(10) \times U(1)$	$(n + 6)(\mathbf{16} + \mathbf{10} + \mathbf{1})$	$3n + 28$
$SU(6) \times SU(2)$	$(n + 6)[(\mathbf{6}, \mathbf{2}) + (\mathbf{15}, \mathbf{1})]$	$3n + 28$
$SO(12)$	$\left(\frac{n+4}{2}\right) \mathbf{32} + (n + 8) \mathbf{12}$	$2n + 18$
$SU(6) \times U(1)$	$\left(\frac{n+4}{2}\right) (\mathbf{15} + \mathbf{15} + \mathbf{1} + \mathbf{1}) + (n + 8)(\mathbf{6} + \mathbf{6})$	$2n + 18$
$SO(10) \times U(1)$	$\left(\frac{n+4}{2}\right) (\mathbf{16} + \mathbf{16}) + (n + 8)(\mathbf{10} + \mathbf{1} + \mathbf{1})$	$2n + 18$
$SO(10)$	$(n + 4) \mathbf{16} + (n + 6) \mathbf{10}$	$4n + 33$
$SU(5) \times U(1)$	$(n + 4)(\mathbf{10} + \mathbf{5} + \mathbf{1}) + (n + 6)(\mathbf{5} + \mathbf{5})$	$4n + 33$
$SO(8) \times U(1)$	$(n + 4)(\mathbf{8}_c + \mathbf{8}_s) + (n + 6)(\mathbf{8}_v + \mathbf{1} + \mathbf{1})$	$4n + 33$
$SU(6)$	$\left(\frac{r}{2}\right) \mathbf{20} + (16 + r + 2n) \mathbf{6} + (2 + n - r) \mathbf{15}$	$3n - r + 21$
$SU(5) \times U(1)$	$\left(\frac{r}{2}\right) (\mathbf{10} + \mathbf{10}) + (16 + r + 2n)(\mathbf{5} + \mathbf{1}) + (2 + n - r)(\mathbf{10} + \mathbf{5})$	$3n - r + 21$
$SO(8)$	$(n + 4)(\mathbf{8}_v + \mathbf{8}_c + \mathbf{8}_s)$	$6n + 44$
$SU(4) \times U(1)$	$(n + 4)[(\mathbf{6} + \mathbf{1} + \mathbf{1}) + (\mathbf{4} + \mathbf{4}) + (\mathbf{4} + \mathbf{4})]$	$6n + 44$
$SU(5)$	$(n + 2) \mathbf{10} + (3n + 16) \mathbf{5}$	$5n + 36$
$SU(4) \times U(1)$	$(n + 2)(\mathbf{6} + \mathbf{4}) + (3n + 16)(\mathbf{4} + \mathbf{1})$	$5n + 36$
$SU(4)$	$(n + 2) \mathbf{6} + (4n + 16) \mathbf{4}$	$8n + 51$
$SU(3) \times U(1)$	$(n + 2)(\mathbf{3} + \mathbf{3}) + (4n + 16)(\mathbf{3} + \mathbf{1})$	$8n + 51$
$SU(3)$	$(6n + 18) \mathbf{3}$	$12n + 66$
$SU(2) \times U(1)$	$(6n + 18)(\mathbf{2} + \mathbf{1})$	$12n + 66$
$SU(2)$	$(6n + 16) \mathbf{2}$	$18n + 83$

Table 5.2: The number of the hypermultiplets.

5.2 Resolutions of Calabi-Yau four-folds from gauge theories

As seen in the previous section, matters arise from codimension-two singularities in the F-theory compactifications. Calabi-Yau three-folds can have codimension-one and two singularities. On the other hand, if we consider more phenomenological physics such as grand unified theories (GUT), we need to deal with Calabi-Yau four-folds in F-theory. The Calabi-Yau four-folds can have not only codimension-one and two but also codimension-three singularities. The codimension-three singularities determine the structure of Yukawa couplings in the four-dimensional theory that is the theory of the 7-branes world-volume.

Supersymmetric gauge theories are a powerful tool for examining structure of geometry. Such gauge theories are realized by string theory compactifications on Calabi-Yau manifolds⁴. Geometry of Calabi-Yau manifolds associates with their moduli spaces. There are many related works. [65–68, 89–101]

In this section, we consider F/M duality. F-theory compactifications on Calabi-Yau four-folds are dual to M-theory compactifications on Calabi-Yau four-folds, which present three-dimensional $\mathcal{N} = 2$ supersymmetric gauge theories. The geometry of the Calabi-Yau four-fold determine the structure of the gauge theory. In particular, the condimension-one singularity decides the gauge group, and the network of the small resolution corresponds to the structure of the classical Coulomb phase since the resolution corresponds to the symmetry breaking [65, 100–102].

As an example, we consider $SU(5)$ gauge theory with N_f chiral multiplets in **5** and **10** representation. We set that masses of the chiral multiplets are zero. In addition, we assume that there is no classical Chern-Simons term. The vector multiplet in the adjoint representation includes a real scalar field ϕ . In general, $SU(5)$ gauge group breaks to $U(1)$ ⁴ by the VEVs of the scalar. The Coulomb branch is described by the Weyl chamber. We choose the fundamental Weyl chamber as

$$\vec{\alpha}_i \cdot \vec{\phi} > 0, \tag{5.2.1}$$

⁴ G_2 and $Spin(7)$ manifolds are also considered, but we do not discuss such manifolds.

where $\vec{\alpha}_i$ ($i = 1, 2, 3, 4$) are the simple roots of $SU(5)$:

$$\vec{\alpha}_1 = (2, -1, 0, 0), \quad \vec{\alpha}_2 = (-1, 2, -1, 0), \quad \vec{\alpha}_3 = (0, -1, 2, -1), \quad \vec{\alpha}_4 = (0, 0, -1, 2). \quad (5.2.2)$$

$\vec{\phi} = (\phi^1, \phi^2, \phi^3, \phi^4)$ is the VEV in the Cartan subalgebra of $SU(5)$.

Now we have the chiral multiplets, which make a substructure in the Coulomb branch. The Lagrangian includes the mass terms of the chiral multiplets $Q^{(f)}$:

$$\mathcal{L}_{\text{mass}} = \sum_f \left| \phi Q^{(f)} \right|^2 = \sum_f \left| \vec{\phi} \cdot \vec{\omega}_f \right|^2 \left| Q^{(f)} \right|^2, \quad (5.2.3)$$

where $f = \mathbf{5}$ or $\mathbf{10}$ representation and $\vec{\omega}_f$ is its weight. Note that when $\vec{\phi} \cdot \vec{\omega}_f = 0$, the corresponding matter becomes massless. In the sense of geometry of Calabi-Yau manifolds, it corresponds to the singularity with higher-codimensions.

Let us classify the region of the Coulomb branch. The region is divided by the zero loci of $\vec{\phi} \cdot \vec{\omega}_f$, namely, the region is characterized by $\vec{\phi} \cdot \vec{\omega}_f > 0$ or $\vec{\phi} \cdot \vec{\omega}_f < 0$. However, not all the regions are allowed since we are working on the fundamental Weyl chamber (5.2.1). We show the consistent phases for $\mathbf{5}$ representation in Table 5.3 and for $\mathbf{10}$ representation in Table 5.4. We have four phases in $\mathbf{5}$ representation and eight phases in $\mathbf{10}$ representation. When we obtain the tables, we use the weights for $\mathbf{5}$ representation,

$$\begin{aligned} \vec{\omega}_1^{\mathbf{5}} &= (1, 0, 0, 0), & \vec{\omega}_2^{\mathbf{5}} &= (-1, 1, 0, 0), & \vec{\omega}_3^{\mathbf{5}} &= (0, -1, 1, 0), \\ \vec{\omega}_4^{\mathbf{5}} &= (0, 0, -1, 1), & \vec{\omega}_5^{\mathbf{5}} &= (0, 0, 0, -1), \end{aligned} \quad (5.2.4)$$

and for $\mathbf{10}$ representation,

$$\begin{aligned} \vec{\omega}_1^{\mathbf{10}} &= (0, 1, 0, 0), & \vec{\omega}_2^{\mathbf{10}} &= (1, -1, 1, 0), & \vec{\omega}_3^{\mathbf{10}} &= (1, 0, -1, 1), & \vec{\omega}_4^{\mathbf{10}} &= (1, 0, 0, -1), \\ \vec{\omega}_5^{\mathbf{10}} &= (-1, 0, 1, 0), & \vec{\omega}_6^{\mathbf{10}} &= (-1, 1, -1, 1), & \vec{\omega}_7^{\mathbf{10}} &= (-1, 1, 0, -1), \\ \vec{\omega}_8^{\mathbf{10}} &= (0, -1, 0, 1), & \vec{\omega}_9^{\mathbf{10}} &= (0, -1, 1, -1), & \vec{\omega}_{10}^{\mathbf{10}} &= (0, 0, -1, 0). \end{aligned} \quad (5.2.5)$$

Since we have the matters in both $\mathbf{5}$ and $\mathbf{10}$ representation in the gauge theory, we need to combine the two phases for $\mathbf{5}$ representation and for $\mathbf{10}$ representation. However, not all combinations are allowed. For instance, let us consider the combination of \mathbf{I}_5 and \mathbf{I}_{10} . We find that the phase \mathbf{I}_5 implies

$$0 < \phi^1 < \phi^2 < \phi^3 < \phi^4. \quad (5.2.6)$$

	$\vec{\omega}_1^5$	$\vec{\omega}_2^5$	$\vec{\omega}_3^5$	$\vec{\omega}_4^5$	$\vec{\omega}_5^5$
I₅	+	+	+	+	-
II₅	+	+	+	-	-
III₅	+	+	-	-	-
IV₅	+	-	-	-	-

Table 5.3: The phases for **5** representation.

	$\vec{\omega}_1^{10}$	$\vec{\omega}_2^{10}$	$\vec{\omega}_3^{10}$	$\vec{\omega}_4^{10}$	$\vec{\omega}_5^{10}$	$\vec{\omega}_6^{10}$	$\vec{\omega}_7^{10}$	$\vec{\omega}_8^{10}$	$\vec{\omega}_9^{10}$	$\vec{\omega}_{10}^{10}$
I₁₀	+	+	+	+	+	+	+	-	-	-
II₁₀	+	+	+	+	+	+	-	-	-	-
III₁₀	+	+	+	+	+	-	-	-	-	-
IV₁₀	+	+	+	+	-	-	-	-	-	-
V₁₀	+	+	+	-	+	+	-	+	-	-
VI₁₀	+	+	+	-	+	+	-	-	-	-
VII₁₀	+	+	+	-	+	-	-	-	-	-
VIII₁₀	+	+	-	-	+	-	-	-	-	-

Table 5.4: The phases for **10** representation.

On the other hand, the condition $\vec{\phi} \cdot \vec{\omega}_4^{10} > 0$ in the phase **I₁₀** provides

$$\phi^1 > \phi^4, \quad (5.2.7)$$

so that the combination of **I₅** and **I₁₀** is empty. The combinations that are not empty are shown in Table 5.5. We have twelve phases, which correspond to the different resolutions of the Calabi-Yau four-fold in the geometric sense.

	1	2	3	4	5	6	7	8	9	10	11	12
5	III ₅	III ₅	II ₅	III ₅	III ₅	IV ₅	I ₅	II ₅	II ₅	III ₅	II ₅	II ₅
10	I ₁₀	II ₁₀	III ₁₀	III ₁₀	IV ₁₀	IV ₁₀	V ₁₀	V ₁₀	VI ₁₀	VI ₁₀	VII ₁₀	VIII ₁₀

Table 5.5: The possible phases.

The boundaries of the phases are codimension-one surface where $\vec{\phi} \cdot \vec{g} = 0$, that is, the phases are cones. The cones are defined as $\vec{\phi} \cdot \vec{g}_i > 0$, where \vec{g}_i with $i = 1, 2, 3, 4$ are the four generators. For each phase, we find the generators in Table 5.6. For example, the phase 1 is represented by

$$\phi \cdot (2, -1, 0, 0) > 0, \phi \cdot (0, -1, 2, -1) > 0, \phi \cdot (0, 0, -1, 2) > 0, \phi \cdot (-1, 1, 0, -1) > 0. \quad (5.2.8)$$

Phase	Generators
1	(2, -1, 0, 0), (0, -1, 2, -1), (0, 0, -1, 2), (-1, 1, 0, -1)
2	(0, -1, 2, -1), (1, 0, 0, -1), (-1, 1, -1, 1), (1, -1, 0, 1)
3	(-1, 2, -1, 0), (0, 0, -1, 2), (1, 0, 0, -1), (0, -1, 1, 0)
4	(0, 0, -1, 2), (-1, 0, 1, 0), (1, -1, 1, -1), (0, 1, -1, 0)
5	(0, -1, 2, -1), (0, 0, -1, 2), (-1, 1, 0, 0), (1, 0, -1, 0)
6	(-1, 2, -1, 0), (0, -1, 2, -1), (0, 0, -1, 2), (1, -1, 0, 0)
7	(2, -1, 0, 0), (-1, 2, -1, 0), (0, -1, 2, -1), (0, 0, -1, 1)
8	(2, -1, 0, 0), (-1, 2, -1, 0), (0, 0, 1, -1), (0, -1, 0, 1)
9	(2, -1, 0, 0), (-1, 1, -1, 1), (0, -1, 1, 0), (0, 1, 0, -1)
10	(2, -1, 0, 0), (0, -1, 2, -1), (-1, 0, 0, 1), (0, 1, -1, 0)
11	(-1, 2, -1, 0), (1, 0, -1, 1), (-1, 0, 0, 1), (1, -1, 1, -1)
12	(2, -1, 0, 0), (-1, 2, -1, 0), (0, 0, -1, 2), (-1, 0, 1, -1)

Table 5.6: The generators of the phases.

The two phases that share the same boundary are adjacent. The two adjacent phases have the generator with the opposite sign each other. For example, the phase 1 and 2 are adjacent. The phase 1 has the generator $\vec{g}_4^{(1)} = (-1, 1, 0, -1)$, and the phase 2 has $\vec{g}_4^{(2)} = (1, -1, 0, 1)$, namely, $\vec{g}_4^{(1)} = -\vec{g}_4^{(2)}$. The phase 1 and 2 share the same boundary represented by

$$\vec{\phi} \cdot (-1, 1, 0, -1) = 0. \quad (5.2.9)$$

In Fig. 5.1, We draw the network of the relations between each phase. The connected two

phases are adjacent. In the Calabi-Yau four-fold, the adjacent phases are related by flop transitions.

Investigating the Coulomb branch of three-dimensional $\mathcal{N} = 2$ gauge theories, we can classify resolutions of Calabi-Yau four-folds. In the case of $SU(5)$, we find the twelve phases. Each phase corresponds to the different resolutions of the Calabi-Yau manifold. All of the resolutions are realized by the toric resolutions, the algebraic resolutions and its flop transitions in [65]. The allowed regions of the Coulomb branch are completely classified by the decorated box graph [66–68]. The box graph is constructed by boxes with signs (or color).

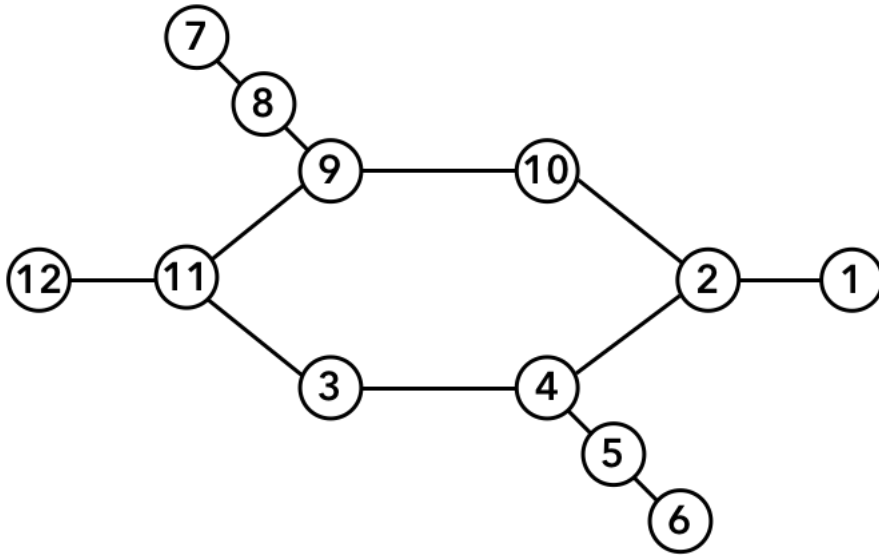


Fig. 5.1: The network of phases of $SU(5)$ gauge theory.

Chapter 6

Half-hypermultiplets and incomplete/complete resolutions

6.1 Half-hypermultiplets in six-dimensional F-theory

Half-hypermultiplets arise when the unbroken gauge group is $SU(6)$, $SO(12)$ or E_7 [53–55, 57, 60]. These models can be systematically obtained by tuning the complex structure of the $SU(5)$ model.

We start with the six-dimensional compactification on F-theory on an elliptically Calabi-Yau three-fold over a Hirzebruch surface F_n [53, 54]. Let z , s be affine coordinates of the fiber and base P^1 's, respectively¹. The Weierstrass equation

$$y^2 = x^3 + f(z, s)x + g(z, s) \tag{6.1.1}$$

develops an $SU(5)$ singularity if [55]

$$f(z, s) = -3h_{n+2}^4 + 12h_{n+2}^2 H_{n+4} z - 12(H_{n+4}^2 - h_{n+2} q_{n+6}) z^2 + f_{n+8} z^3 + f_8 z^4, \tag{6.1.2}$$

$$\begin{aligned} g(z, s) = & 2h_{n+2}^6 - 12h_{n+2}^4 H_{n+4} z + (24h_{n+2}^2 H_{n+4}^2 - 12h_{n+2}^3 q_{n+6}) z^2 \\ & + (-f_{n+8} h_{n+2}^2 + 24h_{n+2} H_{n+4} q_{n+6} - 16H_{n+4}^3) z^3 \\ & + (-f_8 h_{n+2}^2 + 2f_{n+8} H_{n+4} + 12q_{n+6}^2) z^4 + g_{n+12} z^5 + g_{12} z^6, \end{aligned} \tag{6.1.3}$$

¹In Chapter 5, we denoted s as z' .

where h_{n+2} , H_{n+4} , q_{n+6} , f_{n+8} and g_{n+12} are polynomials of s of degrees specified by the subscripts. This Calabi-Yau three-fold admits a K3 fibration, and we work with one of the rational elliptic surfaces in the stable degeneration limit of the K3 so that the orders of the polynomials $f(z, s)$ and $g(z, s)$ are truncated at z^4 and z^6 , respectively. This suffices since the anomalies cancel for each E_8 gauge group, and also we are interested in the local structure of the singularity. x and y are then taken to be sections of $\mathcal{O}(2(-K_{F_n} - C_0))$ and $\mathcal{O}(3(-K_{F_n} - C_0))$, where C_0 is a divisor class with $C_0^2 = -n$, satisfying $-K_{F_n} = 2C_0 + (2+n)f$ with the fiber class f . Similar modifications are necessary for $f(z, z')$ and $g(z, z')$. This deviation from the anti-canonical class (and hence from a Calabi-Yau) is because we consider a rational-elliptic-surface fibration.

The Weierstrass equation (6.1.1) with (6.1.2) and (6.1.3) can be written in Tate's form as

$$y'^2 + x'^3 + \alpha_4 z^4 x' + \alpha_6 z^6 + a_0 z^5 + a_2 z^3 x' + a_3 z^2 y' + a_4 z x'^2 + a_5 x' y' = 0 \quad (6.1.4)$$

with

$$\begin{aligned} a_0 &= g_{n+12} - 2H_{n+4}f_8, & a_2 &= f_{n+8}, & a_3 &= 4\sqrt{3}iq_{n+6}, \\ a_4 &= -6H_{n+4}, & a_5 &= 2\sqrt{3}ih_{n+2}, & \alpha_4 &= f_8, & \alpha_6 &= g_{12}. \end{aligned} \quad (6.1.5)$$

For completeness we write x, y in (6.1.1) in terms of x', y' in (6.1.4):

$$\begin{aligned} x &= x' + \frac{1}{3} \left(a_4 z - \frac{1}{4} a_5^2 \right), \\ y &= i \left(y' + \frac{1}{2} (a_5 x + a_3 z^2) \right). \end{aligned} \quad (6.1.6)$$

6.1.1 $SU(6)$

To obtain an equation for $SU(6)$ gauge group, which yields half-hypermultiplets, we set [55]

$$\begin{aligned} h_{n+2} &= t_r h_{n+2-r}, \\ H_{n+4} &= t_r H_{n+4-r}, \\ q_{n+6} &= u_{r+4} h_{n+2-r}, \\ f_{n+8} &= t_r f_{n+8-r} - 12u_{r+4} H_{n+4-r}, \\ g_{n+12} &= 2(u_{r+4} f_{n-r+8} + f_8 t_r H_{n-r+4}). \end{aligned} \quad (6.1.7)$$

Then the spectral cover factorizes as

$$\begin{aligned} 0 &= a_0 z^5 + a_2 z^3 x' + a_3 z^2 y' + a_4 z x'^2 + a_5 x' y' \\ &= (x' t_r + 2z^2 u_{r+4}) \left(z^3 f_{n-r+8} + 2i\sqrt{3} y' h_{n-r+2} - 6z x' H_{n-r+4} \right), \end{aligned} \quad (6.1.8)$$

indicating that the $SU(5)$ instanton is reduced to an $SU(3) \times SU(2)$ instanton in the heterotic dual. In this specification $f(z, z')$ and $g(z, z')$ become

$$\begin{aligned} f_{SU(6)}(z, s) &= -3t_r^4 h_{n-r+2}^4 + 12zt_r^3 h_{n-r+2}^2 H_{n-r+4} + z^2 (12t_r u_{r+4} h_{n-r+2}^2 - 12t_r^2 H_{n-r+4}^2) \\ &\quad + z^3 (t_r f_{n-r+8} - 12u_{r+4} H_{n-r+4}) + f_8 z^4, \end{aligned} \quad (6.1.9)$$

and

$$\begin{aligned} g_{SU(6)}(z, s) &= 2t_r^6 h_{n-r+2}^6 - 12zt_r^5 h_{n-r+2}^4 H_{n-r+4} \\ &\quad + z^2 (24t_r^4 h_{n-r+2}^2 H_{n-r+4}^2 - 12t_r^3 u_{r+4} h_{n-r+2}^4) \\ &\quad + z^3 (-t_r^3 f_{n-r+8} h_{n-r+2}^2 + 36t_r^2 u_{r+4} h_{n-r+2}^2 H_{n-r+4} - 16t_r^3 H_{n-r+4}^3) \\ &\quad + z^4 (-f_8 t_r^2 h_{n-r+2}^2 + 2t_r^2 f_{n-r+8} H_{n-r+4} + 12u_{r+4}^2 h_{n-r+2}^2 - 24t_r u_{r+4} H_{n-r+4}^2) \\ &\quad + z^5 (2f_8 t_r H_{n-r+4} + 2u_{r+4} f_{n-r+8}) + g_{12} z^6. \end{aligned} \quad (6.1.10)$$

The discriminant reads

$$\begin{aligned} \Delta_{SU(6)} &= 9z^6 t_r^3 h_{n-r+2}^4 (t_r^3 (12g_{12} h_{n-r+2}^2 - f_{n-r+8}^2) \\ &\quad + t_r^2 (-24f_8 u_{r+4} h_{n-r+2}^2 - 24u_{r+4} f_{n-r+8} H_{n-r+4}) \\ &\quad - 144t_r u_{r+4}^2 H_{n-r+4}^2 - 96u_{r+4}^3 h_{n-r+2}^2) + O(z^7). \end{aligned} \quad (6.1.11)$$

Thus the Weierstrass model with (6.1.9),(6.1.10) indeed has a codimension-one $SU(6)$ singularity along $z = 0$.

The zero loci of t_r are the points where the $SU(6)$ singularity is enhanced to E_6 , those of h_{n-r+2} are the ones to D_6 , and those of the remaining factor of degree $2n + r + 16$ are the ones to A_6 . They respectively yield r *half-hypermultiplets* in **20**, $n - r + 2$ hypermultiplets in **15** and $2n + r + 16$ hypermultiplets in **6**.

The number of the complex structure moduli is $3n - r + 21$, which satisfies the anomaly-free constraint

$$\begin{aligned} n_H - n_V &= 20 \cdot \frac{r}{2} + 15(n - r + 2) + 6(2n + r + 16) + 3n - r + 21 - 35 \\ &= 30n + 112. \end{aligned} \quad (6.1.12)$$

Note that this condition does not hold if the multiplets in **20** are ordinary hypermultiplets.

6.1.2 $SO(12)$

To further obtain an equation for $SO(12)$ gauge group, one only needs to set $h_{n+2-r} = 0$ in (6.1.7). The spectral cover is now

$$(x't_r + 2z^2u_{r+4}) \left(x'H_{n-r+4} - \frac{1}{6}z^2f_{n-r+8} \right) = 0. \quad (6.1.13)$$

These factors are in the same form, corresponding to two $SU(2)$'s of the instanton gauge group of the heterotic theory.

Then $f(z, s)$ and $g(z, s)$ are

$$f_{SO(12)}(z, s) = -12z^2t_r^2H_{n-r+4}^2 + z^3(t_rf_{n-r+8} - 12u_{r+4}H_{n-r+4}) + f_8z^4, \quad (6.1.14)$$

and

$$g_{SO(12)}(z, s) = -16z^3t_r^3H_{n-r+4}^3 + 2z^4(t_r^2f_{n-r+8}H_{n-r+4} - 12t_ru_{r+4}H_{n-r+4}^2) + 2z^5(f_8t_rH_{n-r+4} + u_{r+4}f_{n-r+8}) + g_{12}z^6. \quad (6.1.15)$$

The discriminant is given by

$$\Delta_{SO(12)} = -36z^8t_r^2H_{n-r+4}^2(t_rf_{n-r+8} + 12u_{r+4}H_{n-r+4})^2 + O(z^9). \quad (6.1.16)$$

The zero loci of both t_r and H_{n-r+4} give rise to E_7 singularities to yield $n + 4$ half-hypermultiplets. The loci of the remaining factor are A_7 singularities, giving $n + 8$ hypers in **12**. With additional neutral hypermultiplets from the $2n + 18$ complex structure moduli, we have

$$\begin{aligned} n_H - n_V &= 32 \cdot \frac{n+4}{2} + 12(n+8) + 2n + 18 - 66 \\ &= 30n + 112 \end{aligned} \quad (6.1.17)$$

as it should be. Again, if **32** is not a half-hyper, the anomaly does not cancel.

6.1.3 E_7

Finally, the E_7 model can be obtained by setting $H_{n-r+4} = 0$ in the $SO(12)$ model. This amounts to set $h_{n+2} = H_{n+4} = q_{n+6} = 0$ in the $SU(5)$ model. The gauge group of the heterotic vector bundle is $SU(2)$. $f(z, s)$ and $g(z, s)$ are simply given by

$$f_{E_7}(z, s) = f_{n+8}z^3 + f_8z^4, \quad (6.1.18)$$

and

$$g_{E_7}(z, s) = g_{n+12}z^5 + g_{12}z^6. \quad (6.1.19)$$

The discriminant is

$$\Delta_{E_7} = 4f_{n+8}^3z^9 + O(z^{10}) \quad (6.1.20)$$

implies that $n + 8$ half-hypermultiplets in **56** of E_7 arise. Again they must be half-hyper as

$$\begin{aligned} n_H - n_V &= 56 \cdot \frac{n+8}{2} + 2n + 21 - 133 \\ &= 30n + 112. \end{aligned} \quad (6.1.21)$$

6.2 Incomplete resolution: $D_6 \rightarrow E_7$

In this section, we concentrate on the incomplete resolution of the case of $D_6 \rightarrow E_7$ [69]. We consider a Weierstrass model on a base two-fold B_2 with local coordinates $\{z, s\}$, where the codimension one singularity arises along $z = 0$ and the codimension-two singularity arises at $s = 0$ on the $z = 0$ complex line.

6.2.1 Blowing up p_1 first

We consider the model

$$\Phi(x, y, z, s) = -y^2 + x^3 + f(z, s)x + g(z, s) = 0, \quad (6.2.1)$$

where

$$\begin{aligned} f(z, s) &= -3s^2z^2 + z^3, \\ g(z, s) &= 2s^3z^3 - sz^4. \end{aligned} \quad (6.2.2)$$

At $s \neq 0$, the orders of f , g and the discriminant Δ in z are $(2, 3, 6)$, while at $s = 0$, they are $(3, \infty, 9)$. Therefore (6.2.2) describes the enhancement $I_2^* \rightarrow IV^*$ of the Kodaira type, satisfying the requirement.

1st blow up

With (6.2.2), Equation (6.2.1) reads

$$\Phi(x, y, z, s) = xz^2(z - 3s^2) + sz^3(2s^2 - z) + x^3 - y^2 = 0. \quad (6.2.3)$$

This model has a codimension-one singularity at $(0, 0, 0, s)$. We blow up this by replacing the complex line $(x, y, z) = (0, 0, 0)$ with $P^2 \times \mathbb{C}$ in \mathbb{C}^4 by passing to the following charts corresponding to three affine patches of P^2 for fixed s .

Chart 1_x

The Calabi-Yau three-fold that is blown up is given by

$$\Phi(x, xy_1, xz_1, s) = x^2\Phi_x(x, y_1, z_1, s), \quad (6.2.4)$$

where

$$\Phi_x(x, y_1, z_1, s) = x^2(z_1^3 - sz_1^4) + x(sz_1 - 1)^2(2sz_1 + 1) - y_1^2. \quad (6.2.5)$$

The exceptional curve \mathcal{C}_1 and the singularities are

$$\mathcal{C}_1 \text{ in } 1_x : \quad x = 0, \quad y_1 = 0. \quad (6.2.6)$$

$$\text{Singularities :} \quad (x, y_1, z_1, s) = \left(0, 0, \frac{1}{s}, s\right), \left(0, 0, -\frac{1}{2s}, s\right). \quad (6.2.7)$$

These singularities are of codimension-one, which we refer to as p_1 and q_1 , respectively.

Chart 1_y

$$\Phi(x_1y, y, yz_1, s) = y^2\Phi_y(x_1, y, z_1, s), \quad (6.2.8)$$

$$\Phi_y(x_1, y, z_1, s) = 2s^3yz_1^3 + x_1yz_1^2(yz_1 - 3s^2) - sy^2z_1^4 + x_1^3y - 1, \quad (6.2.9)$$

$$\mathcal{C}_1 \text{ in } 1_y : \quad \text{Invisible in this patch,} \quad (6.2.10)$$

$$\text{Singularities :} \quad \text{None.} \quad (6.2.11)$$

In chart 1_y , the exceptional curve cannot be seen, and hence has no singularity.

Chart 1_z

$$\Phi(x_1z, y_1z, z, s) = z^2\Phi_z(x_1, y_1, z, s), \quad (6.2.12)$$

$$\Phi_z(x_1, y_1, z, s) = z(2s^3 - 3s^2x_1 - sz + x_1^3 + x_1z) - y_1^2 \quad (6.2.13)$$

$$\mathcal{C}_1 \text{ in } 1_z : \quad : z = 0, y_1 = 0. \quad (6.2.14)$$

$$\text{Singularities : } (x_1, y_1, z, s) = (s, 0, 0, s), (-2s, 0, 0, s). \quad (6.2.15)$$

The two singularities are the same as (6.2.7). The first singularity is p_1 , while the second is q_1 .

2nd blow up

In the 1st blow up, we have found two singularities. There are two ways to resolve them. Either we blow up at p_1 first, or we do at q_1 first. In this subsection, let us blow up at p_1 first.

In order to blow up the singularities of $\Phi_z(x_1, y_1, z, s) = 0$ at p_1 , we shift the coordinate x_1 so that the singularity comes to $(0, 0, 0, s)$. Defining

$$\Psi_z(\tilde{x}_1, y_1, z, s) = \Phi_z(\tilde{x}_1 + s, y_1, z, s), \quad (6.2.16)$$

the singularities of $\Psi_t(\tilde{x}_1, y_1, z, s)$ are now at $(0, 0, 0, s)$ ($= p_1$) and $(-3s, 0, 0, s)$ ($= q_1$). We blow up the singularities of $\Psi_z(\tilde{x}_1, y_1, z, s)$ at $(0, 0, 0, s)$.

Chart 2_{zx}

$$\Psi_z(\tilde{x}_1, \tilde{x}_1y_2, \tilde{x}_1z_2, s) = \tilde{x}_1^2\Psi_{zx}(\tilde{x}_1, y_2, z_2, s), \quad (6.2.17)$$

$$\Psi_{zx}(\tilde{x}_1, y_2, z_2, s) = \tilde{x}_1z_2(3s + \tilde{x}_1 + z_2) - y_2^2. \quad (6.2.18)$$

$$\mathcal{C}_2 \text{ in } 2_{zx} : \quad \tilde{x}_1 = 0, y_2 = 0. \quad (6.2.19)$$

$$\text{Singularities : } (\tilde{x}_1, y_2, z_2, s) = (0, 0, 0, s), (0, 0, -3s, s), (-3s, 0, 0, s). \quad (6.2.20)$$

We find three singularities in this chart, and we name the first singularity $(0, 0, 0, s)$ as q_2 and the second one $(0, 0, -3s, s)$ as r_2 , respectively. The third one is the same as q_1 .

Chart 2_{zy}

In this chart, we do not have singularities.

Chart 2_{zz}

$$\Psi_z(\tilde{x}_2 z, y_2 z, z, s) = z^2 \Psi_{zz}(\tilde{x}_2, y_2, z, s), \quad (6.2.21)$$

$$\Psi_{zz}(\tilde{x}_2, y_2, z, s) = \tilde{x}_2 z (3s\tilde{x}_2 + \tilde{x}_2^2 z + 1) - y_2^2, \quad (6.2.22)$$

$$\mathcal{C}_2 \text{ in } 2_{zz} : \quad z = 0, \quad y_2 = 0, \quad (6.2.23)$$

$$\text{Singularities : } (\tilde{x}_2, y_2, z, s) = (0, 0, 0, s), \quad \left(-\frac{1}{3s}, 0, 0, s\right). \quad (6.2.24)$$

We observe two singularities. The former, we denote as q_2 , is one which can only be seen in this chart, while the latter is r_2 already seen in chart 2_{zx} .

3rd blow up

We blow up the singularities of $\Psi_{zx}(\tilde{x}_1, y_2, z_2, s) = 0$ at p_2 :

Chart 3_{zxx}

$$\Psi_{zx}(\tilde{x}_1, \tilde{x}_1 y_3, \tilde{x}_1 z_3, s) = \tilde{x}_1^2 \Psi_{zxx}(\tilde{x}_1, y_3, z_3, s), \quad (6.2.25)$$

$$\Psi_{zxx}(\tilde{x}_1, y_3, z_3, s) = z_3 (3s + \tilde{x}_1 z_3 + \tilde{x}_1) - y_3^2, \quad (6.2.26)$$

$$\mathcal{C}_3 \text{ in } 3_{zxx} : \quad \tilde{x}_1 = 0, \quad y_3^2 = 3s z_3, \quad (6.2.27)$$

$$\text{Singularities : } (\tilde{x}_1, y_3, z_3, s) = (-3s, 0, 0, s). \quad (6.2.28)$$

The singularity is q_1 , which we have already seen in Chart 1_x and 1_z . If $s \neq 0$, this singularity is not on the exceptional curve \mathcal{C}_3 .

Chart $\mathfrak{3}_{zzz}$

$$\Psi_{zx}(\tilde{x}_3 z_2, y_3 z_2, z_2, s) = z_2^2 \Psi_{zzz}(\tilde{x}_3, y_3, z_2, s), \quad (6.2.29)$$

$$\Psi_{zzz}(\tilde{x}_3, y_3, z_2, s) = 3s\tilde{x}_3 + \tilde{x}_3(\tilde{x}_3 + 1)z_2 - y_3^2, \quad (6.2.30)$$

$$\mathcal{C}_3 \text{ in } \mathfrak{3}_{zzz} : \quad z_2 = 0, \quad y_3^2 = 3s\tilde{x}_3, \quad (6.2.31)$$

$$\text{Singularities : } (\tilde{x}_3, y_3, z_2, s) = (0, 0, -3s, s) = r_2. \quad (6.2.32)$$

This singularity is also not on \mathcal{C}_3 when $s \neq 0$.

Therefore, there are no singularities on \mathcal{C}_3 when $s \neq 0$. This is the reason why the resolution is incomplete; in the complete case there appears another codimension-two singularity on \mathcal{C}_3 so that the intersection diagram acquires an additional node to comprise the E_7 Dynkin diagram.

The remaining singularities are resolved by blowing up at r_2 , q_1 and q_2 , which are all codimension-one. Since r_2 and q_1 are different points on \mathcal{C}_3 , while q_2 is not on \mathcal{C}_3 but on \mathcal{C}_2 , they can be independently blown up.

The whole process of blowing up is summarized in Table 6.1.

	1st blow up	2nd blow up	3rd blow up	4th blow up
$\overset{\circ}{p}_0 \rightarrow$	$\overset{\circ}{p}_1 (s : 0 : 1) \rightarrow$ $q_1 (-2s : 0 : 1)$	$\overset{\circ}{p}_2 (1 : 0 : 0) \text{ (in } 2_{zx}) \rightarrow$ $q_1 (1 : 0 : 0) (\tilde{x}_1 = -3s)$ $r_2(1 : 0 : -3s)$ $\overset{\circ}{q}_2 (0 : 0 : 1) \text{ (in } 2_{zz}) \rightarrow$	regular $\overset{\circ}{q}_1 (1 : 0 : 0) (\tilde{x}_1 = -3s) \rightarrow$ $\overset{\circ}{r}_2 (0 : 0 : 1) (z_2 = -3s) \rightarrow$ regular	regular regular

Table 6.1: The incomplete case when p_1 is blown up first. The singularities appearing at each step of the process are shown with their homogeneous coordinates on P^2 . The ones marked by a circle are those blown up at the subsequent processes. p_0 denotes the original singularity on the fiber. The notes in the parentheses (such as $\tilde{x}_1 = -3s$ for q_1) imply that they are not generically (*i.e.* unless $s \neq 0$) the points on the P^2 arising at the respective step of the blowing-up process.

6.2.2 Exceptional curves at $s = 0$: change from a root into a weight

Their intersection diagram is D_6 for $s \neq 0$ (upper diagram in Fig. 6.1). On the other hand, when $s = 0$, the singular point r_2 coincides with the intersection of \mathcal{C}_2 and \mathcal{C}_3 . q_1 also coincides with the intersection of \mathcal{C}_1 and \mathcal{C}_3 . Then the exceptional curve arising from the blowing up at r_2 “bridges” between \mathcal{C}_2 and \mathcal{C}_3 , and the one at q_1 does between \mathcal{C}_1 and \mathcal{C}_3 . Writing the exceptional curves for $s = 0$ as δ_i ($i = 1, 2, 3$), δ_{r_2} , δ_{q_1} and δ_{q_2} , we can express them in terms of \mathcal{C} ’s as in [57]:

$$\mathcal{C}_{q_1} = \delta_{q_1}, \quad \mathcal{C}_1 = \delta_1, \quad \mathcal{C}_2 = \delta_2, \quad \mathcal{C}_3 = 2\delta_3 + \delta_{q_1} + \delta_{r_2}, \quad \mathcal{C}_{r_2} = \delta_{r_2}, \quad \mathcal{C}_{q_2} = \delta_{q_2}. \quad (6.2.33)$$

These expressions can be found by carefully up-lifting \mathcal{C} ’s to the chart introduced in a further blow-up and taking the $s \rightarrow 0$ limit. For instance, \mathcal{C}_{r_2} is the exceptional curve arising from the blow-up at r_2 :

Chart 4_{zxzx}

$$\Upsilon_{zxz}(\tilde{x}_3, y_3, \tilde{z}_2, s) = \Psi_{zxz}(\tilde{x}_3, y_3, \tilde{z}_2 - 3s, s), \quad (6.2.34)$$

$$\begin{aligned} \Upsilon_{zxz}(\tilde{x}_3, \tilde{x}_3 y_4, \tilde{x}_3 \tilde{z}_4, s) &= \tilde{x}_3^2 \Upsilon_{zxzx}(\tilde{x}_3, y_4, \tilde{z}_4, s) \\ &= \tilde{x}_3^2 (\tilde{x}_3 \tilde{z}_4 - 3s + \tilde{z}_4 - y_4^2), \end{aligned} \quad (6.2.35)$$

$$\mathcal{C}_{r_2} \text{ in } 4_{zxzx} : \quad \tilde{x}_3 = 0, \quad y_4^2 = \tilde{z}_4 - 3s. \quad (6.2.36)$$

$$\text{Singularities :} \quad \text{None.} \quad (6.2.37)$$

δ_{r_2} is the exceptional curve obtained by taking the $s \rightarrow 0$ limit in \mathcal{C}_{r_2} :

$$\delta_{r_2} \text{ in } 4_{zxzx} : \quad \tilde{x}_3 = 0, \quad y_4^2 = \tilde{z}_4. \quad (6.2.38)$$

On the other hand, \mathcal{C}_3 is

$$z_2 = 0, \quad y_3^2 = 3s\tilde{x}_3 \quad (6.2.39)$$

in Chart 3_{zxz} , and hence $y_4^2 = \tilde{z}_4$ in Chart 4_{zxzx} ; this coincides with δ_{r_2} (6.2.38). Thus we conclude that \mathcal{C}_3 “contains” δ_{r_2} . Likewise, we can verify that \mathcal{C}_3 also contains δ_{q_1} . Finally, \mathcal{C}_3 reduces in the $s \rightarrow 0$ limit to $y_3^2 = 0$ which has multiplicity two, we obtain the expression for \mathcal{C}_3 in (6.2.33).

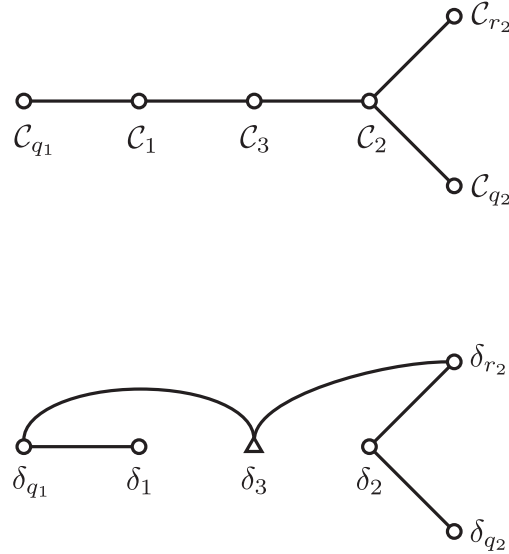


Fig. 6.1: The intersection diagrams of the exceptional curve \mathcal{C} 's and δ 's. We blew up the singularity p_1 first.

Using the fact that the intersection matrix of \mathcal{C} 's is the minus of the $SO(12)$ Cartan matrix:

$$-\mathcal{C}_I \cdot \mathcal{C}_J = \begin{pmatrix} 2 & -1 & 0 & 0 & 0 & 0 \\ -1 & 2 & -1 & 0 & 0 & 0 \\ 0 & -1 & 2 & -1 & 0 & 0 \\ 0 & 0 & -1 & 2 & -1 & -1 \\ 0 & 0 & 0 & -1 & 2 & 0 \\ 0 & 0 & 0 & -1 & 0 & 2 \end{pmatrix}, \quad (6.2.40)$$

where $I, J = q_1, 1, 3, 2, r_2, q_2$. We can obtain by using (6.2.33) the intersection matrix of δ 's:

$$-\delta_I \cdot \delta_J = \begin{pmatrix} 2 & -1 & -1 & 0 & 0 & 0 \\ -1 & 2 & 0 & 0 & 0 & 0 \\ -1 & 0 & \frac{3}{2} & 0 & -1 & 0 \\ 0 & 0 & 0 & 2 & -1 & -1 \\ 0 & 0 & -1 & -1 & 2 & 0 \\ 0 & 0 & 0 & -1 & 0 & 2 \end{pmatrix}. \quad (6.2.41)$$

Interestingly, as was observed in [57], the self-intersection of one of the exceptional curves (δ_3) is $-3/2$, which is the minus of the length squared of a weight in the spinor representation of $SO(12)$. Thus we see that at a generic $s \neq 0$ codimension-one locus of the singularity the exceptional fibers after the resolutions form a root system of $SO(12)$, but at $s = 0$ one of the simple roots is transmuted to a weight in the spinor representation. A similar but slightly different observation was made in [66].

These δ 's form a basis of the two-cycles appearing at the codimension-two singularity after the resolution. On the lattice spanned by these δ 's, there are precisely 32 points of length squared $3/2$. They are of the form $\sum_{I=q_1, 1, 3, 2, r_2, q_2} n_I \delta_I$ with either $n_I \geq 0$ for all I , or $n_I \leq 0$ for all I . Note that, unlike in the the cases of the ordinary or the complete resolutions, there appears only *one* irreducible representation ($= \mathbf{32}$) in the integer span of the two-cycles at the singularity.

6.2.3 Blowing up q_1 first

In Section 6.2.1, between the two singularities, p_1 was blown up first. In this section, let us blow up q_1 first and see the differences. This time we make a shift of the coordinate x_1 so that q_1 comes to $(0, 0, 0, s)$: We define

$$\Sigma_z(\tilde{x}_1, y_1, z, s) \equiv \Phi_z(\tilde{x}_1 - 2s, y_1, z, s), \quad (6.2.42)$$

$\Sigma_z(\tilde{x}_1, y_1, z, s) = 0$ has singularities $(3s, 0, 0, s)$ ($= p_1$) and $(0, 0, 0, s)$ ($= q_1$). We blow up the latter singularity. The process is completely parallel to that in Section 6.2.1 so we will only describe the relevant charts and show the main differences from the previous case.

2nd blow up

Chart 2_{zx}

$$\Sigma_z(\tilde{x}_1, \tilde{x}_1 y_2, \tilde{x}_1 z_2, s) = \tilde{x}_1^2 \Sigma_{zx}(\tilde{x}_1, y_2, z_2, s), \quad (6.2.43)$$

$$\Sigma_{zx}(\tilde{x}_1, y_2, z_2, s) = z_2(3s - \tilde{x}_1)(3s - \tilde{x}_1 - z_2) - y_2^2, \quad (6.2.44)$$

$$\mathcal{C}_2 \text{ in } 2_{zx} : \quad \tilde{x}_1 = 0, \quad y_2^2 = 3s z_2(3s - z_2), \quad (6.2.45)$$

$$\text{Singularities :} \quad (\tilde{x}_1, y_2, z_2, s) = (3s, 0, 0, s) = p_1. \quad (6.2.46)$$

There are no other singularities in chart 2_{zy} or 2_{zz} , so we blow up p_1 in chart 2_{zx} . Again, we need to shift the coordinate so that the singularity we now blow up comes to the origin:

$$\Xi_{zx}(\bar{x}_1, y_2, z_2, s) \equiv \Sigma_{zx}(\bar{x}_1 + 3s, y_2, z_2, s). \quad (6.2.47)$$

3rd blow up

The relevant charts are 3_{zxx} and 3_{zxz} .

Chart 3_{zxx}

$$\Xi_{zx}(\bar{x}_1, \bar{x}_1 y_3, \bar{x}_1 z_3, s) = \bar{x}_1^2 \Xi_{zxx}(\bar{x}_1, y_3, z_3, s), \quad (6.2.48)$$

$$\Xi_{zxx}(\bar{x}_1, y_3, z_3, s) = \bar{x}_1 z_3 (z_3 + 1) - y_3^2, \quad (6.2.49)$$

$$\mathcal{C}_3 \text{ in } 3_{zxx} : \quad \bar{x}_1 = 0, \quad y_3 = 0, \quad (6.2.50)$$

$$\text{Singularities : } (\bar{x}_1, y_3, z_3, s) = (0, 0, -1, s) = r_2, \quad (0, 0, 0, s) = p_2. \quad (6.2.51)$$

Chart 3_{zxz}

$$\Xi_{zx}(\bar{x}_3 z_2, y_3 z_2, z_2, s) = z_2^2 \Xi_{zxz}(\bar{x}_3, y_3, z_2, s), \quad (6.2.52)$$

$$\Xi_{zxz}(\bar{x}_3, y_3, z_2, s) = \bar{x}_3 (\bar{x}_3 + 1) - y_3^2, \quad (6.2.53)$$

$$\mathcal{C}_3 \text{ in } 3_{zxz} : \quad z_2 = 0, \quad y_3 = 0, \quad (6.2.54)$$

$$\text{Singularities : } (\bar{x}_3, y_3, z_2, s) = (-1, 0, 0, s) = r_2, \quad (0, 0, 0, s) = q_2. \quad (6.2.55)$$

The process of blowing up is summarized in Table 6.2.

6.2.4 Exceptional curves at $s = 0$: Differences from the p_1 -first case

δ 's \mathcal{C} 's for the q_1 -first case are given by

$$\mathcal{C}_2 = 2\delta_2 + \delta_{p_2} + 2\delta_3 + 2\delta_{q_2} + \delta_{r_2}, \quad \mathcal{C}_1 = \delta_1, \quad \mathcal{C}_{p_2} = \delta_{p_2}, \quad \mathcal{C}_3 = \delta_3, \quad \mathcal{C}_{q_2} = \delta_{q_2}, \quad \mathcal{C}_{r_2} = \delta_{r_2}. \quad (6.2.56)$$

	1st blow up	2nd blow up	3rd blow up	4th blow up
$\overset{\circ}{p}_0 \rightarrow$	$\overset{\circ}{q}_1 (-2s : 0 : 1) \rightarrow$ $p_1 (s : 0 : 1)$	regular $\overset{\circ}{p}_1 (1 : 0 : 0) (\tilde{x}_1 = 3s) \rightarrow$	$\overset{\circ}{p}_2 (1 : 0 : 0) \rightarrow$ $\overset{\circ}{q}_2 (0 : 0 : 1) \rightarrow$ $\overset{\circ}{r}_2 (1 : 0 : -1) \rightarrow$	regular regular regular

Table 6.2: The incomplete case when q_1 is blown up first.

The intersection matrix of \mathcal{C}_I 's is (6.2.40) with $I, J = 2, 1, p_2, 3, q_2, r_2$. Then (6.2.56) yields the intersections of δ_I 's as

$$-\delta_I \cdot \delta_J = \begin{pmatrix} \frac{3}{2} & 0 & 0 & 0 & -1 & 0 \\ 0 & 2 & -1 & 0 & 0 & 0 \\ 0 & -1 & 2 & -1 & 0 & 0 \\ 0 & 0 & -1 & 2 & -1 & -1 \\ -1 & 0 & 0 & -1 & 2 & 0 \\ 0 & 0 & 0 & -1 & 0 & 2 \end{pmatrix}. \quad (6.2.57)$$

In this case, we obtain an E_6 -like diagram as one representing the intersections of the exceptional curves (6.2.57) at the codimension-two singularity. (6.2.57) is not, however, the E_6 Cartan matrix itself, as the self-intersection of δ_1 is $-3/2$. We show the intersection diagrams of this case in Fig. 6.2.

We can search for the elements of the form $\sum_{I=q_1,1,3,2,r_2,q_2} n_I \delta_I$ whose square is $-3/2$ to find, again, that there are $16 + 16$ such elements, the former of which have $n_I \geq 0$ for all I , and the latter of which have $n_I \leq 0$ for all I . Thus, in this case as well, there is only *one* irreducible representation (= **32**) at the singularity.

6.3 Complete resolution: $D_6 \rightarrow E_7$

In this case we set $H_{n+4} = s^2$ with other parameters being the same as the previous section. The blow-up procedures are almost parallel to the incomplete resolutions, except for the replacement $s \rightarrow s^2$.

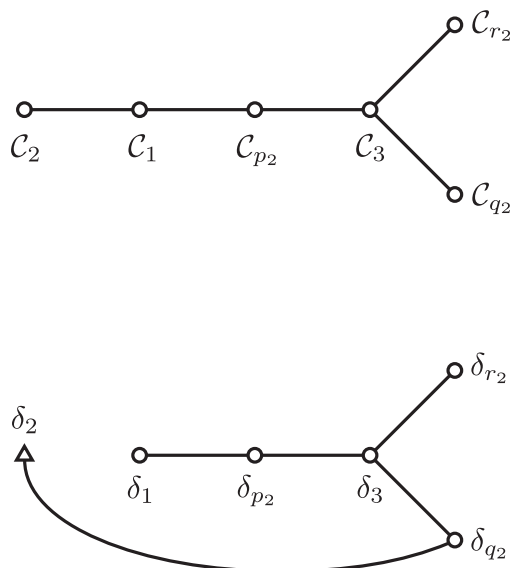


Fig. 6.2: The intersection diagrams of the exceptional curve \mathcal{C} 's and δ 's. We blew up the singularity q_1 first.

6.3.1 Blowing up p_1 first

In this case, a difference arises in chart 3_{zxx} when p_2 is blown up in 2_{zx} , where we have

$$\Psi_{zx}(\tilde{x}_1, \tilde{x}_1 y_3, \tilde{x}_1 z_3, s) = \tilde{x}_1^2 \Psi_{zxx}(\tilde{x}_1, y_3, z_3, s), \quad (6.3.1)$$

$$\Psi_{zxx}(\tilde{x}_1, y_3, z_3, s) = z_3(3s^2 + \tilde{x}_1 z_3 + \tilde{x}_1) - y_3^2, \quad (6.3.2)$$

$$\mathcal{C}_3 \text{ in } 3_{zxx} : \quad \tilde{x}_1 = 0, \quad y_3^2 = 3s^2 z_3, \quad (6.3.3)$$

$$\text{Singularities : } (\tilde{x}_1, y_3, z_3, s) = (-3s^2, 0, 0, s) = q_1, \quad (0, 0, -1, 0) = p_3. \quad (6.3.4)$$

The last one is a new isolated codimension-two singularity, that did not appear in the incomplete resolution in the previous section. This isolated singularity can also be seen in chart 3_{zxx} . By a shift of the coordinate we can see that this is a conifold singularity. The exceptional curve arising from the small resolution intersects with δ_3 at a single point on $s = 0$,

which completes an E_7 intersection diagram (Fig. 6.3). Note that the extra node extends from the one represented by a triangle in the incomplete resolution. In the present complete case, however, this δ_3 is naturally considered to have an ordinary self-intersection number -2 as we will see below.

By carefully examining what becomes of \mathcal{C}_I 's in the small resolution, it can be shown that the relation (6.2.33) is modified to

$$\mathcal{C}_{q_1} = \delta_{q_1}, \quad \mathcal{C}_1 = \delta_1, \quad \mathcal{C}_2 = \delta_2, \quad \mathcal{C}_3 = 2\delta_3 + \delta_{q_1} + \delta_{r_2} + \delta_{\text{complete}}, \quad \mathcal{C}_{r_2} = \delta_{r_2}, \quad \mathcal{C}_{q_2} = \delta_{q_2}, \quad (6.3.5)$$

where δ_{complete} is the new exceptional curve arising from the small resolution of the isolated conifold singularity. Then assuming the ordinary self-intersection numbers among δ 's as specified by the E_7 Dynkin diagram shown in Fig. 6.3, we find that the intersection matrix among \mathcal{C} 's is computed by (6.3.5) to be precisely the minus of the $SO(12)$ Cartan matrix (6.2.40).

The process of blowing up in this subsection is summarized in Table 6.3.

	1st blow up	2nd blow up	3rd blow up	4th blow up
$\overset{\circ}{p}_0 \rightarrow$	$\overset{\circ}{p}_1 (s^2 : 0 : 1) \rightarrow$ $q_1 (-2s^2 : 0 : 1)$	$\overset{\circ}{p}_2 (1 : 0 : 0)$ (in 2_{zx}) \rightarrow $q_1 (1 : 0 : 0)$ ($\tilde{x}_1 = -3s^2$) $r_2(1 : 0 : -3s^2)$ $\overset{\circ}{q}_2 (0 : 0 : 1)$ (in 2_{zz}) \rightarrow	$\overset{\circ}{p}_3 (1 : 0 : 0; s = 0)$ (codim.2) \rightarrow $\overset{\circ}{q}_1 (1 : 0 : 0)$ ($\tilde{x}_1 = -3s^2$) \rightarrow $\overset{\circ}{r}_2 (0 : 0 : 1)$ ($z_2 = -3s^2$) \rightarrow regular	regular regular regular

Table 6.3: The complete case when p_1 is blown up first. The new isolated codimension-two conifold singularity is shown in red. δ_3 is now an ordinary node represented by a circle (cf. Fig. 6.1).

6.3.2 Blowing up q_1 first

When q_1 is blown up first, a difference arises this time in chart 2_{zz} , where a conifold singularity is developed at $(x_2, y_2, z, s) = (0, 0, 0, 0)$, which we denote by q_3 (shown in red in Table 6.4), where the relation to the coordinates in chart 1_z is $(\tilde{x}_1, y_1, z, s) = (\tilde{x}_2 z, y_2 z, z, s)$. This is also

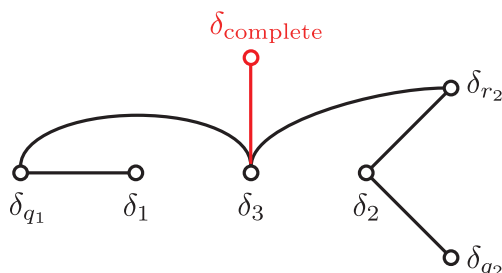


Fig. 6.3: The E_7 Dynkin diagram obtained by a complete resolution with p_1 blow up first.

an isolated codimension-two singularity developed only at $s = 0$. Since this is in chart 2_{zz} , this singularity is located at $(0 : 0 : 1)$ on P^2 emerged by the blow up at $s = 0$. Therefore, it is not visible in chart 2_{zx} or 3_{zx*} . Moreover, after the coordinate shift similar to (6.2.42), Ψ_{zx} becomes identical to the incomplete case. Thus the process is the same as the incomplete case afterwards. Therefore, the only extra exceptional curve is the one arising from the small resolution of the isolated conifold singularity on δ_2 . This adds an extra node to the diagram in the lower panel of Fig. 6.2, as we show in Fig. 6.4. We denote this new curve as δ_{complete} here. This is E_7 , and the extra node again extends from δ_2 that was the “weight” node represented by the triangle in the incomplete case. In the complete resolution, it becomes an ordinary node with self-intersection -2 , being consistent with the modified relation:

$$\begin{aligned} \mathcal{C}_2 &= 2\delta_2 + \delta_{p_2} + 2\delta_3 + 2\delta_{q_2} + \delta_{r_2} + \delta_{\text{complete}}, \\ \mathcal{C}_1 &= \delta_1, \quad \mathcal{C}_{p_2} = \delta_{p_2}, \quad \mathcal{C}_3 = \delta_3, \quad \mathcal{C}_{q_2} = \delta_{q_2}, \quad \mathcal{C}_{r_2} = \delta_{r_2}, \end{aligned} \tag{6.3.6}$$

and the intersection matrix is given by

$$-\delta_I \cdot \delta_J = \begin{pmatrix} 2 & -1 & 0 & 0 & 0 & 0 & 0 \\ -1 & 2 & 0 & 0 & 0 & -1 & 0 \\ 0 & 0 & 2 & -1 & 0 & 0 & 0 \\ 0 & 0 & -1 & 2 & -1 & 0 & 0 \\ 0 & 0 & 0 & -1 & 2 & -1 & -1 \\ 0 & -1 & 0 & 0 & -1 & 2 & 0 \\ 0 & 0 & 0 & 0 & -1 & 0 & 2 \end{pmatrix}, \tag{6.3.7}$$

where $I, J = \text{complete}, 2, 1, p_2, 3, q_2, r_2$. That is, (6.3.6) reproduces the minus of the D_6 Cartan matrix as the intersection matrix among \mathcal{C} 's if the intersections of δ 's are the ones specified by the E_7 Dynkin diagram as shown in Fig. 6.4.

	1st blow up	2nd blow up	3rd blow up	4th blow up
$p_0 \rightarrow$	$q_1 (-2s^2 : 0 : 1) \rightarrow$ $p_1 (s^2 : 0 : 1)$	$q_3 (0 : 0 : 1; s = 0)$ (codim.2) \rightarrow $p_1 (1 : 0 : 0) (\tilde{x}_1 = 3s) \rightarrow$	regular $p_2 (1 : 0 : 0) \rightarrow$ $q_2 (0 : 0 : 1) \rightarrow$ $r_2 (1 : 0 : -1) \rightarrow$	regular regular regular

Table 6.4: The complete case when q_1 is blown up first.

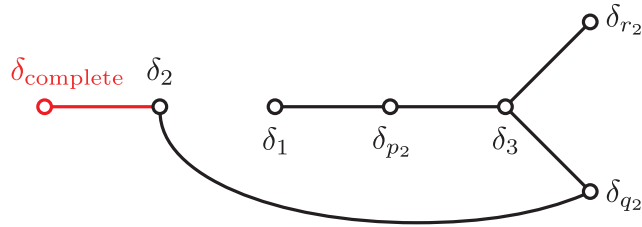


Fig. 6.4: The E_7 Dynkin diagram obtained by a complete resolution with q_1 blow up first.

Chapter 7

Conclusions

In this chapter, we conclude this thesis. We have considered the F-theory compactifications on the K3 manifolds and the Calabi-Yau manifolds. The compact manifolds in F-theory are described by elliptic fibrations, and degeneracy of the elliptic curve corresponds to existence of 7-branes. Physics depends on geometry of the compact manifolds, especially its singularities play important roles.

Codimension-one singularities associate with enhancement of gauge symmetry, which implies a stack of 7-branes. Coexistence of D-branes and non-pure-D7-branes, i.e., (p, q) -brane, is an essential feature of F-theory. Due to this, the gauge enhancements exhibit not only $SU(N)$ but also exceptional gauge groups. We can interpret such gauge enhancements as a spectrum of string junctions. These 7-branes are conventionally described algebraically in terms of **A**, **B** and **C**-branes. Allowed configurations of the 7-branes are decided by types of the singularities, which are classified by the Kodaira classification.

In Chapter 4, noticing that all the discriminant loci are on equal footing and there is no a priori reason to distinguish one from the others, we have considered new complex codimension-one objects consisting of the zero loci of the coefficient functions f and g of the Weierstrass equation, which we referred to as an “ f -plane” and a “ g -plane”, collectively as “elliptic point planes”. They are two kinds of critical points of a “dessin d’enfant” known in mathematics.

Although they do not carry D-brane charges and do not have non-trivial monodromies, they play an essential role in achieving a gauge enhancement by altering the monodromies

around the branes. More precisely, if there are some elliptic point planes, the z -plane is divided into several cell regions, each of which corresponds to a (half of a) fundamental region in the preimage of the J -function. A cell region is bounded by several domain walls extending from these elliptic point planes and D-branes, on which the imaginary part of the J -function vanishes. In particular, the elliptic point planes extend a special kind of domain walls, which we call “ S -walls”, crossing through which implies that the type IIB complex string coupling is S -dualized. Consequently, on the z -plane coexist a theory in the perturbative regime and its nonperturbative S -dual simultaneously. The monodromy around several 7-branes is thus not just a product of monodromy around each 7-brane any more, but they get $SL(2, \mathbb{Z})$ conjugated due to the difference of the corresponding fundamental regions the base points belong to.

In this sense one may say that the nonperturbative properties of F-theory are the consequence of the coexisting “locally S -dualized regions” bounded by the S -walls extended from the elliptic point planes. In the orientifold limit [72], the D-branes and the elliptic point planes gather to form a I_0^* singular fiber, so that the S -walls extended from the elliptic point planes are contracted with each other and confined, so the S -walls are not seen from even a short distance.

We have also considered singularities of Calabi-Yau manifolds with higher-codimensions. In particular, F-theory compactifications on elliptic fibered Calabi-Yau three-folds over Hirzebruch surfaces, which can have codimension-two singularities, are dual to $E_8 \times E_8$ heterotic superstring theory on elliptic fibered K3 surfaces. The codimension-two singularities provide matter fields in six dimensions.

Comparing to dual heterotic theory, we can establish correspondence between geometry of the Calabi-Yau three-folds and information of the matters. We have seen that can interpret the number of the matters as the number of the complex structure moduli, which is the number of the coefficients in the defining equation.

Geometry of Calabi-Yau manifolds is also investigated from insight of supersymmetric gauge theories. In Section 5.2, we have focused on Calabi-Yau four-folds. Based on M-theory compactification, we have provided a brief review of relation between the Coulomb branch of

three-dimensional $\mathcal{N} = 2$ gauge theory and the resolutions of the Calabi-Yau four-fold.

Moreover, we have examined some special cases such that enhancement of gauge symmetry is $SU(6) \rightarrow E_6$, $SO(12) \rightarrow E_7$ or $E_7 \rightarrow E_8$, which yield hypermultiplets in six-dimensions. In particular, we have concentrated on the $SO(12) \rightarrow E_7$ case in Chapter 6. We have performed explicit blowing-ups and investigated the intersection numbers of the exceptional curves.

In the case of the incomplete resolutions, we observe only codimension-one singularities. The intersection matrix of the exceptional curves is the $SO(12)$ Cartan matrix rather than the E_7 one. Taking an another definition, we have referred as δ 's, we obtain a fractional self-intersection number.

For the complete resolutions, the results are completely changed. The codimension-two singularity appear, and the intersection matrix of the exceptional curves becomes E_7 Cartan matrix. In this case, we have not half-hypers but full-hypers in six-dimensional field theory.

We hope that this result of incomplete and complete resolutions will be understood from the point of view of elliptic point planes. Besides, we also hope this new way of presenting the non-localness among 7-branes will be useful for understanding of the structure of higher-codimension singularities with higher-rank enhancement such as discussed in [43, 53–55, 62, 103].

Acknowledgements

The author would like to thank my supervisor Shun'ya Mizoguchi so much for teaching him various physics. NK also express his gratitude to his researching collaborators, Shin Fukuchi, Ryuichiro Kitano, Ryota Kojima, Rinto Kuramochi, Taro Tani, Hitomi Tashiro, Shimon Yankielowicz and Ryo Yokokura.

Finally, NK would like to express the deepest appreciation to the members in KEK Theory Center, especially Toshihiro Aoki, Yuhma Asano, Gabriela Bailas, Takuya Hasegawa, Hiroyuki Ishida, Satoshi Iso, Yusuke Kimura, Yoshihisa Kitazawa, Yusuke Namekawa, Makoto Natsuume, Jun Nishimura, Hikaru Ohta, Hajime Otsuka, Yutaka Sakamura, Takao Suyama, Daiki Ueda and Sumito Yokoo.

Appendix A

The string junctions of E_6

We show the complete set of 72 string junctions in the case of E_6 :

	Q_A^1	Q_A^2	Q_A^3	Q_A^4	Q_A^5	Q_B	Q_C^1	Q_C^2
1	-1	-1	-1	-1	0	2	1	1
2	-1	-1	-1	0	-1	2	1	1
3	-1	-1	0	-1	-1	2	1	1
4	-1	-1	0	0	0	1	0	1
5	-1	-1	0	0	0	1	1	0
6	-1	0	-1	-1	-1	2	1	1
7	-1	0	-1	0	0	1	0	1
8	-1	0	-1	0	0	1	1	0
9	-1	0	0	-1	0	1	0	1
10	-1	0	0	-1	0	1	1	0
11	-1	0	0	0	-1	1	0	1
12	-1	0	0	0	-1	1	1	0
13	-1	0	0	0	1	0	0	0
14	-1	0	0	1	0	0	0	0
15	-1	0	1	0	0	0	0	0
16	-1	1	0	0	0	0	0	0

	Q_A^1	Q_A^2	Q_A^3	Q_A^4	Q_A^5	Q_B	Q_C^1	Q_C^2
17	0	-1	-1	-1	-1	2	1	1
18	0	-1	-1	0	0	1	0	1
19	0	-1	-1	0	0	1	1	0
20	0	-1	0	-1	0	1	0	1
21	0	-1	0	-1	0	1	1	0
22	0	-1	0	0	-1	1	0	1
23	0	-1	0	0	-1	1	1	0
24	0	-1	0	0	1	0	0	0
25	0	-1	0	1	0	0	0	0
26	0	-1	1	0	0	0	0	0
27	0	0	-1	-1	0	1	0	1
28	0	0	-1	-1	0	1	1	0
29	0	0	-1	0	-1	1	0	1
30	0	0	-1	0	-1	1	1	0
31	0	0	-1	0	1	0	0	0
32	0	0	-1	1	0	0	0	0
33	0	0	0	-1	-1	1	0	1
34	0	0	0	-1	-1	1	1	0
35	0	0	0	-1	1	0	0	0
36	0	0	0	0	0	0	-1	1
37	0	0	0	0	0	0	1	-1
38	0	0	0	1	-1	0	0	0
39	0	0	0	1	1	-1	-1	0
40	0	0	0	1	1	-1	0	-1
41	0	0	1	-1	0	0	0	0
42	0	0	1	0	-1	0	0	0
43	0	0	1	0	1	-1	-1	0
44	0	0	1	0	1	-1	0	-1

	Q_A^1	Q_A^2	Q_A^3	Q_A^4	Q_A^5	Q_B	Q_C^1	Q_C^2
45	0	0	1	1	0	-1	-1	0
46	0	0	1	1	0	-1	0	-1
47	0	1	-1	0	0	0	0	0
48	0	1	0	-1	0	0	0	0
49	0	1	0	0	-1	0	0	0
50	0	1	0	0	1	-1	-1	0
51	0	1	0	0	1	-1	0	-1
52	0	1	0	1	0	-1	-1	0
53	0	1	0	1	0	-1	0	-1
54	0	1	1	0	0	-1	-1	0
55	0	1	1	0	0	-1	0	-1
56	0	1	1	1	1	-2	-1	-1
57	1	-1	0	0	0	0	0	0
58	1	0	-1	0	0	0	0	0
59	1	0	0	-1	0	0	0	0
60	1	0	0	0	-1	0	0	0
61	1	0	0	0	1	-1	-1	0
62	1	0	0	0	1	-1	0	-1
63	1	0	0	1	0	-1	-1	0
64	1	0	0	1	0	-1	0	-1
65	1	0	1	0	0	-1	-1	0
66	1	0	1	0	0	-1	0	-1
67	1	0	1	1	1	-2	-1	-1
68	1	1	0	0	0	-1	-1	0
69	1	1	0	0	0	-1	0	-1
70	1	1	0	1	1	-2	-1	-1
71	1	1	1	0	1	-2	-1	-1
72	1	1	1	1	0	-2	-1	-1

Appendix B

Resolutions: $E_7 \rightarrow E_8$

B.1 Incomplete resolution: blowing up p_2 first

In this case we take

$$f(z, s) = sz^3 + z^4, \quad g(z, s) = z^5. \quad (\text{B.1.1})$$

The concrete process of the incomplete resolution of the codimension-two singularity enhancement from E_7 to E_8 goes as follows:

1st blow up

Chart 1_x

$$\Phi(x, xy_1, xz_1, s) = x^2\Phi_x(x, y_1, z_1, s), \quad (\text{B.1.2})$$

$$\Phi_x(x, y_1, z_1, s) = sx^2z_1^3 + x^3(z_1 + 1)z_1^4 + x - y_1^2, \quad (\text{B.1.3})$$

$$\mathcal{C}_1 \text{ in } 1_x : \quad x = 0, \quad y_1 = 0, \quad (\text{B.1.4})$$

$$\text{Singularities :} \quad \text{None.} \quad (\text{B.1.5})$$

Chart 1_y

$$\Phi(x_1 y, y, y z_1, s) = y^2 \Phi_y(x_1, y, z_1, s), \quad (\text{B.1.6})$$

$$\Phi_y(x_1, y, z_1, s) = x_1 y^2 z_1^3 (s + y z_1) + x_1^3 y + y^3 z_1^5 - 1, \quad (\text{B.1.7})$$

$$\mathcal{C}_1 \text{ in } 1_y : \quad \text{Invisible in this patch,} \quad (\text{B.1.8})$$

$$\text{Singularities :} \quad \text{None.} \quad (\text{B.1.9})$$

Chart 1_z

$$\Phi(x_1 z, y_1 z, z, s) = z^2 \Phi_z(x_1, y_1, z, s), \quad (\text{B.1.10})$$

$$\Phi_z(x_1, y_1, z, s) = z (x_1 z (s + z) + x_1^3 + z^2) - y_1^2, \quad (\text{B.1.11})$$

$$\mathcal{C}_1 \text{ in } 1_z : \quad z = 0, \quad y_1 = 0. \quad (\text{B.1.12})$$

$$\text{Singularities :} \quad (x_1, y_1, z, s) = (0, 0, 0, s). \quad (\text{B.1.13})$$

We refer to this singularity as p_1 .

2nd blow upChart 2_{zx}

$$\Phi_z(x_1, x_1 y_2, x_1 z_2, s) = x_1^2 \Phi_{zx}(x_1, y_2, z_2, s), \quad (\text{B.1.14})$$

$$\Phi_{zx}(x_1, y_2, z_2, s) = z_2 x_1 (z_2 (s + z_2) + (z_2^2 + 1) x_1) - y_2^2, \quad (\text{B.1.15})$$

$$\mathcal{C}_2 \text{ in } 2_{zx} : \quad x_1 = 0, \quad y_2 = 0, \quad (\text{B.1.16})$$

$$\text{Singularities :} \quad (x_1, y_2, z_2, s) = (0, 0, -s, s) = q_2, (0, 0, 0, s) = p_2. \quad (\text{B.1.17})$$

Here we see two singularities on \mathcal{C}_2 which coincide with each other at $s = 0$.

Chart 2_{zy}

$$\Phi_z(x_2 y_1, y_1, y_1 z_2, s) = y_1^2 \Phi_{zy}(x_2, y_1, z_2, s), \quad (\text{B.1.18})$$

$$\Phi_{zy}(x_2, y_1, z_2, s) = x_2 y_1 t_2^2 (s + y_1 z_2) + x_2^3 y_1^2 z_2 + y_1 z_2^3 - 1, \quad (\text{B.1.19})$$

$$\mathcal{C}_2 \text{ in } 2_{zy} : \quad \text{Invisible in this patch}, \quad (\text{B.1.20})$$

$$\text{Singularities} : \quad \text{None}. \quad (\text{B.1.21})$$

Chart 2_{zz}

$$\Phi_z(x_2 z, y_2 z, z, s) = z^2 \Phi_{zz}(x_2, y_2, z, s), \quad (\text{B.1.22})$$

$$\Phi_{zz}(x_2, y_2, z, s) = z (s x_2 + z x_2^3 + z x_2 + 1) - y_2^2, \quad (\text{B.1.23})$$

$$\mathcal{C}_2 \text{ in } 2_{zz} : \quad t = 0, \quad y_2 = 0, \quad (\text{B.1.24})$$

$$\text{Singularities} : \quad (x_2, y_2, z, s) = \left(-\frac{1}{s}, 0, 0, s \right). \quad (\text{B.1.25})$$

This singularity is q_2 , which was also seen in chart 2_{zx} . At this stage, we have two singularities p_2 and q_2 . In this section we blow up at p_2 first. We can see this singularity in chart 2_{zx} only, so we consider $\Phi_{zx}(x_1, y_2, z_2, s)$ in the next blow up.

3rd blow upChart 3_{txx}

$$\Phi_{zx}(x_1, x_1 y_3, x_1 z_3, s) = x_1^2 \Phi_{zxx}(x_1, y_3, z_3, s), \quad (\text{B.1.26})$$

$$\Phi_{zxx}(x_1, y_3, z_3, s) = z_3 x_1 (s z_3 + z_3^2 x_1^2 + z_3^2 x_1 + 1) - y_3^2, \quad (\text{B.1.27})$$

$$\mathcal{C}_3 \text{ in } 3_{zxx} : \quad x_1 = 0, \quad y_3 = 0, \quad (\text{B.1.28})$$

$$\text{Singularities} : \quad (x_1, y_3, z_3, s) = \left(0, 0, -\frac{1}{s}, s \right) = r_3, \quad (0, 0, 0, s) = p_3. \quad (\text{B.1.29})$$

We name the first singularity r_3 , and the second singularity p_3 .

Chart 3_{zxz}

$$\Phi_{zx}(x_3z_2, y_3z_2, z_2, s) = z_2^2\Phi_{zxz}(x_3, y_3, z_2, s), \quad (\text{B.1.30})$$

$$\Phi_{zxz}(x_3, y_3, z_2, s) = z_2x_3(s + z_2^2x_3 + z_2 + x_3) - y_3^2, \quad (\text{B.1.31})$$

$$\mathcal{C}_3 \text{ in } 3_{zxz} : \quad z_2 = 0, \quad y_3 = 0, \quad (\text{B.1.32})$$

$$\text{Singularities : } (x_3, y_3, z_2, s) = (0, 0, -s, s) = q_2, (0, 0, 0, s) = q_3, (-s, 0, 0, s) = r_3. \quad (\text{B.1.33})$$

The first singularity is not on \mathcal{C}_3 unless $s = 0$; this is q_2 . We name the second singularity q_3 . The third one is r_3 already seen in chart 3_{zxx} .

Since p_3 and q_3 are different point even when $s \rightarrow 0$, we can blow up at them independently on charts 3_{zxx} and 3_{zxz} , respectively. Let us first blow up at p_3 using $\Phi_{zxx}(x_1, y_3, z_3, s)$:

4th blow up at p_3 Chart 4_{zxxx}

$$\Phi_{zxx}(x_1, x_1y_4, x_1z_4, s) = x_1^2\Phi_{zxxx}(x_1, y_4, z_4, s), \quad (\text{B.1.34})$$

$$\Phi_{zxxx}(x_1, y_4, z_4, s) = sz_4^2x_1 + z_4^3x_1^4 + z_4^3x_1^3 + z_4 - y_4^2, \quad (\text{B.1.35})$$

$$\mathcal{C}_4 \text{ in } 4_{zxxx} : \quad x_1 = 0, \quad y_4^2 = z_4, \quad (\text{B.1.36})$$

$$\text{Singularities : } \quad \text{None.} \quad (\text{B.1.37})$$

Chart 4_{zxzx}

$$\Phi_{zxx}(x_4z_3, y_4z_3, z_3, s) = x_4^2\Phi_{zxzx}(x_4, y_4, z_3, s), \quad (\text{B.1.38})$$

$$\Phi_{zxzx}(x_4, y_4, z_3, s) = sz_3x_4 + z_3^4x_4^3 + z_3^3x_4^2 + x_4 - y_4^2, \quad (\text{B.1.39})$$

$$\mathcal{C}_4 \text{ in } 4_{zxzx} : \quad z_3 = 0, \quad y_4^2 = x_4, \quad (\text{B.1.40})$$

$$\text{Singularities : } (x_4, y_4, z_3, s) = \left(0, 0, -\frac{1}{s}, s\right). \quad (\text{B.1.41})$$

This singularity is not on \mathcal{C}_4 even when $s = 0$; this is r_3 . There is no singularity any more on \mathcal{C}_4 , so let us turn to the singularities observed in chart 3_{zxz} : $(x_1, y_3, z_3, s) = (0, 0, -s, s) = q_2$, $(0, 0, 0, s) = q_3$, $(-s, 0, 0, s) = r_3$.

4th blow up at q_3

We next blow up at q_3 ; using $\Phi_{txt}(x_3, y_3, t_2, s)$, we find

Chart 4_{zxzx}

$$\Phi_{zxz}(x_3, x_3y_4, x_3z_4, s) = x_3^2\Phi_{zxzx}(x_3, y_4, z_4, s), \quad (\text{B.1.42})$$

$$\Phi_{zxzx}(x_3, y_4, z_4, s) = z_4(s + z_4^2x_3^3 + z_4x_3 + x_3) - y_4^2, \quad (\text{B.1.43})$$

$$\mathcal{C}'_4 \text{ in } 4_{zxzx} : \quad x_3 = 0, \quad y_4^2 = sz_4, \quad (\text{B.1.44})$$

$$\text{Singularities : } \quad (x_3, y_4, z_4, s) = (-s, 0, 0, s). \quad (\text{B.1.45})$$

This is r_3 , which is not on \mathcal{C}'_4 unless $s = 0$.

Chart 4_{zxzz}

$$\Phi_{zxz}(x_4z_2, y_4z_2, z_2, s) = z_2^2\Phi_{zxzz}(x_4, y_4, z_2, s), \quad (\text{B.1.46})$$

$$\Phi_{zxzz}(x_4, y_4, z_2, s) = sx_4 + z_2x_4(z_2^2x_4 + x_4 + 1) - y_4^2, \quad (\text{B.1.47})$$

$$\mathcal{C}'_4 \text{ in } 4_{zxzz} : \quad z_2 = 0, \quad y_4^2 = sx_4, \quad (\text{B.1.48})$$

$$\text{Singularities : } \quad (x_4, y_4, z_2, s) = (0, 0, -s, s). \quad (\text{B.1.49})$$

This is q_2 , which is not on \mathcal{C}'_4 unless $s = 0$, either. So far, all the singularities except for q_2 and r_3 are resolved. Since r_3 is located in the $(0 : 0 : 1)$ direction on the P^2 blown up at q_3 , whereas r_3 is in the $(1 : 0 : 0)$ direction on the same P^2 , they are never the same point even when $s = 0$. Thus we can blow up at them independently.

5th blow up at r_3 in chart 4_{zxzx}

To blow up at r_3 , we shift the x_3 coordinate so that this singularity is represented as $(0, 0, 0, s)$ in a new coordinate \tilde{x}_3 :

$$\Psi_{zxzx}(\tilde{x}_3, y_4, z_4, s) \equiv \Phi_{zxzx}(\tilde{x}_3 - s, y_4, z_4, s). \quad (\text{B.1.50})$$

Then it can be verified that no singularity arises in Ψ_{zxzx} or Ψ_{zxzx} defined below. The exceptional curves are:

Chart 5_{zxzxx}

$$\Psi_{zxzx}(\tilde{x}_3, \tilde{x}_3 y_5, \tilde{x}_3 z_5, s) = \tilde{x}_3^2 \Psi_{zxzxx}(\tilde{x}_3, y_5, z_5, s), \quad (\text{B.1.51})$$

$$\Psi_{zxzxx}(\tilde{x}_3, y_5, z_5, s) = z_5^3 \tilde{x}_3 (\tilde{x}_3 - s)^3 + z_5^2 (\tilde{x}_3 - s) + z_5 - y_5^2, \quad (\text{B.1.52})$$

$$\mathcal{C}_5 \text{ in } 5_{zxzxx} : \quad \tilde{x}_3 = 0, \quad y_5^2 = -s z_5^2 + z_5. \quad (\text{B.1.53})$$

Chart 5_{zxzzz}

$$\Psi_{zxzz}(\tilde{x}_5 z_4, y_5 z_4, z_4, s) = z_4^2 \Psi_{zxzzz}(\tilde{x}_5, y_5, z_4, s), \quad (\text{B.1.54})$$

$$\Psi_{zxzzz}(\tilde{x}_5, y_5, z_4, s) = z_4 (z_4 \tilde{x}_5 - s)^3 - s + z_4 \tilde{x}_5 + \tilde{x}_5 - y_5^2, \quad (\text{B.1.55})$$

$$\mathcal{C}_5 \text{ in } 5_{zxzzz} : \quad z_4 = 0, \quad y_5^2 = \tilde{x}_5 - s. \quad (\text{B.1.56})$$

5th blow up at q_2 in chart 4_{txtt}

Having resolved the singularity r_3 , we turn to the resolution of q_2 in chart 4_{zxzz} . For this we need a different coordinate shift:

$$\Sigma_{zxzz}(x_4, y_4, \tilde{z}_2, s) \equiv \Phi_{zxzz}(x_4, y_4, \tilde{z}_2 - s, s). \quad (\text{B.1.57})$$

Then Ψ_{zxzz} has a singularity at $(x_4, y_4, \tilde{z}_2, s) = (0, 0, 0, s)$. Again, Ψ_{zxzzx} and Ψ_{zxzzz} defined below have no singularity. The exceptional curves are:

Chart 5_{zxzzx}

$$\Sigma_{zxzz}(x_4, x_4 y_5, x_4 \tilde{t}_5, s) = x_4^2 \Sigma_{zxzzx}(x_4, y_5, \tilde{t}_5, s), \quad (\text{B.1.58})$$

$$\Sigma_{zxzzx}(x_4, y_5, \tilde{t}_5, s) = (x_4 \tilde{t}_5 - s)^3 + x_4 \tilde{t}_5 - s + \tilde{t}_5 - y_5^2, \quad (\text{B.1.59})$$

$$\mathcal{C}_5 \text{ in } 5_{zxzzx} : \quad x_4 = 0, \quad y_5^2 = \tilde{t}_5 - s - s^3. \quad (\text{B.1.60})$$

Chart 5_{zxzzz}

$$\Sigma_{zxzzz}(x_5 \tilde{z}_2, y_5 \tilde{z}_2, \tilde{z}_2, s) = \tilde{z}_2^2 \Sigma_{zxzzz}(x_5, y_5, \tilde{z}_2, s), \quad (\text{B.1.61})$$

$$\Sigma_{zxzzz}(x_5, y_5, \tilde{z}_2, s) = x_5^2 ((\tilde{z}_2 - s)^3 + \tilde{z}_2 - s) + x_5 - y_5^2, \quad (\text{B.1.62})$$

$$\mathcal{C}_5 \text{ in } 5_{zxzzz} : \quad \tilde{z}_2 = 0, \quad y_5^2 = (-s^3 - s) x_5^2 + x_5. \quad (\text{B.1.63})$$

	1st blow up	2nd blow up	3rd blow up	4th blow up	5th blow up
$\overset{\circ}{p}_0 \rightarrow$	$\overset{\circ}{p}_1 (0 : 0 : 1) \rightarrow$	$\overset{\circ}{p}_2 (1 : 0 : 0) \rightarrow$	$\overset{\circ}{p}_3 (1 : 0 : 0) \rightarrow$	regular	
		$q_2 (1 : 0 : -s)$	$\overset{\circ}{q}_3 (0 : 0 : 1) \rightarrow$	regular	
			$q_2 (0 : 0 : 1) (z_2 = -s) \rightarrow$	$\overset{\circ}{q}_2 (0 : 0 : 1) (z_2 = -s) \rightarrow$	regular
			$r_3 (-s : 0 : 11)$	$\overset{\circ}{r}_3 (1 : 0 : 0) (x_3 = -s) \rightarrow$	regular

Table 2.1: The incomplete case when p_2 is blown up first.

B.2 Exceptional curves at $s = 0$

The intersection matrix among \mathcal{C}_I 's

$$-\mathcal{C}_I \cdot \mathcal{C}_J = \begin{pmatrix} 2 & 0 & 0 & -1 & 0 & 0 & 0 \\ 0 & 2 & 0 & 0 & -1 & 0 & -1 \\ 0 & 0 & 2 & -1 & -1 & -1 & 0 \\ -1 & 0 & -1 & 2 & 0 & 0 & 0 \\ 0 & -1 & -1 & 0 & 2 & 0 & 0 \\ 0 & 0 & -1 & 0 & 0 & 2 & 0 \\ 0 & -1 & 0 & 0 & 0 & 0 & 2 \end{pmatrix} \quad (\text{B.2.1})$$

and the relations

$$\mathcal{C}_1 = \delta_1, \quad \mathcal{C}_2 = \delta_2, \quad \mathcal{C}_3 = \delta_3, \quad \mathcal{C}_4 = \delta_4, \quad \mathcal{C}'_4 = 2\delta'_4 + \delta_{r_3} + \delta_{q_2}, \quad \mathcal{C}_{r_3} = \delta_{r_3}, \quad \mathcal{C}_{q_2} = \delta_{q_2} \quad (\text{B.2.2})$$

imply that the intersection matrix among δ_I 's is

$$-\delta_I \cdot \delta_J = \begin{pmatrix} 2 & 0 & 0 & -1 & 0 & 0 & 0 \\ 0 & 2 & 0 & 0 & 0 & 0 & -1 \\ 0 & 0 & 2 & -1 & 0 & -1 & 0 \\ -1 & 0 & -1 & 2 & 0 & 0 & 0 \\ 0 & 0 & 0 & 0 & \frac{3}{2} & -1 & -1 \\ 0 & 0 & -1 & 0 & -1 & 2 & 0 \\ 0 & -1 & 0 & 0 & -1 & 0 & 2 \end{pmatrix}, \quad (\text{B.2.3})$$

where $I, J = 1, 2, 3, 4, 4', r_3, q_2$.

Similarly to the previous examples, one of the δ 's ($= \delta'_4$) has self-intersection $-3/2$, which equals to the minus of the length squared of a weight in the **56** representation of E_7 . It can also be verified that there are precisely 28 elements of the form $\sum_{I=1,2,3,4,4',r_3,q_2} n_I \delta_I$ with non-negative integer coefficients, $n_I \geq 0$ for all I , such that the length squared is $\frac{3}{2}$, and also there are the same number of elements with non-positive integer coefficients, $n_I \leq 0$ for all I . They all together form the whole weights of the **56** representation. Again, there is only a single set, indicating that it is a half-hypermultiplet.

B.3 Complete resolution: blow up p_2 first

We will now consider the complete resolution. This can be achieved by taking $f_{n+8} = s^2$ instead of s . This amounts to replacing s in (B.1.1) with s^2 . Similarly to the previous sections, we find an additional isolated codimension-two conifold singularity after we blow up q_3 . As shown in red in Table 2.2, this new singularity, which we denote by r_4 , arises at $(1 : 0 : -1)$ on the P^2 particularly at $s = 0$. This adds an extra node to the incomplete intersection diagram to form the correct E_8 Dynkin diagram as we show in Fig. 2.2. The node δ'_4 , which was formerly represented by a triangle in Fig. 2.1, is now an ordinary node consisting of the root system of E_8 . This is consistent with the modified relations:

$$\mathcal{C}_1 = \delta_1, \quad \mathcal{C}_2 = \delta_2, \quad \mathcal{C}_3 = \delta_3, \quad \mathcal{C}_4 = \delta_4, \quad \mathcal{C}'_4 = 2\delta'_4 + \delta_{r_3} + \delta_{q_2} + \delta_{\text{complete}}, \quad \mathcal{C}_{r_3} = \delta_{r_3}, \quad \mathcal{C}_{q_2} = \delta_{q_2}, \quad (\text{B.3.1})$$

which can be verified by a careful up-lifting of \mathcal{C}_I 's into the coordinate system of the small resolution.

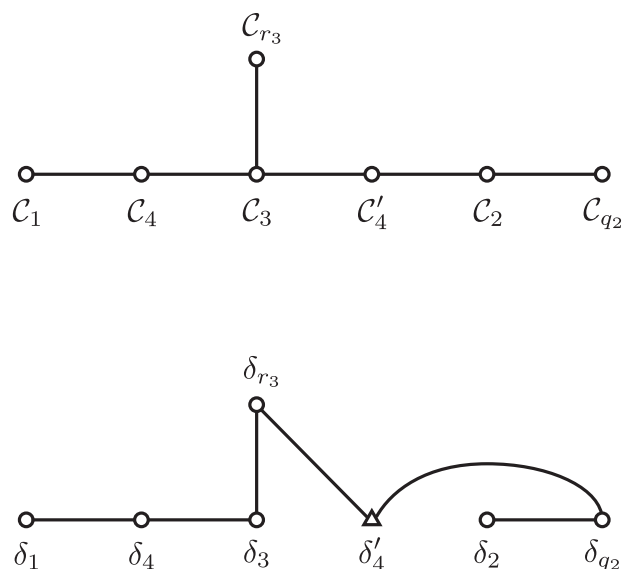


Fig. 2.1: The intersection diagrams of the exceptional curve \mathcal{C} 's and δ 's. We blew up the singularity p_2 first.

	1st blow up	2nd blow up	3rd blow up	4th blow up	5th blow up
$\overset{\circ}{p}_0 \rightarrow$	$\overset{\circ}{p}_1 (0 : 0 : 1) \rightarrow$	$\overset{\circ}{p}_2 (1 : 0 : 0) \rightarrow$	$\overset{\circ}{p}_3 (1 : 0 : 0) \rightarrow$	regular	
		$q_2 (1 : 0 : -s)$	$\overset{\circ}{q}_3 (0 : 0 : 1) \rightarrow$	$\overset{\circ}{r}_4 (1 : 0 : -1; s = 0) \text{ (codim.2)} \rightarrow$	regular
			$q_2 (0 : 0 : 1) (z_2 = -s) \rightarrow$	$\overset{\circ}{q}_2 (0 : 0 : 1) (z_2 = -s) \rightarrow$	regular
			$r_3 (-s : 0 : 11)$	$\overset{\circ}{r}_3 (1 : 0 : 0) (x_3 = -s) \rightarrow$	regular

Table 2.2: The incomplete case when p_2 is blown up first.

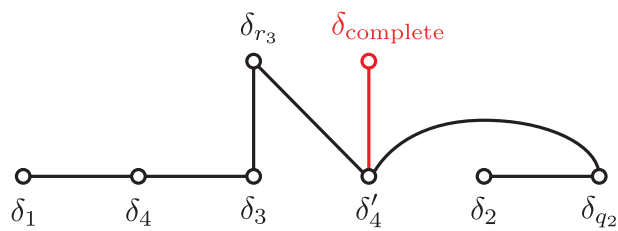


Fig. 2.2: The E_8 Dynkin diagram obtained by a complete resolution with p_2 blow up first.

Reference

- [1] C. Vafa, *Evidence for F theory*, *Nucl. Phys.* **B469** (1996) 403 [[hep-th/9602022](#)].
- [2] T. Weigand, *TASI Lectures on F-theory*, *PoS TASI2017* (2018) 016 [[1806.01854](#)].
- [3] A. Sen, *An Introduction to nonperturbative string theory*, in *Duality and supersymmetric theories. Proceedings, Easter School, Newton Institute, Euroconference, Cambridge, UK, April 7-18, 1997*, pp. 297–413, 1998, [hep-th/9802051](#).
- [4] C. Montonen and D. I. Olive, *Magnetic Monopoles as Gauge Particles?*, *Phys. Lett.* **72B** (1977) 117.
- [5] N. Seiberg and E. Witten, *Monopoles, duality and chiral symmetry breaking in N=2 supersymmetric QCD*, *Nucl. Phys.* **B431** (1994) 484 [[hep-th/9408099](#)].
- [6] T. Banks, M. R. Douglas and N. Seiberg, *Probing F theory with branes*, *Phys. Lett.* **B387** (1996) 278 [[hep-th/9605199](#)].
- [7] M. R. Douglas, D. A. Lowe and J. H. Schwarz, *Probing F theory with multiple branes*, *Phys. Lett.* **B394** (1997) 297 [[hep-th/9612062](#)].
- [8] A. Sen, *BPS states on a three-brane probe*, *Phys. Rev.* **D55** (1997) 2501 [[hep-th/9608005](#)].
- [9] J. Polchinski, *String theory. Vol. 2: Superstring theory and beyond*, Cambridge Monographs on Mathematical Physics. Cambridge University Press, 2007, [10.1017/CBO9780511618123](#).

-
- [10] A. Sen, *Orientifold limit of F theory vacua*, *Phys. Rev.* **D55** (1997) R7345 [hep-th/9702165].
- [11] M. Bianchi, A. Collinucci and L. Martucci, *Magnetized E3-brane instantons in F-theory*, *JHEP* **12** (2011) 045 [1107.3732].
- [12] O. Aharony, J. Sonnenschein and S. Yankielowicz, *Interactions of strings and D-branes from M theory*, *Nucl. Phys.* **B474** (1996) 309 [hep-th/9603009].
- [13] M. R. Gaberdiel and B. Zwiebach, *Exceptional groups from open strings*, *Nucl. Phys.* **B518** (1998) 151 [hep-th/9709013].
- [14] K. Dasgupta and S. Mukhi, *BPS nature of three string junctions*, *Phys. Lett.* **B423** (1998) 261 [hep-th/9711094].
- [15] A. Sen, *String network*, *JHEP* **03** (1998) 005 [hep-th/9711130].
- [16] M. R. Gaberdiel, T. Hauer and B. Zwiebach, *Open string-string junction transitions*, *Nucl. Phys.* **B525** (1998) 117 [hep-th/9801205].
- [17] O. DeWolfe and B. Zwiebach, *String junctions for arbitrary Lie algebra representations*, *Nucl. Phys.* **B541** (1999) 509 [hep-th/9804210].
- [18] M. Krogh and S. Lee, *String network from M theory*, *Nucl. Phys.* **B516** (1998) 241 [hep-th/9712050].
- [19] O. DeWolfe, T. Hauer, A. Iqbal and B. Zwiebach, *Uncovering the symmetries on $[p,q]$ seven-branes: Beyond the Kodaira classification*, *Adv. Theor. Math. Phys.* **3** (1999) 1785 [hep-th/9812028].
- [20] J. H. Schwarz, *LECTURES ON SUPERSTRING THEORY*, *Conf. Proc.* **C841227** (1984) 94.
- [21] O. Bergman, *Three pronged strings and $1/4$ BPS states in $N=4$ superYang-Mills theory*, *Nucl. Phys.* **B525** (1998) 104 [hep-th/9712211].
- [22] O. Bergman and A. Fayyazuddin, *String junctions and BPS states in Seiberg-Witten theory*, *Nucl. Phys.* **B531** (1998) 108 [hep-th/9802033].

-
- [23] O. Bergman and A. Fayyazuddin, *String junction transitions in the moduli space of $N=2$ SYM*, *Nucl. Phys.* **B535** (1998) 139 [[hep-th/9806011](#)].
- [24] K. Hashimoto, H. Hata and N. Sasakura, *Three - string junction and BPS saturated solutions in $SU(3)$ supersymmetric Yang-Mills theory*, *Phys. Lett.* **B431** (1998) 303 [[hep-th/9803127](#)].
- [25] K. Hashimoto, H. Hata and N. Sasakura, *Multipronged strings and BPS saturated solutions in $SU(N)$ supersymmetric Yang-Mills theory*, *Nucl. Phys.* **B535** (1998) 83 [[hep-th/9804164](#)].
- [26] K. Hashimoto, *String junction from world sheet gauge theory*, *Prog. Theor. Phys.* **101** (1999) 1353 [[hep-th/9808185](#)].
- [27] Y. Imamura, *$E(8)$ flavor multiplets*, *Phys. Rev.* **D58** (1998) 106005 [[hep-th/9802189](#)].
- [28] Y. Imamura, *String junctions and their duals in heterotic string theory*, *Prog. Theor. Phys.* **101** (1999) 1155 [[hep-th/9901001](#)].
- [29] T. Tani, *Matter from string junction*, *Nucl. Phys.* **B602** (2001) 434.
- [30] L. Bonora and R. Savelli, *Non-simply-laced Lie algebras via F theory strings*, *JHEP* **11** (2010) 025 [[1007.4668](#)].
- [31] M. Fukae, Y. Yamada and S.-K. Yang, *Mordell-Weil lattice via string junctions*, *Nucl. Phys.* **B572** (2000) 71 [[hep-th/9909122](#)].
- [32] A. Grassi, J. Halverson and J. L. Shaneson, *Matter From Geometry Without Resolution*, *JHEP* **10** (2013) 205 [[1306.1832](#)].
- [33] A. Grassi, J. Halverson and J. L. Shaneson, *Non-Abelian Gauge Symmetry and the Higgs Mechanism in F -theory*, *Commun. Math. Phys.* **336** (2015) 1231 [[1402.5962](#)].
- [34] S. Fukuchi, N. Kan, S. Mizoguchi and H. Tashiro, *A dessin on the base: a description of mutually non-local 7-branes without using branch cuts*, [1808.04135](#).
- [35] S. Fukuchi, N. Kan, R. Kuramochi, S. Mizoguchi and H. Tashiro, *More on a dessin on the base: Kodaira exceptional fibers and mutually (non-)local branes*, [1912.02974](#).

-
- [36] R. Donagi and M. Wijnholt, *Model Building with F-Theory*, *Adv. Theor. Math. Phys.* **15** (2011) 1237 [0802.2969].
- [37] C. Beasley, J. J. Heckman and C. Vafa, *GUTs and Exceptional Branes in F-theory - I*, *JHEP* **01** (2009) 058 [0802.3391].
- [38] C. Beasley, J. J. Heckman and C. Vafa, *GUTs and Exceptional Branes in F-theory - II: Experimental Predictions*, *JHEP* **01** (2009) 059 [0806.0102].
- [39] R. Donagi and M. Wijnholt, *Breaking GUT Groups in F-Theory*, *Adv. Theor. Math. Phys.* **15** (2011) 1523 [0808.2223].
- [40] J. J. Heckman, *Particle Physics Implications of F-theory*, *Ann. Rev. Nucl. Part. Sci.* **60** (2010) 237 [1001.0577].
- [41] T. Weigand, *Lectures on F-theory compactifications and model building*, *Class. Quant. Grav.* **27** (2010) 214004 [1009.3497].
- [42] S. Mizoguchi and T. Sakaguchi, *Note on three-generation models in heterotic string and F-theory on elliptic Calabi–Yau manifolds over Hirzebruch varieties*, *PTEP* **2016** (2016) 101B01 [1607.02890].
- [43] S. Mizoguchi, *F-theory Family Unification*, *JHEP* **07** (2014) 018 [1403.7066].
- [44] Y. Honma and H. Otsuka, *On the Flux Vacua in F-theory Compactifications*, *Phys. Lett.* **B774** (2017) 225 [1706.09417].
- [45] L. Aparicio, D. G. Cerdeno and L. E. Ibanez, *Modulus-dominated SUSY-breaking soft terms in F-theory and their test at LHC*, *JHEP* **07** (2008) 099 [0805.2943].
- [46] H. Hayashi, R. Tatar, Y. Toda, T. Watari and M. Yamazaki, *New Aspects of Heterotic–F Theory Duality*, *Nucl. Phys.* **B806** (2009) 224 [0805.1057].
- [47] E. I. Buchbinder, *Dynamically SUSY Breaking SQCD on F-Theory Seven-Branes*, *JHEP* **09** (2008) 134 [0805.3157].
- [48] J. J. Heckman, J. Marsano, N. Saulina, S. Schafer-Nameki and C. Vafa, *Instantons and SUSY breaking in F-theory*, 0808.1286.

-
- [49] J. Marsano, N. Saulina and S. Schafer-Nameki, *Gauge Mediation in F-Theory GUT Models*, *Phys. Rev.* **D80** (2009) 046006 [0808.1571].
- [50] J. Marsano, N. Saulina and S. Schafer-Nameki, *An Instanton Toolbox for F-Theory Model Building*, *JHEP* **01** (2010) 128 [0808.2450].
- [51] J. J. Heckman and C. Vafa, *From F-theory GUTs to the LHC*, 0809.3452.
- [52] J. J. Heckman and C. Vafa, *F-theory, GUTs, and the Weak Scale*, *JHEP* **09** (2009) 079 [0809.1098].
- [53] D. R. Morrison and C. Vafa, *Compactifications of F theory on Calabi-Yau threefolds. 1*, *Nucl. Phys.* **B473** (1996) 74 [hep-th/9602114].
- [54] D. R. Morrison and C. Vafa, *Compactifications of F theory on Calabi-Yau threefolds. 2.*, *Nucl. Phys.* **B476** (1996) 437 [hep-th/9603161].
- [55] M. Bershadsky, K. A. Intriligator, S. Kachru, D. R. Morrison, V. Sadov and C. Vafa, *Geometric singularities and enhanced gauge symmetries*, *Nucl. Phys.* **B481** (1996) 215 [hep-th/9605200].
- [56] S. H. Katz and C. Vafa, *Matter from geometry*, *Nucl. Phys.* **B497** (1997) 146 [hep-th/9606086].
- [57] D. R. Morrison and W. Taylor, *Matter and singularities*, *JHEP* **01** (2012) 022 [1106.3563].
- [58] D. R. Morrison and W. Taylor, *Non-Higgsable clusters for 4D F-theory models*, *JHEP* **05** (2015) 080 [1412.6112].
- [59] D. R. Morrison and W. Taylor, *Toric bases for 6D F-theory models*, *Fortsch. Phys.* **60** (2012) 1187 [1204.0283].
- [60] D. R. Morrison and W. Taylor, *Classifying bases for 6D F-theory models*, *Central Eur. J. Phys.* **10** (2012) 1072 [1201.1943].
- [61] J. J. Heckman and C. Vafa, *Flavor Hierarchy From F-theory*, *Nucl. Phys.* **B837** (2010) 137 [0811.2417].

-
- [62] H. Hayashi, T. Kawano, R. Tatar and T. Watari, *Codimension-3 Singularities and Yukawa Couplings in F-theory*, *Nucl. Phys.* **B823** (2009) 47 [0901.4941].
- [63] J. de Boer, K. Hori and Y. Oz, *Dynamics of $N=2$ supersymmetric gauge theories in three-dimensions*, *Nucl. Phys.* **B500** (1997) 163 [hep-th/9703100].
- [64] O. Aharony, A. Hanany, K. A. Intriligator, N. Seiberg and M. J. Strassler, *Aspects of $N=2$ supersymmetric gauge theories in three-dimensions*, *Nucl. Phys.* **B499** (1997) 67 [hep-th/9703110].
- [65] H. Hayashi, C. Lawrie and S. Schafer-Nameki, *Phases, Flops and F-theory: $SU(5)$ Gauge Theories*, *JHEP* **10** (2013) 046 [1304.1678].
- [66] H. Hayashi, C. Lawrie, D. R. Morrison and S. Schafer-Nameki, *Box Graphs and Singular Fibers*, *JHEP* **05** (2014) 048 [1402.2653].
- [67] A. P. Braun and S. Schafer-Nameki, *Box Graphs and Resolutions I*, *Nucl. Phys.* **B905** (2016) 447 [1407.3520].
- [68] A. P. Braun and S. Schafer-Nameki, *Box Graphs and Resolutions II: From Coulomb Phases to Fiber Faces*, *Nucl. Phys.* **B905** (2016) 480 [1511.01801].
- [69] N. Kan, S. Mizoguchi and T. Tani, *To appear*, .
- [70] M. Bershadsky, C. Vafa and V. Sadov, *D strings on D manifolds*, *Nucl. Phys.* **B463** (1996) 398 [hep-th/9510225].
- [71] E. G. Gimon and J. Polchinski, *Consistency conditions for orientifolds and d manifolds*, *Phys. Rev.* **D54** (1996) 1667 [hep-th/9601038].
- [72] A. Sen, *F theory and orientifolds*, *Nucl. Phys.* **B475** (1996) 562 [hep-th/9605150].
- [73] K. Dasgupta and S. Mukhi, *F theory at constant coupling*, *Phys. Lett.* **B385** (1996) 125 [hep-th/9606044].
- [74] B. R. Greene, A. D. Shapere, C. Vafa and S.-T. Yau, *Stringy Cosmic Strings and Noncompact Calabi-Yau Manifolds*, *Nucl. Phys.* **B337** (1990) 1.

- [75] E. Witten, *String theory dynamics in various dimensions*, *Nucl. Phys.* **B443** (1995) 85 [[hep-th/9503124](#)].
- [76] J. H. Schwarz, *An $SL(2, Z)$ multiplet of type IIB superstrings*, *Phys. Lett.* **B360** (1995) 13 [[hep-th/9508143](#)].
- [77] A. Giveon and D. Kutasov, *Brane Dynamics and Gauge Theory*, *Rev. Mod. Phys.* **71** (1999) 983 [[hep-th/9802067](#)].
- [78] A. Hanany and E. Witten, *Type IIB superstrings, BPS monopoles, and three-dimensional gauge dynamics*, *Nucl. Phys.* **B492** (1997) 152 [[hep-th/9611230](#)].
- [79] J. H. Schwarz, *Lectures on superstring and M theory dualities: Given at ICTP Spring School and at TASI Summer School*, *Nucl. Phys. Proc. Suppl.* **55B** (1997) 1 [[hep-th/9607201](#)].
- [80] K. Becker, M. Becker and A. Strominger, *Five-branes, membranes and nonperturbative string theory*, *Nucl. Phys.* **B456** (1995) 130 [[hep-th/9507158](#)].
- [81] A. Iqbal, *Selfintersection number of BPS junctions in backgrounds of three-branes and seven-branes*, *JHEP* **10** (1999) 032 [[hep-th/9807117](#)].
- [82] O. DeWolfe, T. Hauer, A. Iqbal and B. Zwiebach, *Constraints on the BPS spectrum of $N=2$, $D=4$ theories with A-D-E flavor symmetry*, *Nucl. Phys.* **B534** (1998) 261 [[hep-th/9805220](#)].
- [83] O. J. Ganor and A. Hanany, *Small $E(8)$ instantons and tensionless noncritical strings*, *Nucl. Phys.* **B474** (1996) 122 [[hep-th/9602120](#)].
- [84] B. Haghighat, G. Lockhart and C. Vafa, *Fusing E-strings to heterotic strings: $E+E \rightarrow H$* , *Phys. Rev.* **D90** (2014) 126012 [[1406.0850](#)].
- [85] J. Kim, S. Kim, K. Lee, J. Park and C. Vafa, *Elliptic Genus of E-strings*, *JHEP* **09** (2017) 098 [[1411.2324](#)].
- [86] J. Gu, B. Haghighat, A. Klemm, K. Sun and X. Wang, *Elliptic Blowup Equations for 6d SCFTs. III: E-strings, M-strings and Chains*, [1911.11724](#).

-
- [87] A. Grothendieck, *Esquisse d'un Programme*, Published in *Schneps and Published in Schneps and Lochak* (1984) 5.
- [88] S. Lando and A. Zvonkin, *Graphs on Surfaces and Their Applications*. Springer, 2004.
- [89] A. Strominger, *Massless black holes and conifolds in string theory*, *Nucl. Phys.* **B451** (1995) 96 [[hep-th/9504090](#)].
- [90] B. R. Greene, D. R. Morrison and A. Strominger, *Black hole condensation and the unification of string vacua*, *Nucl. Phys.* **B451** (1995) 109 [[hep-th/9504145](#)].
- [91] B. R. Greene, D. R. Morrison and C. Vafa, *A Geometric realization of confinement*, *Nucl. Phys.* **B481** (1996) 513 [[hep-th/9608039](#)].
- [92] S. H. Katz, D. R. Morrison and M. R. Plesser, *Enhanced gauge symmetry in type II string theory*, *Nucl. Phys.* **B477** (1996) 105 [[hep-th/9601108](#)].
- [93] A. Klemm and P. Mayr, *Strong coupling singularities and nonAbelian gauge symmetries in $N=2$ string theory*, *Nucl. Phys.* **B469** (1996) 37 [[hep-th/9601014](#)].
- [94] P. Berglund, S. H. Katz, A. Klemm and P. Mayr, *New Higgs transitions between dual $N=2$ string models*, *Nucl. Phys.* **B483** (1997) 209 [[hep-th/9605154](#)].
- [95] K. Hori, H. Ooguri and C. Vafa, *NonAbelian conifold transitions and $N=4$ dualities in three-dimensions*, *Nucl. Phys.* **B504** (1997) 147 [[hep-th/9705220](#)].
- [96] E. Witten, *Phase transitions in M theory and F theory*, *Nucl. Phys.* **B471** (1996) 195 [[hep-th/9603150](#)].
- [97] D. R. Morrison and N. Seiberg, *Extremal transitions and five-dimensional supersymmetric field theories*, *Nucl. Phys.* **B483** (1997) 229 [[hep-th/9609070](#)].
- [98] K. A. Intriligator, D. R. Morrison and N. Seiberg, *Five-dimensional supersymmetric gauge theories and degenerations of Calabi-Yau spaces*, *Nucl. Phys.* **B497** (1997) 56 [[hep-th/9702198](#)].
- [99] D.-E. Diaconescu and R. Entin, *Calabi-Yau spaces and five-dimensional field theories with exceptional gauge symmetry*, *Nucl. Phys.* **B538** (1999) 451 [[hep-th/9807170](#)].

- [100] K. Intriligator, H. Jockers, P. Mayr, D. R. Morrison and M. R. Plesser, *Conifold Transitions in M-theory on Calabi-Yau Fourfolds with Background Fluxes*, *Adv. Theor. Math. Phys.* **17** (2013) 601 [1203.6662].
- [101] D.-E. Diaconescu and S. Gukov, *Three-dimensional N=2 gauge theories and degenerations of Calabi-Yau four folds*, *Nucl. Phys.* **B535** (1998) 171 [hep-th/9804059].
- [102] T. W. Grimm and H. Hayashi, *F-theory fluxes, Chirality and Chern-Simons theories*, *JHEP* **03** (2012) 027 [1111.1232].
- [103] S. Mizoguchi and T. Tani, *Anomaly-free multiple singularity enhancement in F-theory*, *PTEP* **2016** (2016) 073B05 [1508.07423].